

Sign-Based Optimizers Are Effective Under Heavy-Tailed Noise

Dingzhi Yu^{1,2}

YUDZ@LAMDA.NJU.EDU.CN

Hongyi Tao¹

221220032@SMAIL.NJU.EDU.CN

Yuanyu Wan³

WANYY@ZJU.EDU.CN

Luo Luo⁴

LUOLUO@FUDAN.EDU.CN

Lijun Zhang^{1,2}

ZHANGLJ@LAMDA.NJU.EDU.CN

¹*National Key Laboratory for Novel Software Technology, Nanjing University*

²*School of Artificial Intelligence, Nanjing University*

³*School of Software Technology, Zhejiang University*

⁴*School of Data Science, Fudan University*

Abstract

While adaptive gradient methods are the workhorse of modern machine learning, sign-based optimization algorithms such as Lion and Muon have recently demonstrated superior empirical performance over AdamW in training large language models (LLM). However, a theoretical understanding of why sign-based updates outperform variance-adapted methods remains elusive. In this paper, we aim to bridge the gap between theory and practice through the lens of heavy-tailed gradient noise, a phenomenon frequently observed in language modeling tasks. Theoretically, we introduce a novel generalized heavy-tailed noise condition that captures the behavior of LLMs more accurately than standard finite variance assumptions. Under this noise model, we establish sharp convergence rates of SignSGD and Lion for generalized smooth function classes, matching or surpassing previous best-known bounds. Furthermore, we extend our analysis to Muon and Muonlight, providing what is, to our knowledge, the first rigorous analysis of matrix optimization under heavy-tailed stochasticity. These results offer a strong theoretical justification for the empirical superiority of sign-based optimizers, showcasing that they are naturally suited to handle the noisy gradients associated with heavy tails. Empirically, LLM pretraining experiments validate our theoretical insights and confirm that our proposed noise models are well-aligned with practice.

Keywords: Heavy-tailed noise, sign-based methods, Lion and Muon, matrix optimizers, concentration inequalities, LLM pretraining

1. Introduction

The success of large foundation models (Devlin et al., 2019; Brown et al., 2020; Achiam et al., 2023; Touvron et al., 2023a,b; Team et al., 2023; Guo et al., 2025) requires costly pretraining procedures that are supported by stochastic optimization algorithms (Robbins and Monro, 1951). Among them, adaptive gradient methods (Duchi et al., 2011; Kingma and Ba, 2015) prevail, in which AdamW (Loshchilov and Hutter, 2019) is the *de facto* optimizer for training large language models (LLM). Recently, two representative sign-based optimizers, namely Lion (Chen et al., 2023a) and Muon (Jordan et al., 2024) have received significant attention due to their consistent speedup over AdamW (Zhao et al., 2025; Shah et al., 2025; Wen et al., 2025; Semenov et al., 2025), especially in scaling up both LLM pretraining (Liu et al., 2025a; Team et al., 2025; Zeng et al., 2025) and post-training (Team et al., 2026). Despite their huge empirical success, we still lack a complete theoretical understanding of why Lion and Muon outperform AdamW for training LLMs.

In this work, we systematically investigate this phenomenon with theoretical analysis and empirical study. The significant empirical evidence that initiates our work comes from the widely observed heavy-tailed distribution of the stochastic gradients (Simsekli et al., 2019; Zhang et al., 2020c; Gurbuzbalaban et al., 2021), especially in language modeling tasks (Kunstner et al., 2023, 2024; Ahn et al., 2024; Kunstner and Bach, 2025; Yadav et al., 2025) due to Zipf’s Law (Piantadosi, 2014). In sharp contrast to the finite variance condition commonly employed in theoretical studies (Ghadimi and Lan, 2013; Lan, 2020), such a regime only assumes the stochastic noise has a finite p th moment where $p \in (1, 2]$. Under this more realistic noise model, the challenges underlying both theoretical analysis and algorithmic design arise. For instance, SGD is known to diverge (Zhang et al., 2020c), and the convergence theory collapses when $p < 2$.¹ As for the more popular adaptive methods like Adam (Kingma and Ba, 2015) and AdaGrad (Duchi et al., 2011), no rigorous convergence theory has yet been established under heavy-tailed noise. To make things worse, Chezhegov et al. (2025) show that Adam and AdaGrad could suffer from worse convergence when the noise is heavy-tailed. Intriguingly, the empirical advantage of sign-based methods like Lion and Muon is most pronounced in LLM training regimes (Liu et al., 2025a; Wen et al., 2025), where heavy-tailed noise is prevalent. In contrast, this advantage diminishes when it comes to computer vision tasks (Yuan et al., 2025; Liu et al., 2025b), which typically exhibit more concentrated gradient noise (Zhang et al., 2020c; Zhou et al., 2020; Gurbuzbalaban et al., 2021; Ahn et al., 2024). Regarding this disparity, it is natural to ask the following question:

Can we obtain theoretical guarantees of sign-based optimizers to explain their practical effectiveness and justify their advantage over AdamW under heavy-tailed gradient noise?

We answer the above question affirmatively by establishing new convergence theories for a series of representative vector- and matrix-based sign descent methods, including vector sign optimizer SignSGD (Bernstein et al., 2018) and Lion (Chen et al., 2023a), matrix sign optimizer Muon (Jordan et al., 2024) and Muonlight (Liu et al., 2025a). For a heavy-tailed index p and iteration number T , we show that these optimizers converge at $O(T^{-\frac{p-1}{3p-2}})$, matching or surpassing the previous state-of-the-art. Our convergence analysis is derived under a newly proposed generalized heavy-tailed noise condition, allowing the noise level to grow w.r.t. the gradient norm, which is strictly weaker than existing assumptions and is further supported by empirical evidence from LLM pretraining. Furthermore, our theory holds for generalized smooth function classes (Zhang et al., 2020b), which have become a standard deployment in theory (Zhang et al., 2020a; Chen et al., 2023b; Faw et al., 2023; Wang et al., 2023; Li et al., 2023) and proven to align well with practice (Riabinin et al., 2025). The key technical tools that support our analysis are new vector and matrix martingale concentration inequalities in non-Euclidean norms (cf. Section 5.2), which may be of independent interest. Our results suggest that the sign operation, whether applied element-wise or via orthogonalization in the matrix case, acts as a natural robustifier against heavy-tailed stochasticity, thus making sign-based optimizers like Lion and Muon a natural fit for training LLMs. Our main contributions are summarized as follows.

- We propose a generalized heavy-tailed noise framework for both vector and matrix variables and derive sharp convergence rates of $O(T^{-\frac{p-1}{3p-2}})$ for SignSGD, Lion, Muon, and Muonlight.

1. This does not contradict Fatkhullin et al. (2025); Liu (2026), as they impose heavy-tailedness on the stochastic gradient itself. This is a strictly stronger condition than the heavy-tailed noise assumption considered in this work; see Section 2 for details.

- We characterize the mechanism by which the sign operator inherently handles heavy-tailed noise, providing a theoretical justification for their superiority over SGD or AdamW in LLMs.
- We conduct extensive LLM pretraining experiments on GPT2 to validate our theoretical findings and provide empirical evidence that our proposed noise model accurately reflects the stochasticity encountered in practice.

2. Related Work

Heavy-tailed Noise The seminal work of [Zhang et al. \(2020c\)](#) theoretically explains why adaptive gradient methods like Clipped SGD ([Pascanu et al., 2013](#)) have a benefit for Attention models ([Vaswani et al., 2017](#)). Inspired by [Simsekli et al. \(2019\)](#), they identify the heavy-tailed noise distributions in language modeling tasks, and establish a $O(T^{-\frac{p-1}{3p-2}})$ convergence for clipped SGD with a matching lower bound under the standard heavy-tailed gradient noise condition, where the noise is only assumed to have a finite p th momentum where $1 \leq p \leq 2$. After that, a series of works try to study the behavior of this heavy-tailed stochasticity ([Gurbuzbalaban et al., 2021](#); [Kunstner et al., 2024](#); [Kunstner and Bach, 2025](#)), or leverage this phenomenon to explain the empirical success of popular algorithms ([Zhou et al., 2020](#); [Yadav et al., 2025](#)) or model architectures ([Ahn et al., 2024](#)). As for the theory community, heavy-tailedness has been widely adopted and investigated in multiple realms, such as learning theory ([Hsu and Sabato, 2014](#); [Zhang and Zhou, 2018](#)), online learning ([Zhang and Cutkosky, 2022](#); [Liu, 2026b](#)), bandits ([Bubeck et al., 2013](#); [Lu et al., 2019](#); [Xue et al., 2020](#); [Gou et al., 2023](#); [Xue et al., 2023](#); [Ye et al., 2025](#)) and optimization ([Hodgkinson and Mahoney, 2021](#); [Cutkosky and Mehta, 2021](#); [Vural et al., 2022](#); [Liu et al., 2023](#); [Liu and Zhou, 2023](#); [Nguyen et al., 2023](#); [Sadiev et al., 2023](#); [Kornilov et al., 2023](#); [Puchkin et al., 2024](#); [Gorbunov et al., 2024](#); [Liu et al., 2024](#); [Liu and Zhou, 2025](#); [Hübner et al., 2025](#); [Fatkhullin et al., 2025](#); [Liu and Luo, 2025](#); [Wang et al., 2026](#); [Chen et al., 2026](#); [Wu and Luo, 2026](#); [Liu, 2026a](#)).

Sign-based methods: vector optimizers The simplest signed gradient descent algorithm, namely SignSGD, is proposed by [Bernstein et al. \(2018\)](#), where the authors establish convergence rates based on ℓ_1 -norm and discussed its possible complexity improvement over SGD. [Bernstein et al. \(2019\)](#) later shows that SignSGD with majority vote is communication efficient and robust to noise error. Further attempts have been made to improve the convergence of SignSGD for smooth functions ([Safaryan and Richtárik, 2021](#); [Sun et al., 2023](#); [Jiang et al., 2025b](#); [Kornilov et al., 2025](#); [Li et al., 2025b](#)). While for non-smooth functions, [Karimireddy et al. \(2019\)](#) provide a simple convex counterexample where SignSGD fails to converge, which they utilize the error feedback techniques ([Seide et al., 2014](#)) to alleviate the divergence. [Liu et al. \(2019\)](#); [Petrov et al. \(2025\)](#) combine signed gradient with zeroth-order optimization to reduce memory cost in LLM training. SignSGD has also received great attention due to its close relationship with Adam ([Balles and Hennig, 2018](#)). Numerous efforts have been made to theoretically justify the success of Adam through the lens of SignSGD ([Crawshaw et al., 2022](#); [Kunstner et al., 2023](#); [Peng et al., 2025](#)), and of course, study the effectiveness of SignSGD itself ([Balles et al., 2020](#); [Li et al., 2025a](#); [Monzio Compagnoni et al., 2025](#); [Kunstner and Bach, 2025](#)). Another important breakthrough is the Lion optimizer, proposed by [Chen et al. \(2023a\)](#) via symbolic search. By incorporating two momentum buffers, it achieves significant empirical success ([Zhao et al., 2025](#)). Likewise, there exists a rich body of literature that tries to explain its effectiveness ([Chen et al., 2024](#); [Elistratov et al., 2024](#); [Dong et al., 2024](#); [Jiang and Zhang, 2025](#); [Sfyraki and Wang, 2025](#)).

Sign-based methods: matrix optimizers The Muon algorithm is introduced by [Jordan et al. \(2024\)](#), which can be regarded as matrix sign descent. The matrix sign operation $\text{msign}(\cdot)$ is implemented via Newton–Schulz iteration ([Kovarik, 1970](#); [Björck and Bowie, 1971](#)). Built upon [Jordan et al. \(2024\)](#), [Liu et al. \(2025a\)](#) incorporates Nesterov momentum and learning rate alignment techniques into the original version of Muon. The modified algorithm Muonlight, has been applied to train massive-scale LLMs ([Liu et al., 2025a](#); [Zeng et al., 2025](#); [Team et al., 2025, 2026](#)) and exhibits clear performance gains over AdamW ([Wen et al., 2025](#); [Semenov et al., 2025](#); [Shah et al., 2025](#); [Ahn et al., 2025b,a](#)). Many works have tried to theoretically analyze Muon (or its modified versions), or empirically explain its practical efficiency ([Li and Hong, 2025](#); [Shen et al., 2025](#); [Chang et al., 2025](#); [Si et al., 2025](#); [Sfyraki and Wang, 2025](#); [Chen et al., 2025](#); [Huang et al., 2025](#); [Li et al., 2025c](#); [Qian et al., 2025](#); [Tveit et al., 2025](#); [Page et al., 2025](#); [Mehta et al., 2025](#); [Frans et al., 2025](#); [Pan et al., 2025](#); [Wang et al., 2025](#); [Zhang and Gao, 2025](#); [Zhang et al., 2025a](#); [Su, 2025](#); [Crawshaw et al., 2025](#); [Ma et al., 2026](#)).

How to handle heavy-tailed stochasticity? It is well-known that incorporating clipping or normalization into the vanilla SGD provably helps to tackle heavy-tailed noise ([Zhang et al., 2020c](#); [Cutkosky and Mehta, 2021](#); [Liu and Zhou, 2025](#); [Hübler et al., 2025](#); [Sun et al., 2025](#)). [Chezhegov et al. \(2025\)](#) recently prove that Adam and AdaGrad might converge poorly in high probability with the presence of heavy-tailed gradient noise, while their clipped versions effectively fix this issue. Another important line of work focuses on vanilla versions of classic algorithms. [Liu \(2026b\)](#) study SGD ([Zinkevich, 2003](#)), Dual Averaging ([Nesterov, 2009](#)), and AdaGrad ([Duchi et al., 2011](#)) from the perspective of online convex optimization. They show that these algorithms can converge optimally under heavy-tailedness. [Fatkhullin et al. \(2025\)](#) independently derive the same conclusion for SGD. However, a distinct difference between [Fatkhullin et al. \(2025\)](#); [Liu \(2026b\)](#) and our work is that they assume the stochastic gradient itself has p th moment, while we make the assumption on the gradient noise. The former is strictly stronger than the latter², and thus, should be generally regarded as a vertical line of work.

3. Vector Sign Optimizer: SignSGD and Lion

In this section, we first introduce some notations and assumptions, and then present the convergence guarantee. Proofs of the main theorems are deferred to Appendix C.

3.1. Notations and Assumptions

We write $[T]$ for $\{1, 2, \dots, T\}$, $|\mathbf{x}|$ for element-wise absolute value of $\mathbf{x} \in \mathbb{R}^d$, \odot for element-wise product between two vectors. The \mathbf{l} -weighted vector norm for $\mathbf{l} \in \mathbb{R}_+^d$ is defined as $\|\mathbf{x}\|_{\mathbf{l}}^2 := \mathbf{x}^\top \text{diag}(\mathbf{l}) \mathbf{x}$. For vector descent methods, we study the optimization problem $\min_{\mathbf{x} \in \mathbb{R}^d} f(\mathbf{x})$, where $f : \mathbb{R}^d \mapsto \mathbb{R}$ is differentiable. Given a point $\mathbf{x} \in \mathbb{R}^d$, we can only access the gradient $\nabla f(\mathbf{x}) = [\nabla_1 f(\mathbf{x}), \dots, \nabla_d f(\mathbf{x})] \in \mathbb{R}^d$ in a noisy manner, as later specified in Assumption 3a. Below, we list some necessary assumptions.

Assumption 1a (Lower bounded objective) *The objective function f is possibly non-convex, and bounded from below: $f^* := \inf_{\mathbf{x} \in \mathbb{R}^d} f(\mathbf{x}) > -\infty$.*

2. It is also well-known that if the assumption is exerted on the gradient itself, then it would be more natural to consider non-smooth optimization.

Assumption 2a (($\mathbf{l}_0, \mathbf{l}_1$)-vector smoothness) *There exists non-negative vectors $\mathbf{l}_0 = [\mathbf{l}_{0,1}, \dots, \mathbf{l}_{0,d}] \in \mathbb{R}_+^d$ and $\mathbf{l}_1 = [\mathbf{l}_{1,1}, \dots, \mathbf{l}_{1,d}] \in \mathbb{R}_+^d$ such that for all $\|\mathbf{x}' - \mathbf{x}\|_\infty \leq 1/\|\mathbf{l}_1\|_\infty$, it holds that*

$$|f(\mathbf{x}') - (f(\mathbf{x}) + \langle \nabla f(\mathbf{x}), \mathbf{x}' - \mathbf{x} \rangle)| \leq \frac{1}{2} \|\mathbf{x}' - \mathbf{x}\|_{\mathbf{l}_0 + \mathbf{l}_1 \odot |\nabla f(\mathbf{x})|}^2. \quad (1)$$

Assumption 1a is standard and necessary for stochastic non-convex optimization (Arjevani et al., 2023). Assumption 2a is new, which characterizes a class of generalized smooth functions originally proposed in Zhang et al. (2020b). Note that when $\mathbf{l}_1 = \mathbf{0}$, Assumption 2a degenerates to the *coordinate-wise smoothness* condition widely employed in the pioneering works of SignSGD (Bernstein et al., 2018, 2019; Safaryan and Richtárik, 2021), which naturally aligns with sign descent methods due to their coordinate-wise nature (Balles and Hennig, 2018; Balles et al., 2020). When $\mathbf{l}_1 \succ \mathbf{0}$, Assumption 2a can be viewed as an extension of the *coordinate-wise smoothness* assumption, which aligns closely with practice (Crawshaw et al., 2022; Liu et al., 2025c). In general, Assumption 2a is not only weaker than previous assumptions, but also a better fit for sign gradient descent. Detailed discussions are postponed to Appendix B.1.

Assumption 3a (Unbiasedness) *At step t we observe a mini-batch of mutually independent gradients $G_t = \{\mathbf{g}_t^1, \dots, \mathbf{g}_t^B\}$ satisfying $\mathbb{E}[\mathbf{g}_t^b | \mathcal{F}_{t-1}] = \nabla f(\mathbf{x}_t)$, $\forall b \in [B]$ where $\mathcal{F}_t = \sigma(G_1, \dots, G_t)$ denotes the natural filtration.*

Assumption 4a (($\boldsymbol{\sigma}_0, \boldsymbol{\sigma}_1$)-vector heavy-tailed noise) *There exists $p \in (1, 2]$, $\boldsymbol{\sigma}_0 = [\boldsymbol{\sigma}_{0,1}, \dots, \boldsymbol{\sigma}_{0,d}] \in \mathbb{R}_+^d$ and $\boldsymbol{\sigma}_1 = [\boldsymbol{\sigma}_{1,1}, \dots, \boldsymbol{\sigma}_{1,d}] \in \mathbb{R}_+^d$ such that*

$$\mathbb{E} \left[\left| \mathbf{g}_{t,i}^b - \nabla_i f(\mathbf{x}_t) \right|^p \middle| \mathcal{F}_{t-1} \right] \leq \boldsymbol{\sigma}_{0,i}^p + \boldsymbol{\sigma}_{1,i}^p |\nabla_i f(\mathbf{x}_t)|^p, \quad \forall i \in [d], \forall b \in [B].$$

Assumption 4a is new, which generalizes the classic *coordinate-wise* heavy-tailed noise assumption (Kornilov et al., 2025, Assumption 3) where $\boldsymbol{\sigma}_1 = \mathbf{0}$. Assumption 4a is meaningful in two aspects. Theoretically, we demonstrate that the class heavy-tailed noise model ($\boldsymbol{\sigma}_1 = \mathbf{0}$) might fail even on linear regression tasks (see Appendix B.3). Empirically, we draw significant evidence from LLM pretraining to illustrate that Assumption 4a aligns well with practice (see Section 6).

3.2. Convergence Theory for SignSGD

We formally introduce the SignSGD optimizer (Bernstein et al., 2018) in Algorithm 1.³ At step t , Algorithm 1 maintains the momentum buffer \mathbf{m}_t using the batched stochastic gradient \mathbf{g}_t . Then, the sign of the momentum \mathbf{m}_t is utilized to update the current model \mathbf{x}_t . Below, we present the convergence guarantee of Algorithm 1, showcasing that SignSGD remains effective under heavy-tailed gradient noise.

Theorem 1 *Under Assumptions 1a to 4a, define $\Delta_f := f(\mathbf{x}_1) - f^*$. By setting*

$$\begin{aligned} B &= \max \left\{ 1, \left\lceil \left(32\sqrt{2} \|\boldsymbol{\sigma}_1\|_\infty \right)^{\frac{p}{p-1}} \right\rceil \right\}, \quad \beta = \max \left\{ 0, 1 - B^{\frac{2p-2}{3p-2}} \left(\frac{\Delta_f \|\mathbf{l}_0\|_1}{\|\boldsymbol{\sigma}_0\|_1^2 T} \right)^{\frac{p}{3p-2}} \right\}, \\ \eta &= \min \left\{ \sqrt{\frac{2\Delta_f(1-\beta)}{9 \|\mathbf{l}_0\|_1 T}}, \frac{1-\beta}{32 \|\mathbf{l}_1\|_\infty} \right\}, \end{aligned} \quad (2)$$

3. Algorithm 1 is referred to as Signum, signSGD-SIM, or SMM in previous work (Bernstein et al., 2018; Sun et al., 2023; Jiang et al., 2025b). For simplicity, we keep the name SignSGD hereafter.

Algorithm 1 SignSGD (Bernstein et al., 2018)

```

1: Input:  $T \in \mathbb{N}$ ,  $\mathbf{x}_1 \in \mathbb{R}^d$ ,  $\eta \in \mathbb{R}_+$ 
2: for  $t = 1$  to  $T$  do
3:    $\mathbf{g}_t = \frac{1}{B} \sum_{b=1}^B \mathbf{g}_t^b$ 
4:    $\mathbf{m}_t = \beta \mathbf{m}_{t-1} + (1 - \beta) \mathbf{g}_t$  { $\mathbf{m}_0 := \mathbf{g}_1$ }
5:    $\mathbf{x}_{t+1} = \mathbf{x}_t - \eta \text{sign}(\mathbf{m}_t)$ 
6: end for

```

Algorithm 1 ensures

$$\frac{1}{T} \sum_{t=1}^T \mathbb{E} [\|\nabla f(\mathbf{x}_t)\|_1] \leq O \left((\Delta_f \|\mathbf{l}_0\|_1)^{\frac{p-1}{3p-2}} \|\boldsymbol{\sigma}_0\|_1^{\frac{p}{3p-2}} (BT)^{-\frac{p-1}{3p-2}} \right).$$

The convergence rate in Theorem 1 implies a complexity of $O(\epsilon^{-\frac{3p-2}{p-1}})$ to reach an ϵ -stationary point, i.e., $\mathbb{E} [\|\nabla f(\mathbf{x})\|_1] \leq \epsilon$. Since $\|\nabla f(\mathbf{x})\|_1 \geq \|\nabla f(\mathbf{x})\|_2$, this complexity matches the ℓ_2 -norm lower bound in Liu and Zhou (2025, Theorem 3.3) and also recovers the well-known $O(\epsilon^{-4})$ lower bound (Arjevani et al., 2023) when $p = 2$. Unlike previous works (Jiang et al., 2025b; Kornilov et al., 2025), our result does not depend on dimension d explicitly and holds under any $\mathbf{l}_1 \geq \mathbf{0}$, $\boldsymbol{\sigma}_1 \geq \mathbf{0}$ and $p \in (1, 2]$, suggesting that our theory may capture a wider range of objectives. Compared to the well-known gradient normalization or gradient clipping techniques which effectively cope with heavy-tailed noise (Liu and Zhou, 2025; Hübner et al., 2025), our results reveal that the sign operator not only remains robust to heavy-tailed stochasticity but also has an advantage over gradient normalization. Due to space limitations, the comprehensive illustrations can be found in Appendix A.

Remark 1 When $\boldsymbol{\sigma}_1 = \mathbf{0}$, Kornilov et al. (2025) analyze Algorithm 1 and derive a complexity of $O(\Delta_f l_0 d^{\frac{3p-2}{2(p-1)}} \|\boldsymbol{\sigma}_0\|_p^{\frac{p}{p-1}} \epsilon^{-\frac{3p-2}{p-1}})$ under the classic l_0 -smoothness. Compare their result to ours:

$$\text{Kornilov et al. (2025)} : O \left(\frac{\Delta_f \|\mathbf{l}_0\|_1 \|\boldsymbol{\sigma}_0\|_1^{\frac{p}{p-1}} d^{\frac{3p-2}{2(p-1)}}}{\epsilon^{\frac{3p-2}{p-1}} \phi_l \phi_\sigma^{\frac{p}{p-1}}} \right) \text{ vs Ours} : O \left(\frac{\Delta_f \|\mathbf{l}_0\|_1 \|\boldsymbol{\sigma}_0\|_1^{\frac{p}{p-1}}}{\epsilon^{\frac{3p-2}{p-1}}} \right),$$

where $\phi_l := \|\mathbf{l}_0\|_1 / l_0 \in [1, d]$ and $\phi_\sigma := \|\boldsymbol{\sigma}_0\|_1 / \|\boldsymbol{\sigma}_0\|_p \in [1, d^{1-\frac{1}{p}}]$ are two quantities reflecting the problem geometry. When the curvature vector \mathbf{l}_0 is sparse and exhibits axis-alignment phenomenon (Balles et al., 2020), ϕ_l becomes close to 1. If $\boldsymbol{\sigma}_0$ is also sparse (Yuan and Ghanem, 2017; Wu et al., 2020a), then it holds $\phi_\sigma = O(1)$. In this case, Theorem 1 achieves a remarkable complexity improvement of $d^{\frac{3p-2}{2(p-1)}}$. On the other hand, taking the maximum over ϕ_l, ϕ_σ gives the best case complexity of Kornilov et al. (2025), which still suffers from an extra $d^{\frac{2-p}{2(p-1)}}$ factor compared to ours.

3.3. Convergence Theory for Lion

The Lion optimizer is discovered by Chen et al. (2023a) through program search. On top of SignSGD, it incorporates (i) different β values to track the exponential moving average of past

gradients $\{\mathbf{g}_t\}_{t \in [T]}$ thus decoupling the state between stored momentum \mathbf{m}_t and the update momentum \mathbf{v}_t , and (ii) decoupled weight decay into the final update. The whole procedure is summarized in Algorithm 2. The following theorem prescribes the convergence rate of Lion.

Theorem 2 *Under Assumptions 1a to 4a, define $\Delta_f := f(\mathbf{x}_1) - f^*$. Set*

$$B = \max \left\{ 1, \left\lceil \left(72\sqrt{2} \|\boldsymbol{\sigma}_1\|_\infty \right)^{\frac{p}{p-1}} \right\rceil \right\}, \quad \beta_2 = \max \left\{ 0, 1 - B^{\frac{2p-2}{3p-2}} \left(\frac{\Delta_f \|\mathbf{l}_0\|_1}{\|\boldsymbol{\sigma}_0\|_1^2 T} \right)^{\frac{p}{3p-2}} \right\}, \quad (3)$$

$$\eta = \min \left\{ \sqrt{\frac{8\Delta_f(1-\beta_2)}{33\|\mathbf{l}_0\|_1 T}}, \frac{1-\beta_2}{120\|\mathbf{l}_1\|_\infty} \right\}, \quad \beta_1 \in \left[1 - (1-\beta_2)^{\frac{p-1}{p}}, 1 \right], \quad \lambda \in \left[0, \frac{1-2^{-\frac{1}{T}}}{\eta} \right].$$

If $\|\mathbf{x}_1\|_\infty \leq 1/(3\lambda)$, then Algorithm 2 ensures $\|\mathbf{x}_t\|_\infty \leq 2/(3\lambda)$, $\forall t \in [T]$, and

$$\frac{1}{T} \sum_{t=1}^T \mathbb{E} [\|\nabla f(\mathbf{x}_t)\|_1] \leq O \left((\Delta_f \|\mathbf{l}_0\|_1)^{\frac{p-1}{3p-2}} \|\boldsymbol{\sigma}_0\|_1^{\frac{p}{3p-2}} (BT)^{-\frac{p-1}{3p-2}} \right).$$

The above convergence rate matches that of Theorem 1, since Lion reduces to SignSGD when $\beta_1 = \beta_2$. As far as we know, Theorem 2 is the first rigorous theoretical guarantee for Lion under heavy-tailed noise. The implied $O(\epsilon^{-\frac{3p-2}{p-1}})$ complexity, as aforementioned SignSGD, is also optimal.

Remark 2 *In the special case of $\mathbf{l}_1 = \boldsymbol{\sigma}_1 = \mathbf{0}$ and $p = 2$ (finite-variance regime), Jiang and Zhang (2025) establish a convergence rate of $O(\sqrt{d}T^{-1/4})$ for Lion, which our result strictly improves upon. Firstly, our result removes the explicit dimensional dependence. Secondly, we relax their $\beta_1 \in [1 - \sqrt{1 - \beta_2}, 1 - (1 - \beta_2)^2]$ requirement as shown in (3). Thirdly, by a finer analysis of the weight decay dynamics in Lemma C.8, we relax their $\lambda \leq 1/(2\eta T)$ requirement to the milder $\lambda \leq (1 - 2^{-1/T})/\eta$. Lastly, our initialization condition $\|\mathbf{x}_1\|_\infty \leq 1/(3\lambda)$ is more general than their $\|\mathbf{x}_1\|_\infty \leq \eta$, as a large λ ($\sim 10^{-1}$) and a small η ($\sim 10^{-5}$) is typically chosen for Lion (Wen et al., 2025). Furthermore, we establish a uniform constant bound on the iterate trajectory $\|\mathbf{x}_t\|_\infty \leq 2/(3\lambda)$, which is significantly tighter than the $\|\mathbf{x}_t\|_\infty \leq \eta t$ bound in Jiang and Zhang (2025) that grows over time. Our result also aligns with the bounded constraints identified for Lion- \mathcal{K} dynamics in Chen et al. (2024).*

4. Matrix Sign Optimizer: Muon and Muonlight

The organization of this section follows from Section 3. Proofs can be found at Appendix D.

4.1. Notations and Assumptions

We denote the set of $m \times m$ positive semi-definite (PSD) matrices by \mathbb{S}^m . For any $\mathbf{X} \in \mathbb{R}^{m \times n}$, its modulus (or absolute value) is defined as $|\mathbf{X}|_m := (\mathbf{X}\mathbf{X}^\top)^{1/2} \in \mathbb{S}^n$. The matrix sign operator is defined as $\text{msign}(\mathbf{X}) := \mathbf{U}\mathbf{V}^\top$, where $\mathbf{X} = \mathbf{U}\boldsymbol{\Sigma}\mathbf{V}^\top$ is the singular value decomposition (SVD) of $\mathbf{X} \in \mathbb{R}^{m \times n}$. The inner product between matrices $\mathbf{X}, \mathbf{Y} \in \mathbb{R}^{m \times n}$ is denoted by $\langle \mathbf{Y}, \mathbf{X} \rangle := \text{tr}(\mathbf{Y}^\top \mathbf{X})$. We let $\|\cdot\|_{\text{op}}$, $\|\cdot\|_*$, and $\|\cdot\|_{\text{F}}$ denote the matrix operator norm, nuclear norm, and Frobenius norm, respectively. Finally, for any $\mathbf{L} \in \mathbb{S}^n$, the \mathbf{L} -weighted matrix norm is defined as $\|\mathbf{X}\|_{\mathbf{L}}^2 := \text{tr}(\mathbf{X}^\top \mathbf{L} \mathbf{X})$. For Muon and Muonlight, we consider the matrix optimization problem $\min_{\mathbf{X} \in \mathbb{R}^{m \times n}} f(\mathbf{X})$ and list some necessary assumptions in the sequel.

Assumption 1b (Lower bounded objective) *The objective function f is possibly non-convex, and bounded from below: $f^* := \inf_{\mathbf{X} \in \mathbb{R}^{m \times n}} f(\mathbf{X}) > -\infty$.*

Assumption 2b (($\mathbf{L}_0, \mathbf{L}_1$)-matrix smoothness) *There exists matrices $\mathbf{L}_0, \mathbf{L}_1 \in \mathbb{R}^{m \times n}$ such that for all $\|\mathbf{X}' - \mathbf{X}\|_{\text{op}} \leq 1/\|\mathbf{L}_1\|_{\text{op}}$, it holds that*

$$\|\nabla f(\mathbf{X}') - \nabla f(\mathbf{X})\|_{(\mathbf{L}(\mathbf{X}))^{-1}} \leq \|\mathbf{X}' - \mathbf{X}\|_{\mathbf{L}(\mathbf{X})}, \text{ where } \mathbf{L}(\mathbf{X}) = |\mathbf{L}_0|_m + \left| \nabla f(\mathbf{X}) \mathbf{L}_1^\top \right|_m.$$

Assumption 2b serves as the matrix-based counterpart to Assumption 2a and represents, to the best of our knowledge, the first formulation of a matrix generalized smoothness model. In the case where $n = 1$, Assumption 2b recovers the vector generalized smoothness condition introduced in Assumption 2a. Furthermore, when $\mathbf{L}_1 = \mathbf{0}$, this framework encompasses classical matrix L -smoothness, as defined in [An et al. \(2025, Assumption 2\)](#) and [Kovalev and Borodich \(2025, Assumption 1\)](#). As pointed out by [An et al. \(2025\)](#), this formulation effectively models the block-diagonal Hessian structure of transformer-based modern neural networks ([Zhang et al., 2024, 2025b](#)).

Assumption 3b (Unbiasedness) *At step t we observe a mini-batch of mutually independent gradients $\mathbf{G}_t = \{\mathbf{G}_t^1, \dots, \mathbf{G}_t^B\}$ satisfying $\mathbb{E}[\mathbf{G}_t^b | \mathcal{F}_{t-1}] = \nabla f(\mathbf{X}_t), \forall b \in [B]$ where $\mathcal{F}_t = \sigma(G_1, \dots, G_t)$ denotes the natural filtration.*

Assumption 4b (($\mathbf{V}_0, \mathbf{V}_1$)-matrix heavy-tailed noise) *There exists $p \in (1, 2]$, $\mathbf{V}_0, \mathbf{V}_1 \in \mathbb{R}^{m \times n}$ such that*

$$\mathbb{E} \left[\|\mathbf{V}_0\|_*^{p/2} \cdot \left\| \mathbf{G}_t^b - \nabla f(\mathbf{X}_t) \right\|_{|\mathbf{V}_0|_m^{-1}}^p \middle| \mathcal{F}_{t-1} \right] \leq \|\mathbf{V}_0\|_*^p + |\langle \mathbf{V}_1, \nabla f(\mathbf{X}_t) \rangle|^p, \quad \forall b \in [B].$$

Assumption 4b introduces our newly proposed matrix-based generalized heavy-tailed noise model, which generalizes canonical assumptions in several key dimensions (see [Appendix B.4](#) for details). First, when $\mathbf{V}_1 = \mathbf{0}$ and $p = 2$, our condition recovers the adaptive variance assumption $\mathbb{E} \left[\left\| \mathbf{G}_t^b - \nabla f(\mathbf{X}_t) \right\|_{|\mathbf{V}_0|_m^{-1}}^2 \middle| \mathcal{F}_{t-1} \right] \leq \|\mathbf{V}_0\|_*$ in [Kovalev \(2025, Assumption 3\)](#), [Kovalev and Borodich \(2025, Assumption 2\)](#), and [Xie et al. \(2025b, Definition 4.1\)](#). Similar to coordinate-wise bounds in vector settings ([Bernstein et al., 2018; Liu et al., 2025c](#)), this formulation and its variants in [An et al. \(2025, Assumption 3\)](#) and [Pan et al. \(2025, Assumption 3\)](#) better capture the structural properties of the noise matrix. Second, by extending the tail-index to $p \in (1, 2]$, we provide a natural characterization of the heavy-tailed regime. Finally, Assumption 4b allows the p th moment of the noise to grow with the gradient, extending recent vector-based models ([Liu and Zhou, 2025, Assumption 2.4](#)) to matrix optimization—a property we empirically validate in [Section 6](#).

4.2. Convergence Theory for Muon

Muon ([Jordan et al., 2024](#)) ([Algorithm 3](#)) has recently emerged as a powerful optimizer for the hidden layers of large-scale neural networks, utilizing the principle of orthogonalized momentum. [Algorithm 3](#) first tracks a momentum estimate \mathbf{B}_t and subsequently employs the Newton–Schulz iteration ([Kovarik, 1970; Björck and Bowie, 1971](#)) to compute the matrix sign, $\text{msign}(\mathbf{B}_t)$, which is further utilized to update the parameter matrix \mathbf{X}_t . Following common practice ([Li and Hong, 2025; Shen et al., 2025; Sato et al., 2025; Chang et al., 2025; Pan et al., 2025](#)), we assume zero numerical error in Newton–Schulz algorithm, i.e., $\text{NewtonSchulz}(\mathbf{X}) = \text{msign}(\mathbf{X}) = \mathbf{U}\mathbf{V}^\top$

Algorithm 3 Muon (Jordan et al., 2024)

```

1: Input:  $T \in \mathbb{N}$ ,  $\mathbf{X}_1 \in \mathbb{R}^{m \times n}$ ,  $\eta \in \mathbb{R}_+$ 
2: for  $t = 1$  to  $T$  do
3:    $\mathbf{G}_t = \frac{1}{B} \sum_{b=1}^B \mathbf{G}_t^b$ 
4:    $\mathbf{B}_t = \beta \mathbf{B}_{t-1} + \mathbf{G}_t$             $\{\mathbf{B}_0 := \mathbf{0}\}$ 
5:    $\mathbf{O}_t = \text{NewtonSchulz}(\mathbf{B}_t)$ 
6:    $\mathbf{X}_{t+1} = \mathbf{X}_t - \eta \mathbf{O}_t$ 
7: end for

```

Algorithm 4 Muonlight (Liu et al., 2025a)

```

1: Input:  $T \in \mathbb{N}$ ,  $\mathbf{X}_1 \in \mathbb{R}^{m \times n}$ ,  $\eta, \lambda \in \mathbb{R}_+$ 
2: for  $t = 1$  to  $T$  do
3:    $\mathbf{G}_t = \frac{1}{B} \sum_{b=1}^B \mathbf{G}_t^b$ 
4:    $\mathbf{B}_t = \beta_2 \mathbf{B}_{t-1} + \mathbf{G}_t$             $\{\mathbf{B}_0 := \mathbf{0}\}$ 
5:    $\tilde{\mathbf{B}}_t = \beta_1 \mathbf{B}_t + \mathbf{G}_t$ 
6:    $\mathbf{O}_t = \text{NewtonSchulz}(\tilde{\mathbf{B}}_t)$ 
7:    $\mathbf{X}_{t+1} = \mathbf{X}_t - \eta \mathbf{O}_t - \eta \lambda \mathbf{X}_t$ 
8: end for

```

with $\mathbf{X} = \mathbf{U}\Sigma\mathbf{V}^\top$ as the SVD of $\mathbf{X} \in \mathbb{R}^{m \times n}$. We remark that it is introduced for simplicity rather than necessity, with details deferred to Appendix B.5. In the following theorem, we establish the first convergence guarantee for Muon under our generalized heavy-tailed noise framework and matrix-based generalized smoothness conditions.

Theorem 3 *Under Assumptions 1b to 4b, define $\Delta_f := f(\mathbf{X}_1) - f^*$. By setting*

$$B = \max \left\{ 1, \left\lceil \left(32\sqrt{2} \|\mathbf{V}_1\|_{\text{op}} \right)^{\frac{p}{p-1}} \right\rceil \right\}, \quad \beta = \max \left\{ 0, 1 - B^{\frac{2p-2}{3p-2}} \left(\frac{\Delta_f \|\mathbf{L}_0\|_*}{\|\mathbf{V}_0\|_*^2 T} \right)^{\frac{p}{3p-2}} \right\}, \quad (4)$$

$$\eta = \min \left\{ \sqrt{\frac{2\Delta_f(1-\beta)}{5 \|\mathbf{L}_0\|_* T}}, \frac{1-\beta}{16 \|\mathbf{L}_1\|_{\text{op}}} \right\},$$

Algorithm 3 ensures

$$\frac{1}{T} \sum_{t=1}^T \mathbb{E} [\|\nabla f(\mathbf{X}_t)\|_*] \leq O \left((\Delta_f \|\mathbf{L}_0\|_*)^{\frac{p-1}{3p-2}} \|\mathbf{V}_0\|_*^{\frac{p}{3p-2}} (BT)^{-\frac{p-1}{3p-2}} \right).$$

Notably, the convergence rate in Theorem 3 is free of the explicit dimensional dependence, representing a significant advancement over the existing literature on Muon (Li and Hong, 2025; Shen et al., 2025; Chang et al., 2025; Huang et al., 2025). While prior works are restricted to the simpler finite-variance setting ($p = 2$, $\mathbf{L}_1 = \mathbf{V}_1 = \mathbf{0}$), they still suffer from an explicit dependence on the matrix dimensions through the term $\sqrt{\min\{m, n\} \|\mathbf{V}_0\|_{\text{F}}}$. In contrast, our results not only provide the first convergence guarantee for the general heavy-tailed regime ($p \in (1, 2)$) but also yield a sharper bound in the $p = 2$ case, as the nuclear norm $\|\mathbf{V}_0\|_*$ is significantly smaller than the *dimension-dependent* factors in previous bounds. This improvement underscores the strength of our refined noise model in Assumption 4b, which more effectively captures the structural noise properties inherent to matrix optimization.

Remark 3 *Sfyraki and Wang (2025) recently established a suboptimal $O(T^{-\frac{p-1}{3p-2}} \log T)$ convergence rate for clipped versions of Lion and Muon under heavy-tailed noise. Their analysis exhibits several limitations compared to our work: (i) their assumptions and convergence criteria rely on Euclidean norms ($\|\cdot\|_2, \|\cdot\|_{\text{F}}$), which fail to capture the intrinsic geometry of sign-based methods, particularly from their Frank-Wolfe perspective; (ii) they require an additional bounded gradient assumption ($\|\nabla f(\mathbf{X})\|_{\text{F}} \leq G$) and still incur extraneous logarithmic factors; and (iii) their theory is restricted to settings with a strictly positive weight decay parameter ($\lambda > 0$) and provides no guarantees for the standard algorithms without clipping.*

4.3. Convergence Theory for Muonlight

Proposed by Liu et al. (2025a), Muonlight has achieved remarkable success in large-scale LLM pretraining, as evidenced by the Muonlight-16B-A3B, Kimi-K2, GLM-4.5 models. It introduces two primary modifications to the original Muon algorithm⁴: (i) the integration of Nesterov momentum and (ii) the addition of decoupled weight decay. The former is a standard technique in modern optimization (Dozat, 2016; Xie et al., 2024)—already a key feature in the popular PyTorch implementation of Adam (Paszke et al., 2019)—whose effectiveness is often attributed to implicit variance reduction (Wen et al., 2025; Yuan et al., 2025; Liu et al., 2025b). The latter, decoupled weight decay, has proven essential for stabilizing the training trajectories of large foundation models (Team et al., 2025). The complete procedure is detailed in Algorithm 4. Notably, while original implementations often restrict Nesterov momentum to $\beta_1 = \beta_2$, our framework supports a general (β_1, β_2) configuration. We present the theoretical analysis of Muonlight below.

Theorem 4 *Under Assumptions 1b to 4b, define $\Delta_f := f(\mathbf{X}_1) - f^*$. Set*

$$B = \max \left\{ 1, \left\lceil \left(2979 \|\mathbf{V}_1\|_{\text{op}} \right)^{\frac{p}{p-1}} \right\rceil \right\}, \quad \beta_2 = \max \left\{ 0, 1 - B^{\frac{2p-2}{3p-2}} \left(\frac{\Delta_f \|\mathbf{L}_0\|_*}{\|\mathbf{V}_0\|_*^2 T} \right)^{\frac{p}{3p-2}} \right\},$$

$$\eta = \min \left\{ \sqrt{\frac{4\Delta_f(1-\beta_2)}{15 \|\mathbf{L}_0\|_* T}}, \frac{3(1-\beta_2)}{625 \|\mathbf{L}_1\|_{\text{op}}} \right\}, \quad \beta_1 \in \left[\max \left\{ 0, \beta_2 - \frac{3}{20} \right\}, \min \left\{ 1, \beta_2 + \frac{3}{20} \right\} \right], \quad (5)$$

and $\lambda \in \left[0, \left(1 - 2^{-\frac{1}{T}} \right) / \eta \right]$. If $\|\mathbf{X}_1\|_{\text{op}} \leq 1/(3\lambda)$, then Algorithm 4 ensures $\|\mathbf{X}_t\|_{\text{op}} \leq 2/(3\lambda)$, $\forall t \in [T]$, and

$$\frac{1}{T} \sum_{t=1}^T \mathbb{E} [\|\nabla f(\mathbf{X}_t)\|_*] \leq O \left((\Delta_f \|\mathbf{L}_0\|_*)^{\frac{p-1}{3p-2}} \|\mathbf{V}_0\|_*^{\frac{p}{3p-2}} (BT)^{-\frac{p-1}{3p-2}} \right).$$

Several remarks are in order: (i) Muonlight achieves the same convergence bounds as Muon under generalized heavy-tailed noise. (ii) Our result provides the first analysis for $p \in (1, 2)$ and improves upon previous *dimension-dependent* rates for the $p = 2, \mathbf{L}_1 = \mathbf{V}_1 = \mathbf{0}$ case (Sato et al., 2025; Chang et al., 2025). (iii) We establish a uniform trajectory bound $\|\mathbf{X}_t\|_{\text{op}} \leq 2/(3\lambda)$, mirroring the stability of Lion in Theorem 2. (iv) The theory supports a broad range for the Nesterov momentum β_1 , reinforcing the empirical flexibility and practicality of the algorithm.

5. How Sign Operator Works

In this section, we elucidate why the sign operator naturally accommodates heavy-tailed noise, while concurrently presenting our proof sketch and novel analysis techniques. To clearly illustrate the core intuition, we restrict our focus to the simplified setting where $\mathbf{l}_1 = \mathbf{L}_1 = \mathbf{0}$, considering only SignSGD and Muon (Theorems 1 and 3). The core technical intuition is that the sign operator $\text{sign}(\cdot)$ acts as *coordinate-wise* normalization, inheriting the robust properties of gradient normalization under heavy-tailed noise, while shifting the optimization geometry from Euclidean to non-Euclidean space. For matrix sign $\text{msign}(\cdot)$, its effect mirrors the vector case by performing normalization on each singular value.

4. We omit their learning rate alignment with AdamW's update RMS-norm (Kosson et al., 2024) for simplicity, as this implementation detail does not alter our theoretical analysis.

5.1. Signed Gradient As Non-Euclidean Normalized Gradient

We begin by reviewing how the normalized gradient method (Algorithm 5 in Appendix A) mitigates heavy-tailed noise. We invoke the following well-established lemma, attributed to [Cutkosky and Mehta \(2020\)](#); [Jin et al. \(2021\)](#); [Liu and Zhou \(2025\)](#); [Hübler et al. \(2025\)](#).

Lemma 1 *Under the conditions in Theorem 1, Algorithm 5 ensures that*

$$\begin{aligned} \frac{1}{T} \sum_{t=1}^T \mathbb{E} [\|\nabla f(\mathbf{x}_t)\|_2] &\stackrel{(a)}{\leq} \frac{\Delta_f}{\eta T} + \frac{\eta \|\mathbf{L}_0\|_\infty}{2} + \frac{2}{T} \sum_{t=1}^T \mathbb{E} [\|\boldsymbol{\epsilon}_t\|_2] \\ &\stackrel{(b)}{\leq} \frac{\Delta_f}{\eta T} + \frac{\eta \|\mathbf{L}_0\|_\infty}{2} + \frac{2}{T} \sum_{t=1}^T \mathbb{E} \left[\left\| \sum_{k=2}^t \beta^{t-k+1} \mathbf{s}_k \right\|_2 + \beta^{t-1} \|\mathbf{n}_1\|_2 + (1-\beta) \left\| \sum_{k=2}^T \beta^{t-k} \mathbf{n}_k \right\|_2 \right], \end{aligned}$$

where error term $\boldsymbol{\epsilon}_t$, noise term \mathbf{n}_t , and curvature term \mathbf{s}_t are defined in (11).

With Lemma 1, our goal is to bound the three terms in expectation. The first two term, namely the cumulative curvature term $\mathbb{E} [\left\| \sum_{k=2}^T \beta^{t-k+1} \mathbf{s}_k \right\|_2]$ and the initial noise $\mathbb{E} [\beta^{t-1} \|\mathbf{n}_1\|_2]$ admit straightforward upper bounds under Assumptions 2a and 4a. The crux of the analysis lies in controlling the cumulative noise $\mathbb{E} [\left\| \sum_{k=2}^T \beta^{t-k} \mathbf{n}_k \right\|_2]$. This term is bounded by applying Hölder's inequality followed by standard von Bahr-Esseen type concentration inequalities ([von Bahr and Esseen, 1965](#); [Kornilov et al., 2023](#); [Hübler et al., 2025](#)): $\mathbb{E} [\left\| \sum_{k=2}^T \beta^{t-k} \mathbf{n}_k \right\|_2] \leq \left(\mathbb{E} [\left\| \sum_{k=2}^T \beta^{t-k} \mathbf{n}_k \right\|_2^p] \right)^{\frac{1}{p}} \leq \left(2 \sum_{k=2}^T \mathbb{E} [\|\beta^{t-k} \mathbf{n}_k\|_2^p] \right)^{\frac{1}{p}}$. Invoking the heavy-tailed noise assumptions yields the optimal sublinear rate.

We now turn to sign-based gradient methods. The sign operator $\text{sign}(\mathbf{x})$ effectively performs *coordinate-wise* normalization, as it satisfies $\|\text{sign}(\mathbf{x})\|_\infty = 1$ and $\|\text{sign}(\mathbf{x})\|_1 = d$. Indeed, signed gradient and normalized gradient methods can be viewed as instances of normalized steepest descent with respect to the ℓ_∞ - and ℓ_2 -norms, respectively ([Bernstein and Newhouse, 2024](#); [Yadav et al., 2025](#)). This fundamental shift in algorithmic geometry is formalized in the following lemma, with the proof provided in Appendix C.3.

Lemma 2 *Under the same conditions and notations as in Lemma 1, Algorithm 1 ensures that*

$$\begin{aligned} \frac{1}{T} \sum_{t=1}^T \mathbb{E} [\|\nabla f(\mathbf{x}_t)\|_1] &\stackrel{(a)}{\leq} \frac{\Delta_f}{\eta T} + \frac{\eta \|\mathbf{L}_0\|_1}{2} + \frac{2}{T} \sum_{t=1}^T \mathbb{E} [\|\boldsymbol{\epsilon}_t\|_1] \\ &\stackrel{(b)}{\leq} \frac{\Delta_f}{\eta T} + \frac{\eta \|\mathbf{L}_0\|_1}{2} + \frac{2}{T} \sum_{t=1}^T \mathbb{E} \left[\left\| \sum_{k=2}^t \beta^{t-k+1} \mathbf{s}_k \right\|_1 + \beta^{t-1} \|\mathbf{n}_1\|_1 + (1-\beta) \left\| \sum_{k=2}^T \beta^{t-k} \mathbf{n}_k \right\|_1 \right]. \end{aligned}$$

Compared to Lemma 1, the primary distinction lies in the shift from the ℓ_2 -norm to the ℓ_1 -norm for both the convergence criterion $\|\nabla f(\mathbf{x}_t)\|$ and the error term $\|\boldsymbol{\epsilon}_t\|$ (along with the three decomposed components). Lemma 2 demonstrates that *the signed gradient operates as a non-Euclidean form of gradient normalization, fundamentally altering the problem's geometry and the corresponding analysis*. A more comprehensive discussion of these geometric implications is provided in Appendix A. Similar to standard gradient normalization, the principal analytical challenge for Algorithm 1 is bounding the cumulative noise in the ℓ_1 -norm, i.e., $\mathbb{E} [\left\| \sum_{k=2}^T \beta^{t-k} \mathbf{n}_k \right\|_1]$. However, since standard concentration inequalities are typically restricted to Euclidean norms, this necessitates the development of novel techniques to control this critical term.

5.2. New Martingale Concentration Inequalities

To address the major technical challenge identified in Section 5.1, we seek to bound the (discounted) sum of vector martingales in the ℓ_1 -norm, i.e., $\mathbb{E} \left[\left\| \sum_{k=2}^T \beta^{t-k} \mathbf{n}_k \right\|_1 \right]$. A close inspection of the von Bahr-Esseen inequality (e.g., Lemma 10 in Hübler et al. (2025)) reveals its inherent reliance on Euclidean geometry, rendering it ineffective for non-Euclidean norms like $\|\cdot\|_1$. Furthermore, the standard approach of applying Hölder's inequality complicates the analysis by introducing $\|\cdot\|_1^p$. This prompts a key question: *Can we bypass Hölder's inequality and derive a concentration inequality tailored specifically to the ℓ_1 -norm?*

We provide an affirmative answer by establishing a new vector martingale concentration inequality in Lemma 3, which bounds the ℓ_1 -norm of a vector martingale via its *coordinate-wise* variance. By applying Lemma 3 with $\mathbf{g}_k = \beta^{t-k} \mathbf{n}_k$, we recover the tractable term $\mathbb{E} [\beta^{p(t-k)} |\mathbf{n}_{k,i}|^p]$ (following (17) and (18)), which is directly controllable under Assumption 4a.

Lemma 3 (Concentration in ℓ_1 -norm) *Let $\{\mathbf{g}_t\}_{t=1}^T \subset \mathbb{R}^d$ be a vector martingale difference sequence such that $\mathbb{E} [\mathbf{g}_t | \mathcal{F}_{t-1}] = \mathbf{0}$, where $\mathcal{F}_t = \sigma(\mathbf{g}_1, \dots, \mathbf{g}_t)$ is the natural filtration. Then*

$$\mathbb{E} \left[\left\| \sum_{t=1}^T \mathbf{g}_t \right\|_1 \right] \leq 2\sqrt{2} \sum_{i=1}^d \mathbb{E} [\|\mathbf{g}_{1:T,i}\|_2] \leq 2\sqrt{2} \sum_{i=1}^d \mathbb{E} [\|\mathbf{g}_{1:T,i}\|_p], \quad \forall p \in [1, 2],$$

where $\mathbf{g}_{1:t,i} := [\mathbf{g}_{1,i}, \dots, \mathbf{g}_{t,i}] \in \mathbb{R}^t$.

Inspired by Rakhlin and Sridharan (2017); Liu and Zhou (2025), we delve deeply into the regret analysis of diagonal AdaGrad (McMahan and Streeter, 2010; Duchi et al., 2011) to prove this lemma (cf. Lemmas C.6 and C.7). This conceptual strategy—*concentrating vector martingales through the lens of regret analysis in online learning*—will be further leveraged in the matrix setting. Consider the matrix normalized gradient method (Algorithm 6) and Muon (Algorithm 3), where the effect of matrix orthogonalization $\text{msign}(\cdot)$ in Muon plays a role analogous to the vector sign operator $\text{sign}(\cdot)$ discussed in Section 5.1. Concretely, the norms highlighted in Lemmas 1 and 2 map directly to their matrix Schatten p -norm counterparts: $\|\cdot\|_2 \rightarrow \|\cdot\|_F$, $\|\cdot\|_1 \rightarrow \|\cdot\|_*$. Consequently, we face the similar challenge of bounding $\mathbb{E} \left[\left\| \sum_{k=2}^T \beta^{t-k} \mathbf{N}_k \right\|_* \right]$ ($\mathbf{N}_k = \mathbf{G}_k - \nabla f(\mathbf{X}_k)$), necessitating a novel matrix concentration inequality. To resolve this, we present the following lemma to bound $\left\| \sum_{t=1}^T \mathbf{G}_t \right\|_*$ by its covariance.

Lemma 4 (Concentration in nuclear norm, full version in Lemma D.7) *Let $\{\mathbf{G}_t\}_{t=1}^T \subset \mathbb{R}^{m \times n}$ be a matrix martingale difference sequence such that $\mathbb{E} [\mathbf{G}_t | \mathcal{F}_{t-1}] = \mathbf{0}$, where $\mathcal{F}_t = \sigma(\mathbf{G}_1, \dots, \mathbf{G}_t)$ is the natural filtration. Then, it holds that*

$$\mathbb{E} \left[\left\| \sum_{t=1}^T \mathbf{G}_t \right\|_* \right] \leq 2\sqrt{2} \mathbb{E} \left[\left\| \left(\sum_{t=1}^T \mathbf{G}_t \mathbf{G}_t^\top \right)^{1/2} \right\|_* \right].$$

Lemma 4 stands in sharp contrast to existing matrix concentration inequalities, which typically rely on $\|\cdot\|_F$, $\|\cdot\|_{\text{op}}$ or suffer from dimension-dependent factors (Nemirovski, 2007; So, 2011; Tropp et al., 2015). At first glance, this result appears elusive. To derive it, we seek to extend the regret-based concentration argument from Lemma 3 to the matrix setting. The most natural candidate for this extension is Shampoo (Gupta et al., 2018), which serves as the matrix counterpart to AdaGrad.

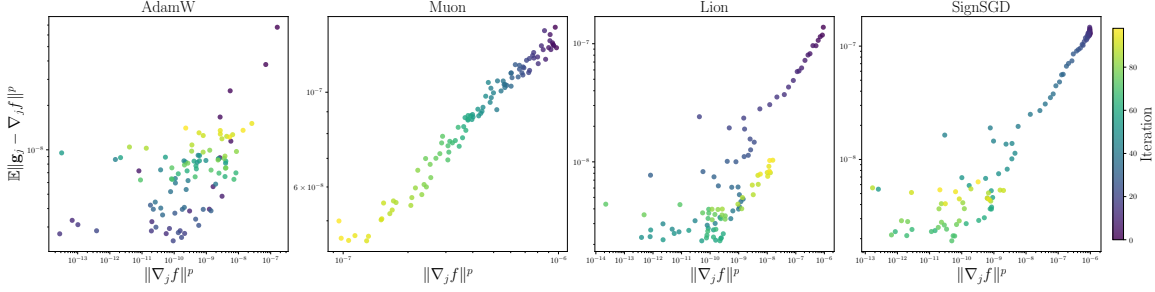


Figure 1: Verification of Assumption 4a. x-axis: $|\nabla_j f|^p$, y-axis: $\mathbb{E} [|\mathbf{g}_j - \nabla_j f|^p]$.

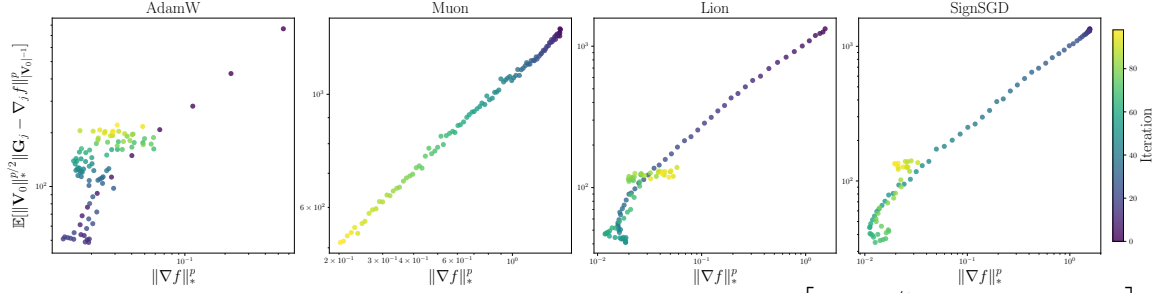


Figure 2: Verification of Assumption 4b. x-axis: $\|\nabla f\|_*^p$, y-axis: $\mathbb{E} \left[\|\mathbf{V}_0\|_*^{p/2} \|\mathbf{G} - \nabla f\|_{|\mathbf{V}_0|_m^{-1}}^p \right]$.

However, this direct path is blocked because the standard Shampoo regret bound incurs explicit dimension dependence. To overcome this barrier, we instead conduct a new regret analysis of *one-sided* Shampoo (An et al., 2025; Xie et al., 2025a). This critical pivot allows us to establish a desirable bound that, equipped with Lemma 4, enables the clean cancellation of terms (cf. (35)) necessary to handle the heavy-tailed noise.

6. Empirical Study

In this section, we provide empirical evidence to (i) demonstrate that our proposed noise models in Assumptions 4a and 4b accurately reflect the stochasticity in LLM training, and (ii) evaluate the efficacy of sign-based optimizers under these heavy-tailed regimes. Code is available at [Heavy-tailed-Noise-in-LLMs](#). Further details regarding hyperparameters and the complete experimental setup are available in Appendix E.

6.1. Validation of Heavy-Tailed Noise

We first verify the validity of our proposed noise assumptions in the LLM pretraining regimes. To this end, we train nanoGPT (Karpathy, 2022) on the C4 dataset (Raffel et al., 2020) using various optimizers and sample the stochastic gradient noise across different mini-batches. We first verify that the noise distributions are heavy-tailed in LLMs, with visualizations in Figure 4. Then, we estimate the tail index p following the methods in Simsekli et al. (2019). After that, we can approximate Assumptions 4a and 4b, where the detailed approach is postponed to Appendix E.3. Figure 1 depicts the relationship between the noise norm and the gradient magnitude for a randomly selected dimension $j \in [d]$ over consecutive iterations, while Figure 2 illustrates the corresponding relationship for the matrix setting. We observe that in both cases, the expected noise norm scales linearly with the gradient norm. These empirical findings strongly corroborate our noise models in As-

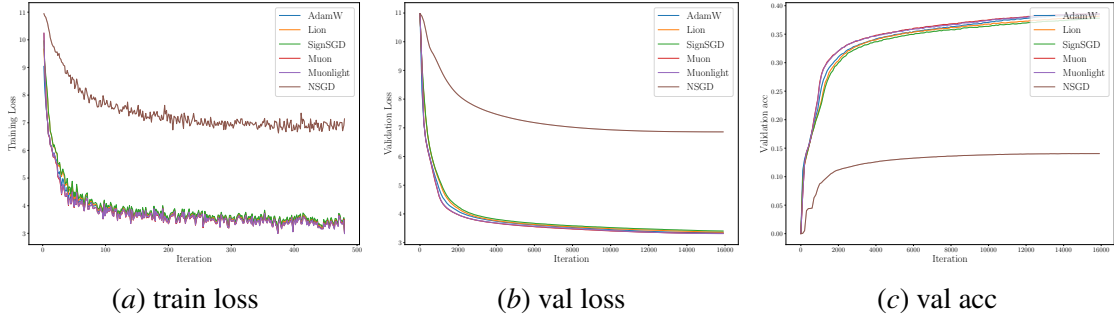


Figure 3: The training loss, validation loss and accuracy for nanoGPT trained on C4.

sumptions 4a and 4b, confirming that the noise magnitude is directly proportional to the gradient magnitude during training.

6.2. Practical Efficiency of Sign-Based Optimizers

Following the setup detailed in Appendix E.1, we train the nanoGPT model on the C4 dataset using Normalized SGD (NSGD) (Nesterov, 1984; Cutkosky and Mehta, 2020), AdamW (Kingma and Ba, 2015; Loshchilov and Hutter, 2019), SignSGD (Bernstein et al., 2018), Lion (Chen et al., 2023a), Muon (Jordan et al., 2024), and Muonlight (Liu et al., 2025a), where the results are shown in Figure 3. We observe a substantial performance gap between NSGD and sign-based methods (Lion and Muon), providing strong empirical evidence that sign-based optimizers are significantly more efficient than NSGD in the presence of heavy-tailed noise. This confirms the theoretical advantages established in Appendix A. Furthermore, the matrix sign methods (Muon and Muonlight) consistently outperform AdamW, aligning with recent empirical findings in Liu et al. (2025a); Shah et al. (2025); Wen et al. (2025); Semenov et al. (2025).

7. Conclusion

This work aims to provide theoretical justifications for the empirical success of sign-based optimization algorithms such as Lion and Muon, particularly in the context of training LLMs. We introduce generalized heavy-tailed gradient noise assumptions that allow the noise magnitude to scale linearly with the gradient norm, a model we empirically validate as accurately reflecting the stochastic dynamics of real-world LLM training. Under this regime, we establish sharp convergence guarantees for SignSGD, Lion, Muon, and Muonlight, achieving rates that match or surpass the best-known bounds. Crucially, our theory indicates provable advantages of sign-based methods over NSGD and AdamW in the presence of heavy-tailedness. These findings are corroborated by LLM pretraining experiments, which confirm the practical superiority of sign-based optimizers.

Acknowledgments

We sincerely appreciate the valuable feedback provided by Weizhong Zhang and Yuxing Liu.

References

Josh Achiam, Steven Adler, Sandhini Agarwal, Lama Ahmad, Ilge Akkaya, Florencia Leoni Aleman, Diogo Almeida, Janko Altenschmidt, Sam Altman, Shyamal Anadkat, et al. GPT-4 technical report. *arXiv preprint arXiv:2303.08774*, 2023.

Kwangjun Ahn, Xiang Cheng, Minhak Song, Chulhee Yun, Ali Jadbabaie, and Suvrit Sra. Linear attention is (maybe) all you need (to understand transformer optimization). In *International Conference on Learning Representations (ICLR)*, pages 16193–16205, 2024.

Kwangjun Ahn, Noah Amsel, and John Langford. Dion2: A simple method to shrink matrix in Muon. *arXiv preprint arXiv:2512.16928*, 2025a.

Kwangjun Ahn, Byron Xu, Natalie Abreu, Ying Fan, Gagik Magakyan, Pratyusha Sharma, Zheng Zhan, and John Langford. Dion: Distributed orthonormalized updates. *arXiv preprint arXiv:2504.05295*, 2025b.

Noah Amsel, David Persson, Christopher Musco, and Robert M Gower. The polar express: Optimal matrix sign methods and their application to the Muon algorithm. *arXiv preprint arXiv:2505.16932*, 2025.

Kang An, Yuxing Liu, Rui Pan, Yi Ren, Shiqian Ma, Donald Goldfarb, and Tong Zhang. ASGO: Adaptive structured gradient optimization. In *Advances in Neural Information Processing Systems 38 (NeurIPS)*, page to appear, 2025.

Yossi Arjevani, Yair Carmon, John C. Duchi, Dylan J Foster, Nathan Srebro, and Blake Woodworth. Lower bounds for non-convex stochastic optimization. *Mathematical Programming*, 199(1):165–214, 2023.

Lukas Balles and Philipp Hennig. Dissecting Adam: The sign, magnitude and variance of stochastic gradients. In *Proceedings of the 35th International Conference on Machine Learning (ICML)*, pages 404–413, 2018.

Lukas Balles, Fabian Pedregosa, and Nicolas Le Roux. The geometry of sign gradient descent. *arXiv preprint arXiv:2002.08056*, 2020.

Jeremy Bernstein and Laker Newhouse. Old optimizer, new norm: An anthology. In *OPT 2024: Optimization for Machine Learning*, 2024. URL <https://openreview.net/forum?id=ux18f5nOpD>.

Jeremy Bernstein and Laker Newhouse. Modular duality in deep learning. In *Proceedings of the 42nd International Conference on Machine Learning (ICML)*, pages 3920–3930, 2025.

Jeremy Bernstein, Yu-Xiang Wang, Kamyar Azizzadenesheli, and Anima Anandkumar. SignSGD: Compressed optimisation for non-convex problems. In *Proceedings of the 35th International Conference on Machine Learning (ICML)*, pages 560–569, 2018.

Jeremy Bernstein, Jiawei Zhao, Kamyar Azizzadenesheli, and Anima Anandkumar. SignSGD with majority vote is communication efficient and fault tolerant. In *International Conference on Learning Representations (ICLR)*, 2019.

Rajendra Bhatia. *Matrix Analysis*, volume 169. Springer Science & Business Media, 1996.

Åke Björck and Clazett Bowie. An iterative algorithm for computing the best estimate of an orthogonal matrix. *SIAM Journal on Numerical Analysis*, 8(2):358–364, 1971.

Tom Brown, Benjamin Mann, Nick Ryder, Melanie Subbiah, Jared D Kaplan, Prafulla Dhariwal, Arvind Neelakantan, Pranav Shyam, Girish Sastry, Amanda Askell, Sandhini Agarwal, Ariel Herbert-Voss, Gretchen Krueger, Tom Henighan, Rewon Child, Aditya Ramesh, Daniel Ziegler, Jeffrey Wu, Clemens Winter, Chris Hesse, Mark Chen, Eric Sigler, Mateusz Litwin, Scott Gray, Benjamin Chess, Jack Clark, Christopher Berner, Sam McCandlish, Alec Radford, Ilya Sutskever, and Dario Amodei. Language models are few-shot learners. In *Advances in Neural Information Processing Systems 33 (NeurIPS)*, pages 1877–1901, 2020.

Sébastien Bubeck, Nicolo Cesa-Bianchi, and Gábor Lugosi. Bandits with heavy tail. *IEEE Transactions on Information Theory*, 59(11):7711–7717, 2013.

Da Chang, Yongxiang Liu, and Ganzhao Yuan. On the convergence of Muon and beyond. *arXiv preprint arXiv:2509.15816*, 2025.

Hongxu Chen, Ke Wei, Xiaoming Yuan, and Luo Luo. Stability and generalization of nonconvex optimization with heavy-tailed noise. *arXiv preprint arXiv:2601.19730*, 2026.

Lizhang Chen, Bo Liu, Kaizhao Liang, and Qiang Liu. Lion secretly solves a constrained optimization: As lyapunov predicts. In *International Conference on Learning Representations (ICLR)*, pages 35404–35439, 2024.

Lizhang Chen, Jonathan Li, and Qiang Liu. Muon optimizes under spectral norm constraints. *arXiv preprint arXiv:2506.15054*, 2025.

Xiangning Chen, Chen Liang, Da Huang, Esteban Real, Kaiyuan Wang, Hieu Pham, Xuanyi Dong, Thang Luong, Cho-Jui Hsieh, Yifeng Lu, et al. Symbolic discovery of optimization algorithms. *Advances in Neural Information Processing systems 36 (NeurIPS)*, pages 49205–49233, 2023a.

Ziyi Chen, Yi Zhou, Yingbin Liang, and Zhaosong Lu. Generalized-smooth nonconvex optimization is as efficient as smooth nonconvex optimization. In *Proceedings of the 40th International Conference on Machine Learning (ICML)*, pages 5396–5427, 2023b.

Savelii Chezhev, Klyukin Yaroslav, Andrei Semenov, Aleksandr Beznosikov, Alexander Gasnikov, Samuel Horváth, Martin Takáč, and Eduard Gorbunov. Clipping improves Adam-norm and AdaGrad-norm when the noise is heavy-tailed. In *Proceedings of the 42nd International Conference on Machine Learning (ICML)*, pages 10269–10333, 2025.

Romain Cosson, Ali Jadbabaie, Anuran Makur, Amirhossein Reisizadeh, and Devavrat Shah. Low-rank gradient descent. *IEEE Open Journal of Control Systems*, 2:380–395, 2023.

Michael Crawshaw, Mingrui Liu, Francesco Orabona, Wei Zhang, and Zhenxun Zhuang. Robustness to unbounded smoothness of generalized SignSGD. In *Advances in Neural Information Processing Systems 35 (NeurIPS)*, pages 9955–9968, 2022.

Michael Crawshaw, Chirag Modi, Mingrui Liu, and Robert M Gower. An exploration of non-Euclidean gradient descent: Muon and its many variants. *arXiv preprint arXiv:2510.09827*, 2025.

Ashok Cutkosky and Harsh Mehta. Momentum improves normalized SGD. In *Proceedings of the 37th International Conference on Machine Learning (ICML)*, pages 2260–2268, 2020.

Ashok Cutkosky and Harsh Mehta. High-probability bounds for non-convex stochastic optimization with heavy tails. In *Advances in Neural Information Processing Systems 34 (NeurIPS)*, pages 4883–4895, 2021.

Jacob Devlin, Ming-Wei Chang, Kenton Lee, and Kristina Toutanova. BERT: Pre-training of deep bidirectional transformers for language understanding. In *Proceedings of the 2019 Conference of the North American Chapter of the Association for Computational Linguistics: Human Language Technologies*, pages 4171–4186, 2019.

Yiming Dong, Huan Li, and Zhouchen Lin. Convergence rate analysis of LION. *arXiv preprint arXiv:2411.07724*, 2024.

Timothy Dozat. Incorporating Nesterov momentum into Adam. In *International Conference on Learning Representations (ICLR) Workshop*, 2016.

John Duchi, Elad Hazan, and Yoram Singer. Adaptive subgradient methods for online learning and stochastic optimization. *Journal of Machine Learning Research (JMLR)*, 12(7), 2011.

Simon Elistratov, Andrey Podivilov, Timofei Iuzhakov, and Dmitry Vetrov. Lion’s sign noise can make training more stable. In *OPT 2024: Optimization for Machine Learning Workshop of NeurIPS 2024*, 2024.

Ilyas Fatkhullin, Florian Hübler, and Guanghui Lan. Can SGD handle heavy-tailed noise? In *OPT 2025: Optimization for Machine Learning*, 2025.

Matthew Faw, Litu Rout, Constantine Caramanis, and Sanjay Shakkottai. Beyond uniform smoothness: A stopped analysis of adaptive SGD. In *Proceedings of the 36th Conference on Learning Theory (COLT)*, pages 89–160, 2023.

Kevin Frans, Pieter Abbeel, and Sergey Levine. What really matters in matrix-whitening optimizers? *arXiv preprint arXiv:2510.25000*, 2025.

Saeed Ghadimi and Guanghui Lan. Stochastic first-and zeroth-order methods for nonconvex stochastic programming. *SIAM Journal on Optimization*, 23(4):2341–2368, 2013.

Eduard Gorbunov, Abdurakhmon Sadiev, Marina Danilova, Samuel Horváth, Gauthier Gidel, Pavel Dvurechensky, Alexander Gasnikov, and Peter Richtárik. High-probability convergence for composite and distributed stochastic minimization and variational inequalities with heavy-tailed noise. In *Proceedings of the 41st International Conference on Machine Learning (ICML)*, pages 15951–16070, 2024.

Yutian Gou, Jinfeng Yi, and Lijun Zhang. Stochastic graphical bandits with heavy-tailed rewards. In *Proceedings of the 39th Conference on Uncertainty in Artificial Intelligence (UAI)*, pages 734–744, 2023.

Daya Guo, Dejian Yang, Haowei Zhang, Junxiao Song, Ruoyu Zhang, Runxin Xu, Qihao Zhu, Shirong Ma, Peiyi Wang, Xiao Bi, et al. DeepSeek-R1: Incentivizing reasoning capability in LLMs via reinforcement learning. *arXiv preprint arXiv:2501.12948*, 2025.

Vineet Gupta, Tomer Koren, and Yoram Singer. Shampoo: Preconditioned stochastic tensor optimization. In *Proceedings of the 35th International Conference on Machine Learning (ICML)*, pages 1842–1850, 2018.

Guy Gur-Ari, Daniel A Roberts, and Ethan Dyer. Gradient descent happens in a tiny subspace. *arXiv preprint arXiv:1812.04754*, 2018.

Mert Gurbuzbalaban, Umut Simsekli, and Lingjiong Zhu. The heavy-tail phenomenon in SGD. In *Proceedings of the 38th International Conference on Machine Learning (ICML)*, pages 3964–3975, 2021.

Elad Hazan, Amit Agarwal, and Satyen Kale. Logarithmic regret algorithms for online convex optimization. *Machine Learning*, 69(2):169–192, 2007.

Elad Hazan, Kfir Levy, and Shai Shalev-Shwartz. Beyond convexity: Stochastic quasi-convex optimization. In *Advances in Neural Information Processing Systems 28 (NIPS)*, pages 1594–1602, 2015.

Liam Hodgkinson and Michael Mahoney. Multiplicative noise and heavy tails in stochastic optimization. In *Proceedings of the 38th International Conference on Machine Learning (ICML)*, pages 4262–4274, 2021.

Jordan Hoffmann, Sebastian Borgeaud, Arthur Mensch, Elena Buchatskaya, Trevor Cai, Eliza Rutherford, Diego de Las Casas, Lisa Anne Hendricks, Johannes Welbl, Aidan Clark, Tom Hennigan, Eric Noland, Katie Millican, George van den Driessche, Bogdan Damoc, Aurelia Guy, Simon Osindero, Karen Simonyan, Erich Elsen, Jack W. Rae, Oriol Vinyals, and Laurent Sifre. Training compute-optimal large language models. In *Advances in Neural Information Processing Systems 35 (NeurIPS)*, pages 30016–30030, 2022.

Roger A Horn and Charles R Johnson. *Matrix analysis*. Cambridge University Press, 2012.

Daniel Hsu and Sivan Sabato. Heavy-tailed regression with a generalized median-of-means. In *Proceedings of the 31st International Conference on Machine Learning (ICML)*, pages 37–45, 2014.

Feihu Huang, Yuning Luo, and Songcan Chen. LiMuon: Light and fast Muon optimizer for large models. *arXiv preprint arXiv:2509.14562*, 2025.

Florian Hübler, Ilyas Fatkhullin, and Niao He. From gradient clipping to normalization for heavy tailed SGD. In *Proceedings of The 28th International Conference on Artificial Intelligence and Statistics (AISTATS)*, pages 2413–2421, 2025.

Ruichen Jiang, Devyani Maladkar, and Aryan Mokhtari. Provable complexity improvement of AdaGrad over SGD: Upper and lower bounds in stochastic non-convex optimization. In *Proceedings of the 38th Conference on Learning Theory (COLT)*, pages 3124–3158, 2025a.

Wei Jiang and Lijun Zhang. Convergence analysis of the Lion optimizer in centralized and distributed settings. *arXiv preprint arXiv:2508.12327*, 2025.

Wei Jiang, Dingzhi Yu, Sifan Yang, Wenhao Yang, and Lijun Zhang. Improved analysis for sign-based methods with momentum updates. *arXiv preprint arXiv:2507.12091*, 2025b.

Jikai Jin, Bohang Zhang, Haiyang Wang, and Liwei Wang. Non-convex distributionally robust optimization: Non-asymptotic analysis. In *Advances in Neural Information Processing Systems 34 (NeurIPS)*, pages 2771–2782, 2021.

Keller Jordan, Yuchen Jin, Vlado Boza, Jiacheng You, Franz Cesista, Laker Newhouse, and Jeremy Bernstein. Muon: An optimizer for hidden layers in neural networks, 2024. URL <https://kellerjordan.github.io/posts/muon/>.

Sai Praneeth Karimireddy, Quentin Rebjock, Sebastian Stich, and Martin Jaggi. Error feedback fixes SignSGD and other gradient compression schemes. In *Proceedings of the 36th International Conference on Machine Learning (ICML)*, pages 3252–3261, 2019.

Andrej Karpathy. NanoGPT, 2022. URL <https://github.com/karpathy/nanoGPT>.

Gyu Yeol Kim and Min-hwan Oh. Convergence of Muon with Newton–Schulz. In *International Conference on Learning Representations (ICLR)*, page to appear, 2026. URL <https://openreview.net/forum?id=1JSfxtLpLm>.

Diederik P. Kingma and Jimmy Ba. Adam: A method for stochastic optimization. In *International Conference on Learning Representations (ICLR)*, 2015.

Nikita Kornilov, Ohad Shamir, Aleksandr Lobanov, Darina Dvinskikh, Alexander Gasnikov, Inokentiy Shibaev, Eduard Gorbunov, and Samuel Horváth. Accelerated zeroth-order method for non-smooth stochastic convex optimization problem with infinite variance. In *Advances in Neural Information Processing Systems 36 (NeurIPS)*, pages 64083–64102, 2023.

Nikita Kornilov, Philip Zmushko, Andrei Semenov, Mark Ikonnikov, Alexander Gasnikov, and Alexander Beznosikov. Sign operator for coping with heavy-tailed noise in non-convex optimization: High probability bounds under (L_0, L_1) -smoothness. *arXiv preprint arXiv:2502.07923*, 2025.

Atli Kosson, Bettina Messmer, and Martin Jaggi. Rotational equilibrium: How weight decay balances learning across neural networks. In *Proceedings of the 41st International Conference on Machine Learning (ICML)*, pages 25333–25369, 2024.

Dmitry Kovalev. SGD with adaptive preconditioning: Unified analysis and momentum acceleration. *arXiv preprint arXiv:2506.23803*, 2025.

Dmitry Kovalev and Ekaterina Borodich. Non-Euclidean SGD for structured optimization: Unified analysis and improved rates. *arXiv preprint arXiv:2511.11466*, 2025.

Zdislav Kovarik. Some iterative methods for improving orthonormality. *SIAM Journal on Numerical Analysis*, 7(3):386–389, 1970.

Frederik Kunstner and Francis Bach. Scaling laws for gradient descent and sign descent for linear bigram models under zipf's law. In *Advances in Neural Information Processing Systems 38 (NeurIPS)*, page to appear, 2025.

Frederik Kunstner, Jacques Chen, Jonathan Wilder Lavington, and Mark Schmidt. Noise is not the main factor behind the gap between SGD and Adam on transformers, but sign descent might be. In *International Conference on Learning Representations (ICLR)*, 2023.

Frederik Kunstner, Alan Milligan, Robin Yadav, Mark Schmidt, and Alberto Bietti. Heavy-tailed class imbalance and why Adam outperforms gradient descent on language models. In *Advances in Neural Information Processing Systems 37 (NeurIPS)*, pages 30106–30148, 2024.

Guanghui Lan. *First-order and stochastic optimization methods for machine learning*, volume 1. Springer, 2020.

Bingrui Li, Wei Huang, Andi Han, Zhanpeng Zhou, Taiji Suzuki, Jun Zhu, and Jianfei Chen. On the optimization and generalization of two-layer transformers with sign gradient descent. In *International Conference on Learning Representations (ICLR)*, pages 64406–64484, 2025a.

Haochuan Li, Alexander Rakhlin, and Ali Jadbabaie. Convergence of Adam under relaxed assumptions. In *Advances in Neural Information Processing Systems 36 (NeurIPS)*, pages 52166–52196, 2023.

Huan Li, Yiming Dong, and Zhouchen Lin. On the $O(\sqrt{d}/T^{1/4})$ convergence rate of rmsprop and its momentum extension measured by ℓ_1 norm. *Journal of Machine Learning Research (JMLR)*, 26(131):1–25, 2025b.

Jiaxiang Li and Mingyi Hong. A note on the convergence of Muon and further. *arXiv preprint arXiv:2502.02900*, 2025.

Zichong Li, Liming Liu, Chen Liang, Weizhu Chen, and Tuo Zhao. NorMuon: Making Muon more efficient and scalable. *arXiv preprint arXiv:2510.05491*, 2025c.

Jingyuan Liu, Jianlin Su, Xingcheng Yao, Zhejun Jiang, Guokun Lai, Yulun Du, Yidao Qin, Weixin Xu, Enzhe Lu, Junjie Yan, et al. Muon is scalable for LLM training. *arXiv preprint arXiv:2502.16982*, 2025a.

Langqi Liu, Yibo Wang, and Lijun Zhang. High-probability bound for non-smooth non-convex stochastic optimization with heavy tails. In *Proceedings of the 41st International Conference on Machine Learning (ICML)*, pages 32122–32138, 2024.

Sijia Liu, Pin-Yu Chen, Xiangyi Chen, and Mingyi Hong. SignSGD via zeroth-order oracle. In *International Conference on Learning Representations (ICLR)*, 2019.

Yifeng Liu, Angela Yuan, and Quanquan Gu. MARS-M: When variance reduction meets matrices. *arXiv preprint arXiv:2510.21800*, 2025b.

Yuxing Liu, Rui Pan, and Tong Zhang. AdaGrad under anisotropic smoothness. In *International Conference on Learning Representations (ICLR)*, pages 19574–19608, 2025c.

Zhuanghua Liu and Luo Luo. Stochastic bilevel optimization with heavy-tailed noise. *arXiv preprint arXiv:2509.14952*, 2025.

Zijian Liu. Clipped gradient methods for nonsmooth convex optimization under heavy-tailed noise: A refined analysis. In *International Conference on Learning Representations (ICLR)*, page to appear, 2026a. URL <https://openreview.net/forum?id=2dbLeXDe39>.

Zijian Liu. Online convex optimization with heavy tails: Old algorithms, new regrets, and applications. In *Proceedings of the 37th International Conference on Algorithmic Learning Theory (ALT)*, page to appear, 2026b.

Zijian Liu and Zhengyuan Zhou. Stochastic nonsmooth convex optimization with heavy-tailed noises: High-probability bound, in-expectation rate and initial distance adaptation. *arXiv preprint arXiv:2303.12277*, 2023.

Zijian Liu and Zhengyuan Zhou. Nonconvex stochastic optimization under heavy-tailed noises: Optimal convergence without gradient clipping. In *International Conference on Learning Representations (ICLR)*, pages 92529–92554, 2025.

Zijian Liu, Jiawei Zhang, and Zhengyuan Zhou. Breaking the lower bound with (little) structure: Acceleration in non-convex stochastic optimization with heavy-tailed noise. In *Proceedings of 36th Conference on Learning Theory (COLT)*, pages 2266–2290, 2023.

Ilya Loshchilov and Frank Hutter. Decoupled weight decay regularization. In *International Conference on Learning Representations (ICLR)*, 2019.

Shiyin Lu, Guanghui Wang, Yao Hu, and Lijun Zhang. Optimal algorithms for Lipschitz bandits with heavy-tailed rewards. In *Proceedings of the 36th International Conference on Machine Learning (ICML)*, pages 4154–4163, 2019.

Jianhao Ma, Yu Huang, Yuejie Chi, and Yuxin Chen. Preconditioning benefits of spectral orthogonalization in Muon. *arXiv preprint arXiv:2601.13474*, 2026.

Brendan McMahan and Matthew Streeter. Adaptive bound optimization for online convex optimization. In *Proceedings of the 23rd Conference on Learning Theory (COLT)*, pages 244–256, 2010.

Sushant Mehta, Raj Dandekar, Rajat Dandekar, and Sreedath Panat. Muon: Training and trade-offs with latent attention and moe. *arXiv preprint arXiv:2509.24406*, 2025.

Enea Monzio Compagnoni, Tianlin Liu, Rustem Islamov, Frank Proske, Antonio Orvieto, and Aurélien Lucchi. Adaptive methods through the lens of sdes: Theoretical insights on the role of noise. In *International Conference on Learning Representations (ICLR)*, pages 95500–95557, 2025.

Arkadi Nemirovski. Sums of random symmetric matrices and quadratic optimization under orthogonality constraints. *Mathematical Programming*, 109(2):283–317, 2007.

Yurii Nesterov. Minimization methods for nonsmooth convex and quasiconvex functions. *Matekon*, 29(3):519–531, 1984.

Yurii Nesterov. Primal-dual subgradient methods for convex problems. *Mathematical Programming*, 120(1):221–259, 2009.

Yurii Nesterov et al. *Lectures on convex optimization*, volume 137. Springer, 2018.

Ta Duy Nguyen, Thien H Nguyen, Alina Ene, and Huy Nguyen. Improved convergence in high probability of clipped gradient methods with heavy tailed noise. In *Advances in Neural Information Processing Systems 36 (NeurIPS)*, pages 24191–24222. Curran Associates, Inc., 2023.

Francesco Orabona. A modern introduction to online learning. *arXiv preprint arXiv:1912.13213v8*, 2019.

Saurabh Page, Advait Joshi, and SS Sonawane. Muonall: Muon variant for efficient finetuning of large language models. *arXiv preprint arXiv:2511.06086*, 2025.

Rui Pan, Yang Luo, Yuxing Liu, Yang You, and Tong Zhang. Unbiased gradient low-rank projection. *arXiv preprint arXiv:2510.17802*, 2025.

Razvan Pascanu, Tomas Mikolov, and Yoshua Bengio. On the difficulty of training recurrent neural networks. In *Proceedings of the 30th International Conference on Machine Learning (ICML)*, pages 1310–1318, 2013.

Adam Paszke, Sam Gross, Francisco Massa, Adam Lerer, James Bradbury, Gregory Chanan, Trevor Killeen, Zeming Lin, Natalia Gimelshein, Luca Antiga, Alban Desmaison, Andreas Kopf, Edward Yang, Zachary DeVito, Martin Raison, Alykhan Tejani, Sasank Chilamkurthy, Benoit Steiner, Lu Fang, Junjie Bai, and Soumith Chintala. Pytorch: An imperative style, high-performance deep learning library. In *Advances in Neural Information Processing Systems 32 (NeurIPS)*, pages 8026–8037, 2019.

Hanyang Peng, Shuang Qin, Yue Yu, Fangqing Jiang, Hui Wang, and Zhouchen Lin. Simple convergence proof of Adam from a sign-like descent perspective. *arXiv preprint arXiv:2507.05966*, 2025.

Thomas Pethick, Wanyun Xie, Kimon Antonakopoulos, Zhenyu Zhu, Antonio Silveti-Falls, and Volkan Cevher. Training deep learning models with norm-constrained lmos. In *Proceedings of the 42nd International Conference on Machine Learning (ICML)*, pages 49069–49104, 2025.

Egor Petrov, Grigoriy Evseev, Aleksey Antonov, Andrey Veprikov, Nikolay Bushkov, Stanislav Moiseev, and Aleksandr Beznosikov. Leveraging coordinate momentum in SignSGD and Muon: Memory-optimized zero-order. *arXiv preprint arXiv:2506.04430*, 2025.

Steven T Piantadosi. Zipf’s word frequency law in natural language: A critical review and future directions. *Psychonomic Bulletin & Review*, 21(5):1112–1130, 2014.

Nikita Puchkin, Eduard Gorbunov, Nickolay Kutuzov, and Alexander Gasnikov. Breaking the heavy-tailed noise barrier in stochastic optimization problems. In *Proceedings of the 27th International Conference on Artificial Intelligence and Statistics (AISTATS)*, pages 856–864, 2024.

Xun Qian, Hussein Rammal, Dmitry Kovalev, and Peter Richtarik. Muon is provably faster with momentum variance reduction. *arXiv preprint arXiv:2512.16598*, 2025.

Colin Raffel, Noam Shazeer, Adam Roberts, Katherine Lee, Sharan Narang, Michael Matena, Yanqi Zhou, Wei Li, and Peter J. Liu. Exploring the limits of transfer learning with a unified text-to-text transformer. *Journal of Machine Learning Research (JMLR)*, 21(140):1–67, 2020.

Alexander Rakhlin and Karthik Sridharan. On equivalence of martingale tail bounds and deterministic regret inequalities. In *Proceedings of the 30th Conference on Learning Theory (COLT)*, pages 1704–1722, 2017.

Artem Riabinin, Egor Shulgin, Kaja Gruntkowska, and Peter Richtárik. Gluon: Making Muon & Scion great again!(bridging theory and practice of LMO-based optimizers for LLMs). *arXiv preprint arXiv:2505.13416*, 2025.

Herbert Robbins and Sutton Monro. A stochastic approximation method. *The Annals of Mathematical Statistics*, pages 400–407, 1951.

Abdurakhmon Sadiev, Marina Danilova, Eduard Gorbunov, Samuel Horváth, Gauthier Gidel, Pavel Dvurechensky, Alexander Gasnikov, and Peter Richtárik. High-probability bounds for stochastic optimization and variational inequalities: the case of unbounded variance. In *Proceedings of the 40th International Conference on Machine Learning (ICML)*, pages 29563–29648, 2023.

Mher Safaryan and Peter Richtárik. Stochastic sign descent methods: New algorithms and better theory. In *Proceedings of the 38th International Conference on Machine Learning (ICML)*, pages 9224–9234, 2021.

Levent Sagun, Leon Bottou, and Yann LeCun. Eigenvalues of the Hessian in deep learning: Singularity and beyond. *arXiv preprint arXiv:1611.07476*, 2016.

Levent Sagun, Utku Evci, V Ugur Guney, Yann Dauphin, and Leon Bottou. Empirical analysis of the Hessian of over-parametrized neural networks. *arXiv preprint arXiv:1706.04454*, 2017.

Naoki Sato, Hiroki Naganuma, and Hideaki Iiduka. Convergence bound and critical batch size of Muon optimizer. *arXiv preprint arXiv:2507.01598*, 2025.

Frank Seide, Hao Fu, Jasha Droppo, Gang Li, and Dong Yu. 1-bit stochastic gradient descent and its application to data-parallel distributed training of speech DNNs. In *Proceedings of Interspeech 2014*, pages 1058–1062, 2014.

Andrei Semenov, Matteo Pagliardini, and Martin Jaggi. Benchmarking optimizers for large language model pretraining. *arXiv preprint arXiv:2509.01440*, 2025.

Maria-Eleni Sfyraki and Jun-Kun Wang. Lions and Muons: Optimization via stochastic frank-wolfe. *arXiv preprint arXiv:2506.04192*, 2025.

Ishaan Shah, Anthony M Polloreno, Karl Stratos, Philip Monk, Adarsh Chaluvaraju, Andrew Hojel, Andrew Ma, Anil Thomas, Ashish Tanwer, Darsh J Shah, et al. Practical efficiency of Muon for pretraining. *arXiv preprint arXiv:2505.02222*, 2025.

Wei Shen, Ruichuan Huang, Minhui Huang, Cong Shen, and Jiawei Zhang. On the convergence analysis of Muon. *arXiv preprint arXiv:2505.23737*, 2025.

Chongjie Si, Debing Zhang, and Wei Shen. Adamuon: Adaptive Muon optimizer. *arXiv preprint arXiv:2507.11005*, 2025.

Umut Simsekli, Levent Sagun, and Mert Gurbuzbalaban. A tail-index analysis of stochastic gradient noise in deep neural networks. In *Proceedings of the 36th International Conference on Machine Learning (ICML)*, pages 5827–5837, 2019.

Anthony Man-Cho So. Moment inequalities for sums of random matrices and their applications in optimization. *Mathematical Programming*, 130(1):125–151, 2011.

Minhak Song, Kwangjun Ahn, and Chulhee Yun. Does SGD really happen in tiny subspaces? In *International Conference on Learning Representations (ICLR)*, pages 8086–8120, 2025.

Matthew J. Streeter and H. Brendan McMahan. Less regret via online conditioning. *arXiv preprint arXiv:1002.4862*, 2010.

Weijie Su. Isotropic curvature model for understanding deep learning optimization: Is gradient orthogonalization optimal? *arXiv preprint arXiv:2511.00674*, 2025.

Tao Sun, Qingsong Wang, Dongsheng Li, and Bao Wang. Momentum ensures convergence of SIGNSGD under weaker assumptions. In *Proceedings of the 40th International Conference on Machine Learning (ICML)*, pages 33077–33099, 2023.

Tao Sun, Xinwang Liu, and Kun Yuan. Revisiting gradient normalization and clipping for nonconvex SGD under heavy-tailed noise: Necessity, sufficiency, and acceleration. *Journal of Machine Learning Research (JMLR)*, 26(237):1–42, 2025.

Gemini Team, Rohan Anil, Sebastian Borgeaud, Jean-Baptiste Alayrac, Jiahui Yu, Radu Soricut, Johan Schalkwyk, Andrew M Dai, Anja Hauth, Katie Millican, et al. Gemini: a family of highly capable multimodal models. *arXiv preprint arXiv:2312.11805*, 2023.

Kimi Team, Yifan Bai, Yiping Bao, Guanduo Chen, Jiahao Chen, Ningxin Chen, Ruijue Chen, Yanru Chen, Yuankun Chen, Yutian Chen, et al. Kimi k2: Open agentic intelligence. *arXiv preprint arXiv:2507.20534*, 2025.

Kimi Team, Tongtong Bai, Yifan Bai, Yiping Bao, SH Cai, Yuan Cao, Y Charles, HS Che, Cheng Chen, Guanduo Chen, et al. Kimi K2.5: Visual Agentic Intelligence. *arXiv preprint arXiv:2602.02276*, 2026.

Hugo Touvron, Thibaut Lavril, Gautier Izacard, Xavier Martinet, Marie-Anne Lachaux, Timothée Lacroix, Baptiste Rozière, Naman Goyal, Eric Hambro, Faisal Azhar, et al. Llama: Open and efficient foundation language models. *arXiv preprint arXiv:2302.13971*, 2023a.

Hugo Touvron, Louis Martin, Kevin Stone, Peter Albert, Amjad Almahairi, Yasmine Babaei, Nikolay Bashlykov, Soumya Batra, Prajwal Bhargava, Shruti Bhosale, et al. Llama 2: Open foundation and fine-tuned chat models. *arXiv preprint arXiv:2307.09288*, 2023b.

Joel A Tropp et al. An introduction to matrix concentration inequalities. *Foundations and Trends® in Machine Learning*, 8(1-2):1–230, 2015.

Amund Tveit, Bjørn Remseth, and Arve Skogvold. Muon optimizer accelerates grokking. *arXiv preprint arXiv:2504.16041*, 2025.

Ashish Vaswani, Noam Shazeer, Niki Parmar, Jakob Uszkoreit, Llion Jones, Aidan N Gomez, Łukasz Kaiser, and Illia Polosukhin. Attention is all you need. In *Advances in Neural Information Processing Systems 30 (NIPS)*, pages 5998–6008, 2017.

Bengt von Bahr and Carl-Gustav Esseen. Inequalities for the r -th absolute moment of a sum of random variables, $1 \leq r \leq 2$. *The Annals of Mathematical Statistics*, 36(1):299 – 303, 1965.

Nuri Mert Vural, Lu Yu, Krishna Balasubramanian, Stanislav Volgushev, and Murat A Erdogdu. Mirror descent strikes again: Optimal stochastic convex optimization under infinite noise variance. In *Proceedings of 35th Conference on Learning Theory (COLT)*, pages 65–102, 2022.

Bohan Wang, Huishuai Zhang, Zhiming Ma, and Wei Chen. Convergence of AdaGrad for non-convex objectives: Simple proofs and relaxed assumptions. In *Proceedings of the 36th Conference on Learning Theory (COLT)*, pages 161–190, 2023.

Menglian Wang, Zhuanghua Liu, and Luo Luo. Near-optimal decentralized stochastic nonconvex optimization with heavy-tailed noise. *arXiv preprint arXiv:2601.11435*, 2026.

Shuche Wang, Fengzhuo Zhang, Jiaxiang Li, Cunxiao Du, Chao Du, Tianyu Pang, Zhuoran Yang, Mingyi Hong, and Vincent YF Tan. Muon outperforms Adam in tail-end associative memory learning. *arXiv preprint arXiv:2509.26030*, 2025.

Kaiyue Wen, David Hall, Tengyu Ma, and Percy Liang. Fantastic pretraining optimizers and where to find them. *arXiv preprint arXiv:2509.02046*, 2025.

Jingfeng Wu, Wenqing Hu, Haoyi Xiong, Jun Huan, Vladimir Braverman, and Zhanxing Zhu. On the noisy gradient descent that generalizes as SGD. In *Proceedings of the 37th International Conference on Machine Learning (ICML)*, pages 10367–10376, 2020a.

Yidong Wu and Luo Luo. Optimal asynchronous stochastic nonconvex optimization under heavy-tailed noise. *arXiv preprint arXiv:2601.19379*, 2026.

Yikai Wu, Xingyu Zhu, Chenwei Wu, Annie Wang, and Rong Ge. Dissecting Hessian: Understanding common structure of Hessian in neural networks. *arXiv preprint arXiv:2010.04261*, 2020b.

Shuo Xie, Tianhao Wang, Sashank J. Reddi, Sanjiv Kumar, and Zhiyuan Li. Structured preconditioners in adaptive optimization: A unified analysis. In *Proceedings of the 42nd International Conference on Machine Learning (ICML)*, pages 68746–68776, 2025a.

Shuo Xie, Tianhao Wang, Beining Wu, and Zhiyuan Li. A tale of two geometries: Adaptive optimizers and non-Euclidean descent. *arXiv preprint arXiv:2511.20584*, 2025b.

Xingyu Xie, Pan Zhou, Huan Li, Zhouchen Lin, and Shuicheng Yan. Adan: Adaptive nesterov momentum algorithm for faster optimizing deep models. *IEEE Transactions on Pattern Analysis and Machine Intelligence*, 46(12):9508–9520, 2024.

Bo Xue, Guanghui Wang, Yimu Wang, and Lijun Zhang. Nearly optimal regret for stochastic linear bandits with heavy-tailed payoffs. In *Proceedings of the 29th International Joint Conference on Artificial Intelligence (IJCAI)*, pages 2936–2942, 2020.

Bo Xue, Yimu Wang, Yuanyu Wan, Jinfeng Yi, and Lijun Zhang. Efficient algorithms for generalized linear bandits with heavy-tailed rewards. In *Advances in Neural Information Processing Systems 36 (NeurIPS)*, pages 70880–70891, 2023.

Robin Yadav, Shuo Xie, Tianhao Wang, and Zhiyuan Li. Provable benefit of sign descent: A minimal model under heavy-tail class imbalance. In *OPT 2025: Optimization for Machine Learning*, 2025.

Greg Yang, James B Simon, and Jeremy Bernstein. A spectral condition for feature learning. *arXiv preprint arXiv:2310.17813*, 2023.

Chenlu Ye, Yujia Jin, Alekh Agarwal, and Tong Zhang. Catoni contextual bandits are robust to heavy-tailed rewards. In *Proceedings of the 42nd International Conference on Machine Learning (ICML)*, pages 71998–72040, 2025.

Yang You, Igor Gitman, and Boris Ginsburg. Large batch training of convolutional networks. *arXiv preprint arXiv:1708.03888*, 2017.

Yang You, Jing Li, Sashank Reddi, Jonathan Hseu, Sanjiv Kumar, Srinadh Bhojanapalli, Xiaodan Song, James Demmel, Kurt Keutzer, and Cho-Jui Hsieh. Large batch optimization for deep learning: Training BERT in 76 minutes. In *International Conference on Learning Representations (ICLR)*, 2020.

Ganzhao Yuan and Bernard Ghanem. ℓ_0 TV: A sparse optimization method for impulse noise image restoration. *IEEE Transactions on Pattern Analysis and Machine Intelligence*, 41(2):352–364, 2017.

Huizhuo Yuan, Yifeng Liu, Shuang Wu, Zhou Xun, and Quanquan Gu. MARS: Unleashing the power of variance reduction for training large models. In *Proceedings of the 42nd International Conference on Machine Learning (ICML)*, pages 73553–73587, 2025.

Aohan Zeng, Xin Lv, Qinkai Zheng, Zhenyu Hou, Bin Chen, Chengxing Xie, Cunxiang Wang, Da Yin, Hao Zeng, Jiajie Zhang, et al. Glm-4.5: Agentic, reasoning, and coding (arc) foundation models. *arXiv preprint arXiv:2508.06471*, 2025.

Bohang Zhang, Jikai Jin, Cong Fang, and Liwei Wang. Improved analysis of clipping algorithms for non-convex optimization. In *Advances in Neural Information Processing Systems 33 (NeurIPS)*, pages 15511–15521, 2020a.

Jingzhao Zhang, Tianxing He, Suvrit Sra, and Ali Jadbabaie. Why gradient clipping accelerates training: A theoretical justification for adaptivity. In *International Conference on Learning Representations (ICLR)*, 2020b.

Jingzhao Zhang, Sai Praneeth Karimireddy, Andreas Veit, Seungyeon Kim, Sashank Reddi, Sanjiv Kumar, and Suvrit Sra. Why are adaptive methods good for attention models? In *Advances in Neural Information Processing Systems 33 (NeurIPS)*, pages 15383–15393, 2020c.

Jiujia Zhang and Ashok Cutkosky. Parameter-free regret in high probability with heavy tails. In *Advances in Neural Information Processing Systems 35 (NeurIPS)*, pages 8000–8012, 2022.

Lijun Zhang and Zhi-Hua Zhou. ℓ_1 -regression with heavy-tailed distributions. In *Advances in Neural Information Processing Systems 31 (NeurIPS)*, pages 1076–1086, 2018.

Minxin Zhang, Yuxuan Liu, and Hayden Schaeffer. Adagrad meets Muon: Adaptive stepsizes for orthogonal updates. *arXiv preprint arXiv:2509.02981*, 2025a.

Xinwen Zhang and Hongchang Gao. On provable benefits of Muon in federated learning. *arXiv preprint arXiv:2510.03866*, 2025.

Yushun Zhang, Congliang Chen, Tian Ding, Ziniu Li, Ruoyu Sun, and Zhi-Quan Luo. Why Transformers need Adam: A Hessian perspective. In *Advances in Neural Information Processing Systems 37 (NeurIPS)*, pages 131786–131823, 2024.

Yushun Zhang, Congliang Chen, Ziniu Li, Tian Ding, Chenwei Wu, Diederik (Durk) Kingma, Yinyu Ye, Zhi-Quan Luo, and Ruoyu Sun. Adam-mini: Use fewer learning rates to gain more. In *International Conference on Learning Representations (ICLR)*, pages 28033–28063, 2025b.

Jiawei Zhao, Florian Tobias Schaefer, and Anima Anandkumar. Zero initialization: Initializing neural networks with only zeros and ones. *Transactions on Machine Learning Research*, 2022. ISSN 2835-8856. URL <https://openreview.net/forum?id=1AxQpKmiTc>.

Rosie Zhao, Depen Morwani, David Brandfonbrener, Nikhil Vyas, and Sham Kakade. Deconstructing what makes a good optimizer for autoregressive language models. In *International Conference on Learning Representations (ICLR)*, pages 2830–2850, 2025.

Pan Zhou, Jiashi Feng, Chao Ma, Caiming Xiong, Steven Chu Hong Hoi, and Weinan E. Towards theoretically understanding why SGD generalizes better than Adam in deep learning. In *Advances in Neural Information Processing Systems 33 (NeurIPS)*, pages 21285–21296, 2020.

Martin Zinkevich. Online convex programming and generalized infinitesimal gradient ascent. In *Proceedings of the 20th International Conference on Machine Learning (ICML)*, page 928–935, 2003.

Appendix A. Provable Complexity Improvement of Sign Gradient Descent over Normalized Gradient Descent

This section provides a theoretical comparison between the complexities of sign-based methods and Normalized Stochastic Gradient Descent (NSGD) (Nesterov, 1984; Hazan et al., 2015; You et al., 2017, 2020; Cutkosky and Mehta, 2020), highlighting scenarios where the former offers provable advantages. The comparison is motivated by two key observations: (i) NSGD is a robust baseline for heavy-tailed noise (Liu and Zhou, 2025; Hübner et al., 2025), and (ii) both methods can be interpreted as steepest descent algorithms—or Linear Minimization Oracles (LMOs)—operating under distinct geometric constraints (Bernstein and Newhouse, 2024; Pethick et al., 2025; Sfyraki and Wang, 2025). Consistent with the main text, both methods incorporate momentum, which is essential for tight convergence rates (Cutkosky and Mehta, 2020).

Algorithm 5 Normalized Stochastic Gradient Descent (NSGD) **Algorithm 6** Matrix Normalized Stochastic Gradient Descent (MNSGD)

1: Input: $T \in \mathbb{N}$, $\mathbf{x}_1 \in \mathbb{R}^d$, $\eta \in \mathbb{R}_+$ 2: for $t = 1$ to T do 3: $\mathbf{g}_t = \frac{1}{B} \sum_{b=1}^B \mathbf{g}_t^b$ 4: $\mathbf{m}_t = \beta \mathbf{m}_{t-1} + (1 - \beta) \mathbf{g}_t$ { $\mathbf{m}_0 := \mathbf{g}_1$ } 5: $\mathbf{x}_{t+1} = \mathbf{x}_t - \eta \frac{\mathbf{m}_t}{\ \mathbf{m}_t\ _2}$ 6: end for	1: Input: $T \in \mathbb{N}$, $\mathbf{x}_1 \in \mathbb{R}^d$, $\eta \in \mathbb{R}_+$, $\lambda \in \mathbb{R}_+$ 2: for $t = 1$ to T do 3: $\mathbf{G}_t = \frac{1}{B} \sum_{b=1}^B \mathbf{G}_t^b$ 4: $\mathbf{M}_t = \beta_1 \mathbf{M}_{t-1} + (1 - \beta_1) \mathbf{G}_t$ { $\mathbf{M}_0 := \mathbf{G}_1$ } 5: $\mathbf{X}_{t+1} = \mathbf{X}_t - \eta \frac{\mathbf{M}_t}{\ \mathbf{M}_t\ _F}$ 6: end for
---	--

To quantify these geometric differences, we utilize the notion of *vector density function* following [Bernstein et al. \(2018\)](#); [Jiang et al. \(2025a\)](#):

$$\phi_q(\mathbf{v}) := \frac{\|\mathbf{v}\|_1}{\|\mathbf{v}\|_q} \in [1, d^{1-\frac{1}{q}}], \forall \mathbf{v} \in \mathbb{R}^d, q \in [1, \infty],$$

where a higher $\phi_q(\mathbf{v})$ indicates a denser vector. To compare different stationary measures, we define the trajectory-wide density as $\phi_2(\nabla_T) := \min_{t \in [T]} \phi_2(\nabla f(\mathbf{x}_t))$. This concept extends naturally to the matrix setting via the *matrix density function*:

$$\psi_q(\mathbf{Y}) := \frac{\|\mathbf{Y}\|_{S_1}}{\|\mathbf{Y}\|_{S_q}} \in [1, (\text{rank}(\mathbf{Y}))^{1-\frac{1}{q}}], \forall \mathbf{Y} \in \mathbb{R}^{m \times n}, q \in [1, \infty],$$

where $\|\cdot\|_{S_q}$ denotes the Schatten q -norm (the ℓ_q -norm of the singular values). Notably, $\|\cdot\|_{S_1}$, $\|\cdot\|_{S_2}$, and $\|\cdot\|_{S_\infty}$ correspond to the nuclear norm $\|\cdot\|_*$, Frobenius norm $\|\cdot\|_F$, and operator norm $\|\cdot\|_{\text{op}}$, respectively. Intuitively, the matrix density function $\psi_q(\cdot)$ measures the distribution of singular values, capturing the “flatness” of the matrix spectrum. We define the matrix trajectory density as $\psi_2(\nabla_T) := \min_{t \in [T]} \psi_2(\nabla f(\mathbf{X}_t))$. To simplify the comparison, we focus on the case where $\mathbf{l}_1 = \mathbf{L}_1 = \boldsymbol{\sigma}_1 = \mathbf{V}_1 = \mathbf{0}$. The complete versions of normalized gradient descent for vectors and matrices are listed in Algorithms 5 and 6, respectively.

Vector Optimization Under the conditions of Assumptions 2a and 4a, the objective f is effectively $\|\mathbf{l}_0\|_\infty$ -smooth with $\|\boldsymbol{\sigma}_0\|_2$ -heavy-tailed noise⁵. As established in [Liu and Zhou \(2025\)](#), Algorithm 5 achieves a complexity of $O(\Delta_f \|\mathbf{l}_0\|_\infty \|\boldsymbol{\sigma}_0\|_2^{\frac{p}{p-1}} \epsilon^{-\frac{3p-2}{p-1}})$ for finding ℓ_2 -stationary points, i.e., $\mathbb{E}[\|\nabla f(\mathbf{x})\|_2] \leq \epsilon$. Using density functions to convert the complexity notion, we obtain the following bounds for identifying ℓ_2 -stationary points.

$$\begin{aligned} \text{SignSGD \& Lion (Theorems 1 and 2):} \quad & O\left(\frac{\Delta_f \|\mathbf{l}_0\|_\infty \|\boldsymbol{\sigma}_0\|_2^{\frac{p}{p-1}} \phi_\infty(\mathbf{l}_0) (\phi_2(\boldsymbol{\sigma}_0))^{\frac{p}{p-1}}}{\epsilon^{\frac{3p-2}{p-1}} (\phi_2(\nabla_T))^{\frac{3p-2}{p-1}}}\right) \\ \text{NSGD (Liu and Zhou, 2025):} \quad & O\left(\frac{\Delta_f \|\mathbf{l}_0\|_\infty \|\boldsymbol{\sigma}_0\|_2^{\frac{p}{p-1}}}{\epsilon^{\frac{3p-2}{p-1}}}\right) \end{aligned}$$

5. Technically speaking, we reparameterize the original $\boldsymbol{\sigma}_0$ by $\|\boldsymbol{\sigma}_0\|_2$, which shares the same range as $\boldsymbol{\sigma}_0$ in $\phi_2(\boldsymbol{\sigma}_0)$ and does not affect our later discussions.

Evidently, the relative complexity is governed by the ratio

$$R = R_1(R_2)^{\frac{p}{2(p-1)}}, \quad \text{where } R_1 := \frac{\phi_\infty(\mathbf{l}_0)}{\phi_2^2(\nabla_T)} \text{ and } R_2 = \frac{\phi_2^2(\sigma_0)}{\phi_2^2(\nabla_T)}.$$

Based on the empirical evidence in [Bernstein et al. \(2018, Figure 1\)](#), we shall see that R_2 is a mild constant ($R_2 \leq 5$). For the dominant factor R_1 , the extensive experiments on language modeling as well as computer vision tasks in [Bernstein et al. \(2018\)](#); [Dong et al. \(2024\)](#); [Li et al. \(2025b\)](#) show that the gradients $\{\nabla f(\mathbf{x}_t)\}_{t \in [T]}$ along the optimization trajectory remain dense, and the ratio $\phi_2(\nabla_T)$ is close to $\Theta(\sqrt{d})$. Since $\phi_\infty(\mathbf{l}_0) \in [1, d]$, so we have that $R_1 = O(1)$ in the worst case. When the curvature vector \mathbf{l}_0 exhibits axis-alignment properties ([Balles et al., 2020](#)) such that $\phi_\infty(\mathbf{l}_0) \approx 1$, SignSGD and Lion achieve a remarkable dimension-wise speedup of factor d over NSGD.

Matrix Optimization Consider the MNSGD method shown in [Algorithm 6](#). The trajectory of [Algorithm 6](#) is equivalent to [Algorithm 5](#) since $\|\mathbf{Y}\|_F = \|\text{vec}(\mathbf{Y})\|_2$. Under [Assumptions 2b](#) and [4b](#) and by the same reparameterization trick as in the vector case, we can deduce that the objective f is $\|\mathbf{L}_0\|_{\text{op}}$ -smooth and $\|\mathbf{V}_0\|_F$ -heavytailed. The results in [Liu and Zhou \(2025\)](#) suggest that MNSGD require $O(\Delta_f \|\mathbf{L}_0\|_{\text{op}} \|\mathbf{V}_0\|_F^{\frac{p}{p-1}} \epsilon^{-\frac{3p-2}{p-1}})$ iterations to reach $\mathbb{E} [\|\nabla f(\mathbf{X})\|_F] \leq \epsilon$. Leveraging matrix density functions, we obtain the following complexity comparison:

$$\begin{aligned} \text{Muon \& Muonlight (Theorems 3 and 4):} \quad & O\left(\frac{\Delta_f \|\mathbf{L}_0\|_{\text{op}} \|\mathbf{V}_0\|_F^{\frac{p}{p-1}} \psi_\infty(\mathbf{L}_0) (\psi_2(\mathbf{V}_0))^{\frac{p}{p-1}}}{\epsilon^{\frac{3p-2}{p-1}} (\psi_2(\nabla_T))^{\frac{3p-2}{p-1}}}\right) \\ \text{MNSGD (Liu and Zhou, 2025):} \quad & O\left(\frac{\Delta_f \|\mathbf{L}_0\|_{\text{op}} \|\mathbf{V}_0\|_F^{\frac{p}{p-1}}}{\epsilon^{\frac{3p-2}{p-1}}}\right) \end{aligned}$$

As in the vector case, the comparison is dominated by the ratios below:

$$R = R_1(R_2)^{\frac{p}{2(p-1)}}, \quad \text{where } R_1 := \frac{\psi_\infty(\mathbf{L}_0)}{\psi_2^2(\nabla_T)} \text{ and } R_2 = \frac{\psi_2^2(\mathbf{V}_0)}{\psi_2^2(\nabla_T)}.$$

The Hessians in modern deep neural networks (DNN) are typically low-rank ([Sagun et al., 2016, 2017](#); [Wu et al., 2020b](#); [An et al., 2025](#)), implying $\psi_\infty(\mathbf{L}_0)$ is close to 1. Furthermore, while gradients in DNNs frequently exhibit low-rank structures ([Gur-Ari et al., 2018](#); [Zhao et al., 2022](#); [Cosson et al., 2023](#); [Yang et al., 2023](#)), recent evidence ([Song et al., 2025](#)) suggests that gradient components aligning with the low-rank eigenspace may not effectively reduce training loss. When the variance and gradient matrices share a similar effective rank—particularly under Muon or Muonlight, which balance singular values via orthogonalization—the gradients can maintain a high effective rank ([Pan et al., 2025](#)). In this scenario, $R_1 \approx 1/\min\{m, n\}$ and R_2 remains a mild constant, highlighting a significant $\min\{m, n\}$ complexity improvement of Muon over MNSGD.

Lower Bounds The comparisons above follow the approach of [Bernstein et al. \(2018\)](#) by evaluating the upper bounds of both method classes. However, this argument can be significantly strengthened by comparing the *upper bounds* of sign-based optimizers directly against the *lower bounds* of gradient normalization. Given that the complexity results for NSGD and MNSGD are tight ([Liu and](#)

Table 1: Complexity comparison to find an ϵ -stationary point.

Setting	Algorithm	Criterion	Complexity	Improvement
Vector	NSGD	$\mathbb{E}[\ \nabla\ _2] \leq \epsilon$	$O\left(\frac{\Delta_f \ \mathbf{l}_0\ _\infty \ \boldsymbol{\sigma}_0\ _2^{\frac{p}{p-1}}}{\epsilon^{\frac{3p-2}{p-1}}}\right)$	= lower bound
	SignSGD & Lion	$\mathbb{E}[\ \nabla\ _1] \leq \epsilon$	$O\left(\frac{\Delta_f \ \mathbf{l}_0\ _1 \ \boldsymbol{\sigma}_0\ _1^{\frac{p}{p-1}}}{\epsilon^{\frac{3p-2}{p-1}}}\right)$	Up to d
Matrix	MNSGD	$\mathbb{E}[\ \nabla\ _F] \leq \epsilon$	$O\left(\frac{\Delta_f \ \mathbf{L}_0\ _{\text{op}} \ \mathbf{V}_0\ _F^{\frac{p}{p-1}}}{\epsilon^{\frac{3p-2}{p-1}}}\right)$	= lower bound
	Muon & Muonlight	$\mathbb{E}[\ \nabla\ _*] \leq \epsilon$	$O\left(\frac{\Delta_f \ \mathbf{L}_0\ _* \ \mathbf{V}_0\ _*^{\frac{p}{p-1}}}{\epsilon^{\frac{3p-2}{p-1}}}\right)$	Up to $\min\{m, n\}$

Zhou, 2025), this comparison highlights a fundamental, provable advantage of sign-descent methods. Similar to the approach in Jiang et al. (2025a), evaluating our upper bounds against established lower bounds rigorously demonstrates the superiority of sign-based optimization in these specific geometric settings.

We consolidate these findings in Table 1. This table explicitly illustrates how sign-based algorithms leverage problem geometry to achieve superior convergence rates compared to the established lower bounds of normalized gradient methods.

Appendix B. Further Discussions on Assumptions

In this section, we complete the omitted discussions in Sections 3 and 4.

B.1. Generalized Smoothness: Assumption 2a

Below, we briefly compare Assumption 2a with other $(\mathbf{l}_0, \mathbf{l}_1)$ -coordinate-wise smooth conditions. Consider the generalized smoothness model proposed in Crawshaw et al. (2022, Assumption 2):

$$|\nabla_i f(\mathbf{x}') - \nabla_i f(\mathbf{x})| \leq (\mathbf{l}_{0,i} + \mathbf{l}_{1,i} |\nabla_i f(\mathbf{x})|) \|\mathbf{x}' - \mathbf{x}\|_2, \forall i \in [d], \|\mathbf{x}' - \mathbf{x}\|_2 \leq \frac{1}{\|\mathbf{l}_1\|_\infty}. \quad (6)$$

Evidently, the above assumption is stronger than Assumption 2a in the sense that it requires (6) to hold for all coordinates, and that the requested domain is larger as $\|\mathbf{x}' - \mathbf{x}\|_\infty \leq \|\mathbf{x}' - \mathbf{x}\|_2$. Also, (6) will incur an explicit dimensional factor of d , which is unfavorable for LLMs. Liu et al. (2025c) further refined the condition in (6) into

$$\|\nabla f(\mathbf{x}') - \nabla f(\mathbf{x})\|_{(\mathbf{l}_0 + \mathbf{l}_1 \odot |\nabla f(\mathbf{x})|)^{-1}} \leq \|\mathbf{x}' - \mathbf{x}\|_{\mathbf{l}_0 + \mathbf{l}_1 \odot |\nabla f(\mathbf{x})|}, \quad \forall \|\mathbf{x}' - \mathbf{x}\|_{\mathbf{l}_1^2} \leq \sqrt{d}. \quad (7)$$

By standard calculus, it's easy to see that (7) implies Assumption 2c, a variant of Assumption 2a to be introduced later. Note that all of our theoretical results also hold under Assumption 2c (see discussions below Assumption 2c). We deduce that our smoothness model based on the quadratic bound (1) is generally weaker than the gradient curvature bound in (6) and (7). On the other hand, (6)

leverages ℓ_2 -norm while (7) utilizes ℓ_1^2 -weighted norm, both of which fail to align with the geometry of sign gradient descent (Bernstein and Newhouse, 2024, 2025). On the contrary, our ℓ_∞ -norm formulation perfectly matches the interpretation of sign descent from the perspective of linear minimization oracle (Pethick et al., 2025). Lastly, the empirical validations in Crawshaw et al. (2022); Liu et al. (2025c) confirms the practical value of Assumption 2a.

The following condition is a variant of Assumption 2a, and can be inferred from (7).

Assumption 2c (Variant of Assumption 2a) *There exists non-negative vectors $\mathbf{l}_0 = [\mathbf{l}_{0,1}, \dots, \mathbf{l}_{0,d}] \in \mathbb{R}_+^d$ and $\mathbf{l}_1 = [\mathbf{l}_{1,1}, \dots, \mathbf{l}_{1,d}] \in \mathbb{R}_+^d$ such that for all $\|\mathbf{x}' - \mathbf{x}\|_{\mathbf{l}_1^2} \leq 1/\sqrt{d}$:*

$$|f(\mathbf{x}') - (f(\mathbf{x}) + \langle \nabla f(\mathbf{x}), \mathbf{x}' - \mathbf{x} \rangle)| \leq \frac{1}{2} \|\mathbf{x}' - \mathbf{x}\|_{\mathbf{l}_0 + \mathbf{l}_1 \odot |\nabla f(\mathbf{x})|}^2. \quad (8)$$

Ignoring the absolute value on the LHS of (8), then Assumption 2c admits the exact same form as Lemma C.3 in Liu et al. (2025c), which is derived under condition (7) (Liu et al., 2025c, Assumption 5.1). According to the textbook analysis (Nesterov et al., 2018), we can expand their proof to derive (8), which indicates that the type of gradient curvature bound in (6) and (7) is *stronger* than the function value quadratic bound in Assumptions 2a and 2c. To illustrate that the theoretical guarantee in Section 3 still holds under Assumption 2c, note that the only difference between Assumptions 2a and 2c lies in the condition $\|\mathbf{x}' - \mathbf{x}\|_\infty \leq 1/\|\mathbf{l}_1\|_\infty$ versus $\|\mathbf{x}' - \mathbf{x}\|_{\mathbf{l}_1^2} \leq \sqrt{d}$. Delving into the analysis of SignSGD in Appendix C.3, Assumption 2a is used under

$$\eta \leq 1/\|\mathbf{l}_1\|_\infty \implies \|\mathbf{x}_{t+1} - \mathbf{x}_t\|_\infty = \eta \|\text{sign}(\mathbf{m}_t)\|_\infty \leq 1/\|\mathbf{l}_1\|_\infty.$$

Since we have

$$\eta \leq 1/\|\mathbf{l}_1\|_\infty \implies \|\mathbf{x}_{t+1} - \mathbf{x}_t\|_{\mathbf{l}_1^2} = \eta \sqrt{\sum_{i=1}^d (\text{sign}(\mathbf{m}_{t,i})^2 \cdot \mathbf{l}_{1,i}^2)} \leq \frac{\|\mathbf{l}_1\|_2}{\|\mathbf{l}_1\|_\infty} \leq \sqrt{d},$$

so we can replace Assumption 2a by Assumption 2c. The same arguments are still valid for Lion, which we omit here for brevity.

B.2. Generalized Smoothness: Assumption 2b

For completeness, we also provide the following assumption for Muon and Muonlight.

Assumption 2d (Variant of Assumption 2b) *There exists non-negative constants $\|\mathbf{L}_0\|_*, \|\mathbf{L}_1\|_{\text{op}} \in \mathbb{R}$ such that for all $\|\mathbf{X}' - \mathbf{X}\|_{\text{op}} \leq 1/\|\mathbf{L}_1\|_{\text{op}}$:*

$$\|\nabla f(\mathbf{X}') - \nabla f(\mathbf{X})\|_* \leq (\|\mathbf{L}_0\|_* + \|\mathbf{L}_1\|_{\text{op}} \|\nabla f(\mathbf{X})\|_*) \|\mathbf{X}' - \mathbf{X}\|_{\text{op}}. \quad (9)$$

Assumption 2d mirrors the original (L_0, L_1) -smoothness formulation in Zhang et al. (2020b) by utilizing scalar constants $(\|\mathbf{L}_0\|_*, \|\mathbf{L}_1\|_{\text{op}})$. This is a milder condition than Assumption 2b, as the latter necessitates the specification of two full matrices \mathbf{L}_0 and \mathbf{L}_1 . To demonstrate that Assumption 2d is a weaker requirement, consider the case where Assumption 2b holds. We have

$$\|\nabla f(\mathbf{X}') - \nabla f(\mathbf{X})\|_* \stackrel{\text{Lemma D.4}}{\leq} \sqrt{\|\mathbf{L}(\mathbf{X})\|_*} \|\nabla f(\mathbf{X}') - \nabla f(\mathbf{X})\|_{(\mathbf{L}(\mathbf{X}))^{-1}}$$

6. The requirement $\|\mathbf{x}' - \mathbf{x}\|_{\mathbf{l}_1^2} \leq \sqrt{d}$ here as well as in (7) is stated as $\|\mathbf{x}' - \mathbf{x}\|_{\mathbf{l}_1} \leq \sqrt{d}$ in Liu et al. (2025c), which is not correct after private communications with the authors of Liu et al. (2025c). Thus, we discuss under the right condition here.

$$\begin{aligned}
 & \stackrel{\text{Assumption 2b}}{\leq} \sqrt{\|\mathbf{L}(\mathbf{X})\|_*} \|\mathbf{X}' - \mathbf{X}\|_{\mathbf{L}(\mathbf{X})} = \sqrt{\|\mathbf{L}(\mathbf{X})\|_* \text{tr} \left((\mathbf{X}' - \mathbf{X})^\top \mathbf{L}(\mathbf{X}) (\mathbf{X}' - \mathbf{X}) \right)} \\
 & \leq \sqrt{\|\mathbf{L}(\mathbf{X})\|_* \cdot \left(\|\mathbf{L}(\mathbf{X})\|_* \left\| (\mathbf{X}' - \mathbf{X}) (\mathbf{X}' - \mathbf{X})^\top \right\|_{\text{op}} \right)} \\
 & \stackrel{\text{Lemma D.1}}{\leq} \|\mathbf{L}(\mathbf{X})\|_* \|\mathbf{X}' - \mathbf{X}\|_{\text{op}} \leq \left(\|\mathbf{L}_0\|_* + \|\mathbf{L}_1\|_{\text{op}} \|\nabla f(\mathbf{X})\|_* \right) \|\mathbf{X}' - \mathbf{X}\|_{\text{op}},
 \end{aligned}$$

suggesting that Assumption 2b implies Assumption 2d. In order to be more consistent with prior work (An et al., 2025; Kovalev and Borodich, 2025) and address the matrix structures, we adopt the formulation in the main text.

B.3. Heavy-Tailed Noise: Assumption 4a

Our theoretical justification mainly follows from Liu and Zhou (2025). The following lemma shows that Assumption 4a is meaningful for non-zero σ_1 .

Lemma B.1 (Based on Example A.1 in Liu and Zhou (2025)) *Given $\mathbf{x}_* = [x_{*,1}, \dots, x_{*,d}] \in \mathbb{R}^d$, define the separable function $h(\mathbf{x}) := \sum_{i=1}^d h_i(x_i)$, $\forall \mathbf{x} = [x_1, \dots, x_d] \in \mathbb{R}^d$ with*

$$h_i(x_i) := \frac{1}{2} \mathbb{E} \left[(a_i x_i - b_i)^2 \right], \quad a_i \sim \text{Bernoulli}(0.5), b = a_i x_{*,i} + \xi_i,$$

where ξ_i is a centered random variable independent of a_i and further satisfy $\mathbb{E} [|\xi_i|^p] \leq \sigma_i^p$ for some $\sigma_i \geq 0$. Then, for any h defined above, it holds that

1. $\sigma_1 = \mathbf{0}$: Assumption 4a can not be satisfied.
2. $\sigma_1 > \mathbf{0}$: Assumption 4a is satisfied with $\sigma_{0,i} = \sigma 2^{1-\frac{2}{p}}$, $\sigma_{1,i} = 2^{-\frac{1}{p}} + 2^{1-\frac{2}{p}}$, $\forall i \in [d]$.

Proof The stochastic gradient, as well as the true gradient at point \mathbf{x} is given by

$$\mathbf{g}_i = a_i (a_i x_i - b_i), \quad \nabla_i f(\mathbf{x}) = \mathbb{E}[a_i^2] \mathbf{x} - \mathbb{E}[a_i b_i].$$

Then, the function h_i is reduced to the one-dimensional case in Liu and Zhou (2025, Example A.1). Thus, we apply their results to deduce that when $\sigma_1 = \mathbf{0}$, for all $h_i, i \in [d]$, Assumption 4a can not be satisfied. Also, their results indicate that for any $i \in [d]$, we can select $\sigma_{0,i}^p = 2^{p-2} \sigma^p$ and $\sigma_{1,i}^p = 0.5 + 2^{p-2}$. Due to our separate construction of h and the independence between all coordinates, we can extend this conclusion to finish the second part of the proof. \blacksquare

B.4. Heavy-Tailed Noise: Assumption 4b

The following assumption is a relaxation of Assumption 4b.

Assumption 4c (Variant of Assumption 4b) *There exists $p \in (1, 2]$, $\mathbf{V}_0 \in \mathbb{R}^{m \times n}$, $\|\mathbf{V}_1\|_{\text{op}} \in \mathbb{R}_+$ such that*

$$\mathbb{E} \left[\left\| \mathbf{G}_t^b - \nabla f(\mathbf{X}_t) \right\|_{|\mathbf{V}_0|_m^{-1}}^p \middle| \mathcal{F}_{t-1} \right] \leq \|\mathbf{V}_0\|_*^{p/2} + \frac{\|\mathbf{V}_1\|_{\text{op}}^p \|\nabla f(\mathbf{X}_t)\|_*^p}{\|\mathbf{V}_0\|_*^{p/2}}, \quad \forall b \in [B]. \quad (10)$$

By the Cauchy-Schwarz inequality, $|\langle \mathbf{V}_1, \nabla f(\mathbf{X}_t) \rangle|^p \leq \|\mathbf{V}_1\|_{\text{op}}^p \|\nabla f(\mathbf{X}_t)\|_*^p$, which implies that Assumption 4b is a stronger condition than Assumption 4c. The latter is more amenable to empirical verification, as it replaces the full matrix \mathbf{V}_1 with a scalar coefficient $\|\mathbf{V}_1\|_{\text{op}}$, an approach we adopt in Section 6. We also underline that in both assumptions, the term $\|\mathbf{V}_0\|_*^{p/2}$ is introduced to maintain the homogeneity of the p th moment, ensuring that the scaling of the $|\mathbf{V}_0|_m^{-1}$ -weighted metric remains consistent with the noise magnitude.

Crucially, the use of the $\|\cdot\|_{|\mathbf{V}_0|_m^{-1}}$ weighted norm allows our model to capture the anisotropic structural properties of the noise (Xie et al., 2025b; An et al., 2025). Specifically, An et al. (2025, Assumption 3) and Pan et al. (2025, Assumption 3) assume a PSD constraint on the noise covariance: $\mathbb{E}[(\mathbf{G}_t^b - \nabla f(\mathbf{X}_t))(\mathbf{G}_t^b - \nabla f(\mathbf{X}_t))^\top | \mathcal{F}_{t-1}] \preceq \mathbf{V}_0 \mathbf{V}_0^\top$. This condition directly implies $\mathbb{E} \left[\|\mathbf{G}_t^b - \nabla f(\mathbf{X}_t)\|_{|\mathbf{V}_0|_m^{-1}}^2 \mid \mathcal{F}_{t-1} \right] \leq \|\mathbf{V}_0\|_*$ (Xie et al., 2025b, Proposition A.10), illustrating how our framework encapsulates the geometry of the gradient's principal directions.

B.5. Exact Newton–Schulz Oracle

In practice, Algorithms 3 and 4 often runs in $q = 5$ Newton–Schulz iterations (Kovarik, 1970; Björck and Bowie, 1971). The numerical error of the Newton–Schulz algorithm has been observed to exert little error on the optimization trajectory (Jordan et al., 2024; Liu et al., 2025a). Kim and Oh (2026) investigate this phenomenon theoretically and show that Muon with inexact Newton–Schulz converges at the same rate compared to the exact SVD realization, up to a constant factor which converges to 1 *double exponentially* in q . After reading their proof, it should be evident that their analysis can serve as a black box compatible with ours. It suffices to adapt (33) in Appendix D.3 to equation (5) in Kim and Oh (2026). Ultimately, we only need to pay the same constant factor for the convergence of Muon without assuming exact Newton–Schulz oracle. The same technique can be extended to other numerical algorithms that compute $\text{msign}(\cdot)$ in Muon, e.g., the recent hit PolarExpress (Amsel et al., 2025).

Appendix C. Analysis for SignSGD and Lion

To facilitate the theoretical analysis, we define

$$\epsilon_t := \mathbf{m}_t - \nabla f(\mathbf{x}_t), \quad \mathbf{n}_t := \mathbf{g}_t - \nabla f(\mathbf{x}_t), \quad \mathbf{s}_t := \nabla f(\mathbf{x}_{t-1}) - \nabla f(\mathbf{x}_t). \quad (11)$$

C.1. Vector Calculus

Lemma C.1 (Minkowski's inequality) *For any $p \geq 1$, $x, y \in \mathbb{R}_+$, it holds that $(x + y)^{1/p} \leq x^{1/p} + y^{1/p}$.*

Proof Applying Minkowski's inequality $\|\mathbf{x} + \mathbf{y}\|_p \leq \|\mathbf{x}\|_p + \|\mathbf{y}\|_p$ for two-dimensional vectors $\mathbf{x} = (x^{1/p}, 0)$, $\mathbf{y} = (0, y^{1/p})$ yields the result. \blacksquare

Lemma C.2 (Jensen's inequality for ℓ_p -means) *Let $p \in [1, +\infty]$ and let X_1, \dots, X_n be non-negative scalar random variables on some probability space, then*

$$\mathbb{E} \left[\sum_{i=1}^n X_i^p \right]^{1/p} \leq \left(\sum_{i=1}^n \mathbb{E}[X_i^p] \right)^{1/p}$$

Proof Let $Y = (X_1, \dots, X_n)$ be a random vector in \mathbb{R}_+^n . By Jensen's inequality as well as the convexity of $x \mapsto x^p, p \geq 1$:

$$\left(\mathbb{E} [\|Y\|_p] \right)^p \leq \mathbb{E} [\|Y\|_p^p] = \mathbb{E} \left[\sum_{i=1}^n X_i^p \right] = \sum_{i=1}^n \mathbb{E}[X_i^p].$$

Taking the $1/p$ -th power on both sides yields the result. \blacksquare

Lemma C.3 (Sign-difference Bound) *For any $\mathbf{x}, \mathbf{y} \in \mathbb{R}^d$, it holds that $\langle \mathbf{x}, \text{sign}(\mathbf{x}) - \text{sign}(\mathbf{y}) \rangle \leq 2 \|\mathbf{x} - \mathbf{y}\|_1$.*

Proof Let $\mathbf{x} = [\mathbf{x}_1, \dots, \mathbf{x}_d] \in \mathbb{R}^d, \mathbf{y} = [\mathbf{y}_1, \dots, \mathbf{y}_d] \in \mathbb{R}^d$, then

$$\begin{aligned} \langle \mathbf{x}, \text{sign}(\mathbf{x}) - \text{sign}(\mathbf{y}) \rangle &= \sum_{i=1}^d \mathbf{x}_i \cdot [\text{sign}(\mathbf{x}_i) - \text{sign}(\mathbf{y}_i)] \leq \sum_{i=1}^d 2 |\mathbf{x}_i| \cdot \mathbb{I}(\text{sign}(\mathbf{x}_i) \neq \text{sign}(\mathbf{y}_i)) \\ &\leq \sum_{i=1}^d 2 |\mathbf{x}_i - \mathbf{y}_i| \cdot \mathbb{I}(\text{sign}(\mathbf{x}_i) \neq \text{sign}(\mathbf{y}_i)) \leq \sum_{i=1}^d 2 |\mathbf{x}_i - \mathbf{y}_i| = 2 \|\mathbf{x} - \mathbf{y}\|_1. \end{aligned}$$

\blacksquare

C.2. Technical Lemmas

Lemma C.4 (Based on Lemma F.3 in Bernstein et al. (2018)) *Under Assumption 2a, for any sign vector $\mathbf{s} \in \{-1, 1\}^d$ and any $\eta \leq 1/\|\mathbf{l}_1\|_\infty$,*

$$\|\nabla f(\mathbf{x} + \eta\mathbf{s}) - \nabla f(\mathbf{x})\|_1 \leq 2\eta (\|\mathbf{l}_0\|_1 + \langle \mathbf{l}_1, |\nabla f(\mathbf{x})| \rangle).$$

Proof For any f twice-differentiable on the line segment between $\mathbf{x} + \eta\mathbf{s}$ and \mathbf{x} , by Taylor's theorem,

$$\nabla f(\mathbf{x} + \eta\mathbf{s}) - \nabla f(\mathbf{x}) = \int_0^1 \nabla^2 f(\mathbf{x} + t\eta\mathbf{s}) \eta\mathbf{s} dt = \left(\int_0^1 \nabla^2 f(\mathbf{x} + t\eta\mathbf{s}) dt \right) \cdot \eta\mathbf{s}.$$

Define

$$\mathbf{g} := \nabla f(\mathbf{x} + \eta\mathbf{s}) - \nabla f(\mathbf{x}), \quad \mathbf{H} := \int_0^1 \nabla^2 f(\mathbf{x} + t\eta\mathbf{s}) dt = \mathbf{H}_+ - \mathbf{H}_-, \text{ where } \mathbf{H}_+ \succeq \mathbf{0}, \mathbf{H}_- \preceq \mathbf{0},$$

which implies $\mathbf{g} = \eta\mathbf{H}\mathbf{s}$. Since $\eta \leq 1/\|\mathbf{l}_1\|_\infty$ guarantees $\|\eta\mathbf{s}\|_\infty \leq 1/\|\mathbf{l}_1\|_\infty$, Assumption 2a indicates that

$$\mathbf{H}_+ \preceq \text{diag}(\mathbf{l}_0 + \mathbf{l}_1 \odot |\nabla f(\mathbf{x})|), \quad \mathbf{H}_- \preceq \text{diag}(\mathbf{l}_0 + \mathbf{l}_1 \odot |\nabla f(\mathbf{x})|).$$

Therefore, the objective can be bounded by

$$\begin{aligned} \|\mathbf{g}\|_1 &= \langle \text{sign}(\mathbf{g}), \mathbf{g} \rangle = \langle \text{sign}(\mathbf{g}), (\mathbf{H}_+ - \mathbf{H}_-) \eta\mathbf{s} \rangle \\ &= \eta \langle \text{sign}(\mathbf{g}), \mathbf{H}_+ \mathbf{s} \rangle - \eta \langle \text{sign}(\mathbf{g}), \mathbf{H}_- \mathbf{s} \rangle \leq 2\eta \|\mathbf{l}_0 + \mathbf{l}_1 \odot |\nabla f(\mathbf{x})|\|_1. \end{aligned}$$

\blacksquare

Lemma C.5 (pth moment of mini-batch noise) *Under Assumptions 3a and 4a, the following holds for any $i \in [d], t \in [T]$:*

$$\mathbb{E} [|\mathbf{N}_t|^p | \mathcal{F}_{t-1}] \leq B^{1-p} \left(\boldsymbol{\sigma}_{0,i}^p + \boldsymbol{\sigma}_{1,i}^p |\nabla_i f(\mathbf{x}_t)|^p \right),$$

where \mathbf{n}_t is defined in (11).

Proof We denote $\mathbf{n}_{t,i}^b := \mathbf{g}_{t,i}^b - \nabla_i f(\mathbf{x}_t)$. So $\mathbf{n}_{t,i} = \frac{1}{B} \sum_{b=1}^B \mathbf{n}_{t,i}^b$. Under Assumption 4a and Jensen's inequality, we have

$$\begin{aligned} \mathbb{E} [|\mathbf{n}_{t,i}|^p | \mathcal{F}_{t-1}] &= \mathbb{E} \left[\left| \frac{1}{B} \sum_{b=1}^B \mathbf{n}_{t,i}^b \right|^p \middle| \mathcal{F}_{t-1} \right] \leq \mathbb{E} \left[\frac{1}{B^p} \sum_{b=1}^B \left| \mathbf{n}_{t,i}^b \right|^p \middle| \mathcal{F}_{t-1} \right] \\ &\leq \frac{1}{B^p} \sum_{b=1}^B \left(\boldsymbol{\sigma}_{0,i}^p + \boldsymbol{\sigma}_{1,i}^p |\nabla_i f(\mathbf{x}_t)|^p \right) = B^{1-p} \left(\boldsymbol{\sigma}_{0,i}^p + \boldsymbol{\sigma}_{1,i}^p |\nabla_i f(\mathbf{x}_t)|^p \right). \end{aligned}$$

■

Lemma C.6 (Regret Analysis of Diagonal AdaGrad) *Given an arbitrary sequence of vectors $\{\mathbf{v}_t\}_{t=1}^T \subset \mathbb{R}^d, T \in \mathbb{N}$, there exists a sequence of vectors $\{\mathbf{w}_t\}_{t=1}^T \subset \mathbb{R}^d$ such that (i) $\|\mathbf{w}_t\|_\infty \leq 1$, (ii) every \mathbf{w}_t only depends on $\mathbf{v}_1, \dots, \mathbf{v}_{t-1}$, and (iii) they further satisfy*

$$\sum_{t=1}^T \langle \mathbf{v}_t, \mathbf{w}_t \rangle \leq \sum_{i=1}^d 2 \sqrt{2 \sum_{t=1}^T \mathbf{v}_{t,i}^2} - \left\| \sum_{t=1}^T \mathbf{v}_t \right\|_1.$$

Proof The proof of this lemma stems from the regret analysis of AdaGrad-Norm (Streeter and McMahan, 2010; Duchi et al., 2011) in Liu and Zhou (2025), which is based on Rakhlin and Sridharan (2017, Lemma 2). Here, we adapt their analysis to the diagonal version of AdaGrad (McMahan and Streeter, 2010; Duchi et al., 2011). Define

$$\mathbf{w}_1 := \mathbf{0}, \quad \mathbf{w}_{t+1,i} := \Pi_{[-1,1]} [\mathbf{w}_{t,i} - \gamma_t \mathbf{v}_{t,i}], \quad \gamma_{t,i} = \begin{cases} \sqrt{\frac{2}{\sum_{s=1}^t \mathbf{v}_{s,i}^2}}, & t \geq 1 \\ +\infty, & t = 0 \end{cases}, \quad \forall i \in [d], \quad (12)$$

which ensures (i) and (ii) in Lemma C.6. By standard analysis of projected online subgradient descent (Orabona, 2019, Lemma 2.30), for any $\mathbf{u}_i \in [-1, 1]$,

$$\mathbf{v}_{t,i} \cdot (\mathbf{w}_{t,i} - \mathbf{u}_i) \leq \frac{(\mathbf{u}_i - \mathbf{w}_{t,i})^2}{2\gamma_{t,i}} - \frac{(\mathbf{u}_i - \mathbf{w}_{t+1,i})^2}{2\gamma_{t,i}} + \frac{\gamma_{t,i} \mathbf{v}_{t,i}^2}{2}.$$

Summing from 1 to T :

$$\begin{aligned} \sum_{t=1}^T \mathbf{v}_{t,i} \cdot (\mathbf{w}_{t,i} - \mathbf{u}_i) &\leq \sum_{t=1}^T \left(\frac{(\mathbf{u}_i - \mathbf{w}_{t,i})^2}{2\gamma_{t,i}} - \frac{(\mathbf{u}_i - \mathbf{w}_{t+1,i})^2}{2\gamma_{t,i}} + \frac{\gamma_{t,i} \mathbf{v}_{t,i}^2}{2} \right) \\ &= \frac{(\mathbf{u}_i - \mathbf{w}_{1,i})^2}{2\gamma_{1,i}} - \frac{(\mathbf{u}_i - \mathbf{w}_{T+1,i})^2}{2\gamma_{T,i}} + \sum_{t=2}^T (\mathbf{u}_i - \mathbf{w}_{t,i})^2 \left(\frac{1}{2\gamma_{t,i}} - \frac{1}{2\gamma_{t-1,i}} \right) + \sum_{t=1}^T \frac{\gamma_{t,i} \mathbf{v}_{t,i}^2}{2} \end{aligned}$$

$$\begin{aligned}
 &\leq \frac{1}{2\gamma_{1,i}} + \sum_{t=2}^T \left(\frac{2}{\gamma_{t,i}} - \frac{2}{\gamma_{t-1,i}} \right) + \sum_{t=1}^T \gamma_{t,i} \left(\frac{1}{2\gamma_{t,i}^2} - \frac{1}{2\gamma_{t-1,i}^2} \right) \\
 &\leq \frac{2}{\gamma_{T,i}} + \sum_{t=1}^T 2 \left(\frac{1}{\gamma_{t,i}} - \frac{1}{\gamma_{t-1,i}} \right) \leq \frac{4}{\gamma_{T,i}} = 2 \sqrt{2 \sum_{t=1}^T \mathbf{v}_{t,i}^2},
 \end{aligned}$$

where we utilize $\mathbf{u}_i \in [-1, 1]$, $\mathbf{w}_{1,i} = 0$, $\gamma_t \leq \gamma_{t-1}$, $\mathbf{u}_i - \mathbf{w}_{t,i} \in [-2, 2]$, $1/\gamma_{0,i} = 0$ in the second inequality. Rearranging the above relation and taking minimum over $\mathbf{u}_i \in [-1, 1]$,

$$\sum_{t=1}^T \mathbf{v}_{t,i} \cdot \mathbf{w}_{t,i} \leq 2 \sqrt{2 \sum_{t=1}^T \mathbf{v}_{t,i}^2} + \min_{\mathbf{u}_i \in [-1, 1]} \sum_{t=1}^T \mathbf{v}_{t,i} \cdot \mathbf{u}_i = 2 \sqrt{2 \sum_{t=1}^T \mathbf{v}_{t,i}^2} - \left| \sum_{t=1}^T \mathbf{v}_{t,i} \right|.$$

Summing the regret across all coordinates $i \in [d]$ finishes the proof. \blacksquare

Lemma C.7 (ℓ_1 -norm vector martingale concentration, Lemma 3 in Section 5.2) *Given a sequence of integrable random vectors $\mathbf{v}_t \in \mathbb{R}^d$, $\forall t \in \mathbb{N}$ such that $\mathbb{E}[\mathbf{v}_t | \mathcal{F}_{t-1}] = \mathbf{0}$ where $\mathcal{F}_t = \sigma(\mathbf{v}_1, \dots, \mathbf{v}_t)$ is the natural filtration, then for any $p \in [1, 2]$, there is*

$$\mathbb{E} \left[\left\| \sum_{t=1}^T \mathbf{v}_t \right\|_1 \right] \leq 2\sqrt{2} \sum_{i=1}^d \mathbb{E} \left[\|\mathbf{v}_{1:T,i}\|_p \right], \quad \forall T \in \mathbb{N},$$

where $\mathbf{v}_{1:T,i} := [\mathbf{v}_{1,i}, \dots, \mathbf{v}_{T,i}] \in \mathbb{R}^T$.

Proof According to Lemma C.6, there exists a sequence of random vectors $\{\mathbf{w}_t\}_{t=1}^T \subset \mathbb{R}^d$ such that (i) $\|\mathbf{w}_t\|_\infty \leq 1$, (ii) every $\mathbf{w}_t \in \mathcal{F}_{t-1}$, and (iii) they further satisfy

$$\sum_{t=1}^T \langle \mathbf{v}_t, \mathbf{w}_t \rangle \leq \sum_{i=1}^d 2\sqrt{2} \|\mathbf{v}_{1:T,i}\|_2 - \left\| \sum_{t=1}^T \mathbf{v}_t \right\|_1.$$

Rearranging this inequality and taking expectations yields

$$\mathbb{E} \left[\left\| \sum_{t=1}^T \mathbf{v}_t \right\|_1 \right] \leq 2\sqrt{2} \sum_{i=1}^d \mathbb{E} [\|\mathbf{v}_{1:T,i}\|_2] - \sum_{t=1}^T \mathbb{E} [\langle \mathbf{v}_t, \mathbf{w}_t \rangle] \leq 2\sqrt{2} \sum_{i=1}^d \mathbb{E} [\|\mathbf{v}_{1:T,i}\|_p],$$

where the last step is due to $\|\cdot\|_2 \leq \|\cdot\|_p$ and the tower rule:

$$\mathbb{E} [\langle \mathbf{v}_t, \mathbf{w}_t \rangle] = \mathbb{E} [\mathbb{E} [\langle \mathbf{v}_t, \mathbf{w}_t \rangle | \mathcal{F}_{t-1}]] = \mathbb{E} [\langle \mathbb{E} [\mathbf{v}_t | \mathcal{F}_{t-1}], \mathbf{w}_t \rangle] = 0. \quad \blacksquare$$

Lemma C.8 (Stability with weight decay) *Running Algorithm 2 with*

$$\lambda \leq \frac{1}{\eta} \left(1 - \frac{1}{2^{1/T}} \right), \text{ and } \|\mathbf{x}_1\|_\infty \leq \frac{a}{\lambda}, \quad \forall a \in (0, 1),$$

ensures that

$$\|\mathbf{x}_t\|_\infty \leq \frac{a+1}{2\lambda}, \quad \|\mathbf{x}_{t+1} - \mathbf{x}_t\|_\infty \leq \frac{a+3}{2}\eta, \quad \forall t \in [T].$$

Proof We first show that the trajectory is bounded if the model is appropriately initialized with $\|\mathbf{x}_1\|_\infty \leq a/\lambda$. Denote $1 - \eta\lambda$ by q , suggesting $q \in (1/2^{1/T}, 1)$ by the choice of λ . By the update rule of Algorithm 2, we have

$$\begin{aligned}\|\mathbf{x}_t\|_\infty &= \|(1 - \eta\lambda)\mathbf{x}_{t-1} - \eta \operatorname{sign}(\mathbf{v}_{t-1})\|_\infty \leq q \|\mathbf{x}_{t-1}\|_\infty + \eta \\ &\leq q^2 \|\mathbf{x}_{t-2}\|_\infty + q\eta + \eta \leq \dots \leq q^{t-1} \|\mathbf{x}_1\|_\infty + \eta \sum_{i=0}^{t-2} q^i \leq \frac{aq^{t-1}}{\lambda} + \frac{\eta(1 - q^{t-1})}{1 - q} \\ &= \frac{1 - (1 - a)q^{t-1}}{\lambda} \leq \frac{1 - (1 - a) \left(\frac{1}{2}\right)^{\frac{t-1}{T}}}{\lambda} \leq \frac{a+1}{2\lambda},\end{aligned}$$

which holds for any $t \in [T]$. Therefore, we can deduce

$$\|\mathbf{x}_{t+1} - \mathbf{x}_t\|_\infty = \|\eta\lambda\mathbf{x}_t + \eta \operatorname{sign}(\mathbf{v}_t)\|_\infty \leq \eta\lambda \|\mathbf{x}_t\|_\infty + \eta \leq \frac{a+3}{2}\eta, \quad \forall t \in [T].$$

■

Lemma C.9 (Lemma C.4 with weight decay) *For any sign vector $\mathbf{s} \in \{-1, 1\}^d$ and any $\eta \leq 1/((c+1)\|\mathbf{l}_1\|_\infty)$, $c > 0$, consider the sign-based update with weight decay:*

$$\mathbf{x}' := \mathbf{x} + \eta\mathbf{s}', \quad \mathbf{s}' = -\mathbf{s} - \lambda\mathbf{x}, \quad \forall \lambda \geq 0, \mathbf{x} \in \mathbb{R}^d \text{ such that } \|\mathbf{x}\|_\infty \leq c/\lambda.$$

Under Assumption 2a, it holds that

$$\|\nabla f(\mathbf{x}') - \nabla f(\mathbf{x})\|_1 \leq (2+2c)\eta (\|\mathbf{l}_0\|_1 + \langle \mathbf{l}_1, |\nabla f(\mathbf{x})| \rangle).$$

Proof For any f twice-differentiable on the line segment between \mathbf{x}' and \mathbf{x} , by Taylor's theorem,

$$\nabla f(\mathbf{x}') - \nabla f(\mathbf{x}) = \int_0^1 \nabla^2 f(\mathbf{x} + t\eta\mathbf{s}') \eta\mathbf{s}' dt = \left(\int_0^1 \nabla^2 f(\mathbf{x} + t\eta\mathbf{s}') dt \right) \cdot \eta\mathbf{s}'.$$

Define

$$\mathbf{g} := \nabla f(\mathbf{x}') - \nabla f(\mathbf{x}), \quad \mathbf{H} := \int_0^1 \nabla^2 f(\mathbf{x} + t\eta\mathbf{s}') dt = \mathbf{H}_+ - \mathbf{H}_-, \text{ where } \mathbf{H}_+ \succeq \mathbf{0}, \mathbf{H}_- \preceq \mathbf{0},$$

which implies $\mathbf{g} = \eta\mathbf{H}\mathbf{s}'$. Since

$$\|\mathbf{x}' - \mathbf{x}\|_\infty = \eta \|\mathbf{s}'\|_\infty \leq \eta \|\mathbf{s}\|_\infty + \eta\lambda \|\mathbf{x}\|_\infty \leq \eta + \eta c \leq 1/\|\mathbf{l}_1\|_\infty,$$

so Assumption 2a indicates that

$$\mathbf{H}_+ \preceq \operatorname{diag}(\mathbf{l}_0 + \mathbf{l}_1 \odot |\nabla f(\mathbf{x})|), \quad \mathbf{H}_- \preceq \operatorname{diag}(\mathbf{l}_0 + \mathbf{l}_1 \odot |\nabla f(\mathbf{x})|).$$

Thus, we can derive

$$\begin{aligned}\|\mathbf{g}\|_1 &= \langle \operatorname{sign}(\mathbf{g}), \mathbf{g} \rangle = \langle \operatorname{sign}(\mathbf{g}), (\mathbf{H}_+ - \mathbf{H}_-) \eta\mathbf{s}' \rangle = \eta \langle \operatorname{sign}(\mathbf{g}), \mathbf{H}_+ \mathbf{s}' \rangle - \eta \langle \operatorname{sign}(\mathbf{g}), \mathbf{H}_- \mathbf{s}' \rangle \\ &= \eta \langle \operatorname{sign}(\mathbf{g}), \mathbf{H}_- \mathbf{s} \rangle - \eta \langle \operatorname{sign}(\mathbf{g}), \mathbf{H}_+ \mathbf{s} \rangle + \eta\lambda \langle \operatorname{sign}(\mathbf{g}), \mathbf{H}_- \mathbf{x} \rangle - \eta\lambda \langle \operatorname{sign}(\mathbf{g}), \mathbf{H}_+ \mathbf{x} \rangle \\ &\leq 2\eta \|\mathbf{l}_0 + \mathbf{l}_1 \odot |\nabla f(\mathbf{x})|\|_1 + 2\eta\lambda \|\mathbf{x}\|_\infty \|\mathbf{l}_0 + \mathbf{l}_1 \odot |\nabla f(\mathbf{x})|\|_1 \\ &\leq (2+2c)\eta (\|\mathbf{l}_0\|_1 + \langle \mathbf{l}_1, |\nabla f(\mathbf{x})| \rangle).\end{aligned}$$

■

C.3. Proof of Theorem 1

For any $t \in [T]$, we have $\|\mathbf{x}_{t+1} - \mathbf{x}_t\|_\infty = \eta \|\text{sign}(\mathbf{m}_t)\|_\infty \leq 1/\|\mathbf{l}_1\|_\infty$ by the choice of $\eta \leq 1/\|\mathbf{l}_1\|_\infty$. Thus, under Assumption 2a, it holds that

$$\begin{aligned}
 f(\mathbf{x}_{t+1}) - f(\mathbf{x}_t) &\leq \langle \nabla f(\mathbf{x}_t), \mathbf{x}_{t+1} - \mathbf{x}_t \rangle + \frac{1}{2} \|\mathbf{x}_{t+1} - \mathbf{x}_t\|_{\mathbf{l}_0 + \mathbf{l}_1 \odot |\nabla f(\mathbf{x}_t)|}^2 \\
 &= \langle \nabla f(\mathbf{x}_t), -\eta \text{sign}(\mathbf{m}_t) \rangle + \frac{1}{2} \sum_{i=1}^d (\mathbf{l}_0 + \mathbf{l}_1 |\nabla_i f(\mathbf{x}_t)|) (\eta \text{sign}(\mathbf{m}_{t,i}))^2 \\
 &= \eta \langle \nabla f(\mathbf{x}_t), -\text{sign}(\nabla f(\mathbf{x}_t)) \rangle + \eta \langle \nabla f(\mathbf{x}_t), \text{sign}(\nabla f(\mathbf{x}_t)) - \text{sign}(\mathbf{m}_t) \rangle \\
 &\quad + \frac{\eta^2 \|\mathbf{l}_0\|_1}{2} + \frac{\eta^2 \langle \mathbf{l}_1, |\nabla f(\mathbf{x}_t)| \rangle}{2} \\
 &\leq -\eta \|\nabla f(\mathbf{x}_t)\|_1 + 2\eta \|\mathbf{m}_t - \nabla f(\mathbf{x}_t)\|_1 + \frac{\eta^2 \|\mathbf{l}_0\|_1}{2} + \frac{\eta^2 \|\mathbf{l}_1\|_\infty \|\nabla f(\mathbf{x}_t)\|_1}{2} \\
 &\leq -\frac{\eta}{2} \|\nabla f(\mathbf{x}_t)\|_1 + 2\eta \|\mathbf{m}_t - \nabla f(\mathbf{x}_t)\|_1 + \frac{\eta^2 \|\mathbf{l}_0\|_1}{2},
 \end{aligned}$$

where the second inequality is due to Lemma C.3; the last step utilizes $\eta \leq 1/\|\mathbf{l}_1\|_\infty$. Rearranging the above relation and summing up yields

$$\mathbb{E} \left[\frac{1}{T} \sum_{t=1}^T \|\nabla f(\mathbf{x}_t)\|_1 \right] \leq \frac{2\Delta_f}{\eta T} + 4\mathbb{E} \left[\frac{1}{T} \sum_{t=1}^T \|\mathbf{m}_t - \nabla f(\mathbf{x}_t)\|_1 \right] + \eta \|\mathbf{l}_0\|_1, \quad (13)$$

where we use $\Delta_f = f(\mathbf{x}_1) - f_* \geq f(\mathbf{x}_1) - f(\mathbf{x}_{T+1})$. Next, we proceed to bound the deviation between the momentum and the true gradient (Cutkosky and Mehta, 2020). By (11), we have

$$\begin{aligned}
 \boldsymbol{\epsilon}_t &= \mathbf{m}_t - \nabla f(\mathbf{x}_t) = \beta \mathbf{m}_{t-1} + (1-\beta) \mathbf{g}_t - \nabla f(\mathbf{x}_t) \\
 &= \beta (\mathbf{m}_{t-1} - \nabla f(\mathbf{x}_{t-1})) + \beta (\nabla f(\mathbf{x}_{t-1}) - \nabla f(\mathbf{x}_t)) + (1-\beta) (\mathbf{g}_t - \nabla f(\mathbf{x}_t)) \\
 &= \beta \boldsymbol{\epsilon}_{t-1} + \beta \mathbf{s}_t + (1-\beta) \mathbf{n}_t.
 \end{aligned} \quad (14)$$

Applying the above relation recursively yields

$$\boldsymbol{\epsilon}_t = \beta^{t-1} \mathbf{n}_1 + (1-\beta) \sum_{k=2}^t \beta^{t-k} \mathbf{n}_k + \sum_{k=2}^t \beta^{t-k+1} \mathbf{s}_k,$$

where we utilize $\boldsymbol{\epsilon}_1 = \mathbf{m}_1 - \nabla f(\mathbf{x}_1) = \mathbf{g}_1 - \nabla f(\mathbf{x}_1) = \mathbf{n}_1$. Next, we decompose $\boldsymbol{\epsilon}_t$ into

$$\mathbb{E} [\|\boldsymbol{\epsilon}_t\|_1] \leq \underbrace{\mathbb{E} [\|\beta^{t-1} \mathbf{n}_1\|_1]}_{A_t} + \underbrace{\mathbb{E} \left[\left\| (1-\beta) \sum_{k=2}^t \beta^{t-k} \mathbf{n}_k \right\|_1 \right]}_{B_t} + \underbrace{\mathbb{E} \left[\left\| \sum_{k=2}^t \beta^{t-k+1} \mathbf{s}_k \right\|_1 \right]}_{C_t}, \quad (15)$$

and bound these terms separately.

Initial noise A_t We have

$$\begin{aligned}
 A_t &= \beta^{t-1} \sum_{i=1}^d \mathbb{E} [|\mathbf{n}_{1,i}|] \stackrel{\text{Lemma C.2}}{\leq} \beta^{t-1} \sum_{i=1}^d (\mathbb{E} [|\mathbf{n}_{1,i}|^p])^{1/p} \\
 &\stackrel{\text{Lemma C.5}}{\leq} \beta^{t-1} \sum_{i=1}^d \left(B^{1-p} \left(\boldsymbol{\sigma}_{0,i}^p + \boldsymbol{\sigma}_{1,i}^p |\nabla_i f(\mathbf{x}_1)|^p \right) \right)^{1/p} \\
 &\stackrel{\text{Lemma C.1}}{\leq} \beta^{t-1} \sum_{i=1}^d B^{\frac{1-p}{p}} (\boldsymbol{\sigma}_{0,i} + \boldsymbol{\sigma}_{1,i} |\nabla_i f(\mathbf{x}_1)|) \\
 &\leq \beta^{t-1} B^{\frac{1-p}{p}} (\|\boldsymbol{\sigma}_0\|_1 + \|\boldsymbol{\sigma}_1\|_\infty \|\nabla f(\mathbf{x}_1)\|_1).
 \end{aligned} \tag{16}$$

Cumulative noise B_t Define $\mathbf{v}_k := \beta^{t-k} \mathbf{n}_k$, $k \in [2, t]$. It holds that

$$\frac{B_t}{1-\beta} \leq \mathbb{E} \left[\left\| \sum_{k=2}^t \mathbf{v}_k \right\|_1 \right] \stackrel{\text{Lemma C.7}}{\leq} 2\sqrt{2} \sum_{i=1}^d \mathbb{E} \left[\sum_{k=2}^t |\mathbf{v}_{k,i}|^p \right]^{1/p}. \tag{17}$$

Here, we cannot directly bound the above noise terms using similar procedures as in A_t due to technical reasons. As an alternative, we recursively expand the conditional expectation.

$$\begin{aligned}
 &\mathbb{E} \left[\left(\sum_{k=2}^t |\mathbf{v}_{k,i}|^p \right)^{1/p} \middle| \mathcal{F}_{t-1} \right] \stackrel{\text{Lemma C.2}}{\leq} \left(\sum_{k=2}^t \mathbb{E} [|\mathbf{v}_{t,i}|^p \mid \mathcal{F}_{t-1}] \right)^{1/p} \\
 &= \left(\sum_{k=2}^{t-1} |\mathbf{v}_{k,i}|^p + \mathbb{E} [|\mathbf{v}_{t,i}|^p \mid \mathcal{F}_{t-1}] \right)^{1/p} \\
 &\stackrel{\text{Lemma C.5}}{\leq} \left(\sum_{k=2}^{t-1} |\mathbf{v}_{k,i}|^p + \beta^{p(t-t)} B^{1-p} \left(\boldsymbol{\sigma}_{0,i}^p + \boldsymbol{\sigma}_{1,i}^p |\nabla_i f(\mathbf{x}_t)|^p \right) \right)^{1/p} \\
 &\stackrel{\text{Lemma C.1}}{\leq} \left(\sum_{k=2}^{t-1} |\mathbf{v}_{k,i}|^p + \beta^{p(t-t)} B^{1-p} \boldsymbol{\sigma}_{0,i}^p \right)^{1/p} + \beta^{t-t} B^{\frac{1-p}{p}} \boldsymbol{\sigma}_{1,i} |\nabla_i f(\mathbf{x}_t)|.
 \end{aligned} \tag{18}$$

Taking total expectations on both sides and applying the relation in (18) recursively:

$$\begin{aligned}
 &\mathbb{E} \left[\sum_{k=2}^t |\mathbf{v}_{k,i}|^p \right]^{1/p} \\
 &\leq \mathbb{E} \left[\sum_{k=2}^{t-1} |\mathbf{v}_{k,i}|^p + \beta^{p(t-t)} B^{1-p} \boldsymbol{\sigma}_{0,i}^p \right]^{1/p} + \beta^{t-t} B^{\frac{1-p}{p}} \boldsymbol{\sigma}_{1,i} \mathbb{E} [|\nabla_i f(\mathbf{x}_t)|] \\
 &\stackrel{\text{Lemma C.2}}{\leq} \left(\mathbb{E} \left[\sum_{k=2}^{t-1} |\mathbf{v}_{k,i}|^p + \beta^{p(t-t)} B^{1-p} \boldsymbol{\sigma}_{0,i}^p \right] \right)^{1/p} + \beta^{t-t} B^{\frac{1-p}{p}} \boldsymbol{\sigma}_{1,i} \mathbb{E} [|\nabla_i f(\mathbf{x}_t)|] \\
 &= \left(\mathbb{E} \left[\mathbb{E} \left[\sum_{k=2}^{t-1} |\mathbf{v}_{k,i}|^p \middle| \mathcal{F}_{t-2} \right] \right] + \beta^{p(t-t)} B^{1-p} \boldsymbol{\sigma}_{0,i}^p \right)^{1/p} + \beta^{t-t} B^{\frac{1-p}{p}} \boldsymbol{\sigma}_{1,i} \mathbb{E} [|\nabla_i f(\mathbf{x}_t)|]
 \end{aligned}$$

$$\begin{aligned}
 &\stackrel{(18)}{\leq} \left(\mathbb{E} \left[\mathbb{E} \left[\sum_{k=2}^{t-2} |\mathbf{v}_{k,i}|^p \middle| \mathcal{F}_{t-3} \right] \right] + \beta^{p(t-(t-1))} B^{1-p} \boldsymbol{\sigma}_{0,i}^p + \beta^{p(t-t)} B^{1-p} \boldsymbol{\sigma}_{0,i}^p \right)^{1/p} \\
 &\quad + \beta^{t-(t-1)} B^{\frac{1-p}{p}} \boldsymbol{\sigma}_{1,i} \mathbb{E} [|\nabla_i f(\mathbf{x}_{t-1})|] + \beta^{t-t} B^{\frac{1-p}{p}} \boldsymbol{\sigma}_{1,i} \mathbb{E} [|\nabla_i f(\mathbf{x}_t)|] \\
 &\leq \dots \\
 &\leq \left(\sum_{k=2}^t \beta^{p(t-k)} B^{1-p} \boldsymbol{\sigma}_{0,i}^p \right)^{1/p} + \sum_{k=2}^t \beta^{t-k} B^{\frac{1-p}{p}} \boldsymbol{\sigma}_{1,i} \mathbb{E} [|\nabla_i f(\mathbf{x}_k)|] \\
 &\leq \frac{B^{\frac{1-p}{p}} \boldsymbol{\sigma}_{0,i}}{(1-\beta^p)^{1/p}} + B^{\frac{1-p}{p}} \sum_{k=2}^t \beta^{t-k} \boldsymbol{\sigma}_{1,i} \mathbb{E} [|\nabla_i f(\mathbf{x}_k)|].
 \end{aligned}$$

Thus, combining with (17), we conclude that

$$\begin{aligned}
 \mathbf{B}_t &\leq 2\sqrt{2}(1-\beta)B^{\frac{1-p}{p}} \sum_{i=1}^d \left(\frac{\boldsymbol{\sigma}_{0,i}}{(1-\beta^p)^{1/p}} + \sum_{k=2}^t \beta^{t-k} \boldsymbol{\sigma}_{1,i} \mathbb{E} [|\nabla_i f(\mathbf{x}_k)|] \right) \\
 &\leq 2\sqrt{2}(1-\beta)B^{\frac{1-p}{p}} \left(\frac{\|\boldsymbol{\sigma}_0\|_1}{(1-\beta)^{1/p}} + \sum_{k=2}^t \beta^{t-k} \|\boldsymbol{\sigma}_1\|_\infty \mathbb{E} [\|\nabla f(\mathbf{x}_k)\|_1] \right) \\
 &\leq 2\sqrt{2}B^{\frac{1-p}{p}} (1-\beta)^{\frac{p-1}{p}} \|\boldsymbol{\sigma}_0\|_1 + 2\sqrt{2}B^{\frac{1-p}{p}} (1-\beta) \|\boldsymbol{\sigma}_1\|_\infty \sum_{k=2}^t \beta^{t-k} \mathbb{E} [\|\nabla f(\mathbf{x}_k)\|_1].
 \end{aligned} \tag{19}$$

Trajectory curvature \mathbf{C}_t Since $\{\mathbf{x}_t\}_{t \in [T]}$ are generated by sign-based updates, we can apply Lemma C.4 to bound $\|\mathbf{s}_k\|_1$:

$$\begin{aligned}
 \mathbf{C}_t &\leq \mathbb{E} \left[\sum_{k=2}^t \beta^{t-k+1} \|\mathbf{s}_k\|_1 \right] \leq \sum_{k=2}^t \beta^{t-k+1} \cdot \mathbb{E} [2\eta (\|\mathbf{l}_0\|_1 + \langle \mathbf{l}_1, |\nabla f(\mathbf{x}_k)| \rangle)] \\
 &\leq \frac{2\eta\beta \|\mathbf{l}_0\|_1}{1-\beta} + \sum_{k=2}^t 2\eta\beta^{t-k+1} \|\mathbf{l}_1\|_\infty \mathbb{E} [\|\nabla f(\mathbf{x}_k)\|_1].
 \end{aligned} \tag{20}$$

Combining the bounds for \mathbf{A}_t , \mathbf{B}_t , \mathbf{C}_t (adding (16), (19) and (20) together), we obtain

$$\begin{aligned}
 \mathbb{E} [\|\boldsymbol{\epsilon}_t\|_1] &\leq \beta^{t-1} B^{\frac{1-p}{p}} (\|\boldsymbol{\sigma}_0\|_1 + \|\boldsymbol{\sigma}_1\|_\infty \|\nabla f(\mathbf{x}_1)\|_1) \\
 &\quad + 2\sqrt{2}B^{\frac{1-p}{p}} (1-\beta)^{\frac{p-1}{p}} \|\boldsymbol{\sigma}_0\|_1 + 2\sqrt{2}B^{\frac{1-p}{p}} (1-\beta) \|\boldsymbol{\sigma}_1\|_\infty \sum_{k=2}^t \beta^{t-k} \mathbb{E} [\|\nabla f(\mathbf{x}_k)\|_1] \\
 &\quad + \frac{2\eta\beta \|\mathbf{l}_0\|_1}{1-\beta} + \sum_{k=2}^t 2\eta\beta^{t-k+1} \|\mathbf{l}_1\|_\infty \mathbb{E} [\|\nabla f(\mathbf{x}_k)\|_1].
 \end{aligned}$$

Summing from 1 to T :

$$\mathbb{E} \left[\frac{1}{T} \sum_{t=1}^T \|\boldsymbol{\epsilon}_t\|_1 \right] \leq \frac{B^{\frac{1-p}{p}}}{T(1-\beta)} (\|\boldsymbol{\sigma}_0\|_1 + \|\boldsymbol{\sigma}_1\|_\infty \|\nabla f(\mathbf{x}_1)\|_1) + 2\sqrt{2}B^{\frac{1-p}{p}} (1-\beta)^{\frac{p-1}{p}} \|\boldsymbol{\sigma}_0\|_1$$

$$\begin{aligned}
 & + 2\sqrt{2}B^{\frac{1-p}{p}}(1-\beta)\|\boldsymbol{\sigma}_1\|_\infty \sum_{t=1}^T \sum_{k=2}^t \frac{\beta^{t-k}}{T} \mathbb{E}[\|\nabla f(\mathbf{x}_k)\|_1] \\
 & + \frac{2\eta\beta\|\mathbf{l}_0\|_1}{1-\beta} + 2\eta\|\mathbf{l}_1\|_\infty \sum_{t=1}^T \sum_{k=2}^t \frac{\beta^{t-k+1}}{T} \mathbb{E}[\|\nabla f(\mathbf{x}_k)\|_1].
 \end{aligned}$$

Note that

$$\sum_{t=1}^T \sum_{k=2}^t \beta^{t-k} \mathbb{E}[\|\nabla f(\mathbf{x}_k)\|_1] = \sum_{t=2}^T \left(\sum_{k=0}^{T-t} \beta^k \right) \mathbb{E}[\|\nabla f(\mathbf{x}_t)\|_1] \leq \sum_{t=2}^T \frac{\mathbb{E}[\|\nabla f(\mathbf{x}_t)\|_1]}{(1-\beta)}. \quad (21)$$

Hence,

$$\begin{aligned}
 & \mathbb{E} \left[\frac{1}{T} \sum_{t=1}^T \|\boldsymbol{\epsilon}_t\|_1 \right] \\
 & \leq \frac{B^{\frac{1-p}{p}}}{T(1-\beta)} (\|\boldsymbol{\sigma}_0\|_1 + \|\boldsymbol{\sigma}_1\|_\infty \|\nabla f(\mathbf{x}_1)\|_1) + 2\sqrt{2}B^{\frac{1-p}{p}}(1-\beta)^{\frac{p-1}{p}} \|\boldsymbol{\sigma}_0\|_1 + \frac{2\eta\beta\|\mathbf{l}_0\|_1}{1-\beta} \\
 & \quad + 2\sqrt{2}B^{\frac{1-p}{p}} \|\boldsymbol{\sigma}_1\|_\infty \sum_{t=2}^T \frac{1}{T} \mathbb{E}[\|\nabla f(\mathbf{x}_k)\|_1] + 2\eta\|\mathbf{l}_1\|_\infty \sum_{t=2}^T \frac{\beta}{T(1-\beta)} \mathbb{E}[\|\nabla f(\mathbf{x}_t)\|_1] \quad (22) \\
 & = 2\sqrt{2}(1-\beta)^{\frac{p-1}{p}} B^{\frac{1-p}{p}} \|\boldsymbol{\sigma}_0\|_1 + \frac{B^{\frac{1-p}{p}} \|\boldsymbol{\sigma}_0\|_1 + B^{\frac{1-p}{p}} \|\boldsymbol{\sigma}_1\|_\infty \|\nabla f(\mathbf{x}_1)\|_1}{T(1-\beta)} + \frac{2\eta\beta\|\mathbf{l}_0\|_1}{1-\beta} \\
 & \quad + \sum_{t=2}^T \left(2\sqrt{2}B^{\frac{1-p}{p}} \|\boldsymbol{\sigma}_1\|_\infty + \frac{2\eta\|\mathbf{l}_1\|_\infty\beta}{1-\beta} \right) \frac{1}{T} \mathbb{E}[\|\nabla f(\mathbf{x}_t)\|_1].
 \end{aligned}$$

By (2), we deduce that

$$2\sqrt{2}B^{\frac{1-p}{p}} \|\boldsymbol{\sigma}_1\|_\infty + \frac{2\eta\|\mathbf{l}_1\|_\infty\beta}{1-\beta} \leq \frac{1}{16} + \frac{1}{16} = \frac{1}{8}.$$

Plugging the above relation into the last line of (22) and recall (13), we get

$$\begin{aligned}
 \mathbb{E} \left[\frac{1}{T} \sum_{t=1}^T \|\nabla f(\mathbf{x}_t)\|_1 \right] & \leq \frac{2\Delta_f}{\eta T} + \eta\|\mathbf{l}_0\|_1 + \mathbb{E} \left[\frac{1}{2T} \sum_{t=1}^T \mathbb{E}[\|\nabla f(\mathbf{x}_t)\|_1] \right] \\
 & + 8\sqrt{2}(1-\beta)^{\frac{p-1}{p}} B^{\frac{1-p}{p}} \|\boldsymbol{\sigma}_0\|_1 + \frac{4B^{\frac{1-p}{p}} (\|\boldsymbol{\sigma}_0\|_1 + \|\boldsymbol{\sigma}_1\|_\infty \|\nabla f(\mathbf{x}_1)\|_1)}{T(1-\beta)} + \frac{8\eta\beta\|\mathbf{l}_0\|_1}{1-\beta},
 \end{aligned}$$

Rearranging the above relation yields

$$\begin{aligned}
 \mathbb{E} \left[\frac{1}{T} \sum_{t=1}^T \|\nabla f(\mathbf{x}_t)\|_1 \right] & \leq \frac{4\Delta_f}{\eta T} + \frac{18\eta\beta\|\mathbf{l}_0\|_1}{1-\beta} + 16\sqrt{2}(1-\beta)^{\frac{p-1}{p}} B^{\frac{1-p}{p}} \|\boldsymbol{\sigma}_0\|_1 \\
 & \quad + \frac{8B^{\frac{1-p}{p}} (\|\boldsymbol{\sigma}_0\|_1 + \|\boldsymbol{\sigma}_1\|_\infty \|\nabla f(\mathbf{x}_1)\|_1)}{T(1-\beta)}.
 \end{aligned}$$

In view of η in (2), it holds that

$$\begin{aligned}
 \frac{4\Delta_f}{\eta T} + \frac{18\eta\beta\|\mathbf{l}_0\|_1}{1-\beta} &\leq 12\sqrt{\frac{2\Delta_f\|\mathbf{l}_0\|_1}{T(1-\beta)}} + \frac{128\beta\Delta_f\|\mathbf{l}_1\|_\infty}{T(1-\beta)} + \frac{9\|\mathbf{l}_0\|_1}{16\|\mathbf{l}_1\|_\infty} \\
 &\leq 12\sqrt{\frac{2\Delta_f\|\mathbf{l}_0\|_1}{T(1-\beta)}} + \frac{256\beta\Delta_f\|\mathbf{l}_1\|_\infty}{T(1-\beta)} \\
 &\leq \frac{12\sqrt{2}(\Delta_f\|\mathbf{l}_0\|_1)^{\frac{p-1}{3p-2}}\|\boldsymbol{\sigma}_0\|_1^{\frac{p}{3p-2}}}{(BT)^{\frac{p-1}{3p-2}}} + \frac{256\Delta_f^{\frac{2p-2}{3p-2}}\|\boldsymbol{\sigma}_0\|_1^{\frac{2p}{3p-2}}\|\mathbf{l}_1\|_\infty}{\|\mathbf{l}_0\|_1^{\frac{p}{3p-2}}(BT)^{\frac{2p-2}{3p-2}}},
 \end{aligned} \tag{23}$$

where the second inequality holds when $\sqrt{\frac{2\Delta_f(1-\beta)}{9\beta\|\mathbf{l}_0\|_1 T}} \geq \frac{1-\beta}{32\beta\|\mathbf{l}_1\|_\infty}$. Similarly, the rest terms are bounded by

$$\begin{aligned}
 &16\sqrt{2}(1-\beta)^{\frac{p-1}{p}}B^{\frac{1-p}{p}}\|\boldsymbol{\sigma}_0\|_1 + \frac{8B^{\frac{1-p}{p}}(\|\boldsymbol{\sigma}_0\|_1 + \|\boldsymbol{\sigma}_1\|_\infty\|\nabla f(\mathbf{x}_1)\|_1)}{T(1-\beta)} \\
 &\leq \frac{16\sqrt{2}(\Delta_f\|\mathbf{l}_0\|_1)^{\frac{p-1}{3p-2}}\|\boldsymbol{\sigma}_0\|_1^{\frac{p}{3p-2}}}{(BT)^{\frac{p-1}{3p-2}}} + \frac{8B^{\frac{1-p}{p}}(\|\boldsymbol{\sigma}_0\|_1 + \|\boldsymbol{\sigma}_1\|_\infty\|\nabla f(\mathbf{x}_1)\|_1)\|\boldsymbol{\sigma}_0\|_1^{\frac{2p}{3p-2}}}{(\Delta_f\|\mathbf{l}_0\|_1)^{\frac{p}{3p-2}}(BT)^{\frac{2p-2}{3p-2}}}
 \end{aligned} \tag{24}$$

Combining (24) with (23), we finally obtain

$$\begin{aligned}
 \mathbb{E}\left[\frac{1}{T}\sum_{t=1}^T\|\nabla f(\mathbf{x}_t)\|_1\right] &\leq \frac{28\sqrt{2}(\Delta_f\|\mathbf{l}_0\|_1)^{\frac{p-1}{3p-2}}\|\boldsymbol{\sigma}_0\|_1^{\frac{p}{3p-2}}}{(BT)^{\frac{p-1}{3p-2}}} \\
 &+ \frac{8B^{\frac{1-p}{p}}(\|\boldsymbol{\sigma}_0\|_1 + \|\boldsymbol{\sigma}_1\|_\infty\|\nabla f(\mathbf{x}_1)\|_1)\|\boldsymbol{\sigma}_0\|_1^{\frac{2p}{3p-2}}}{(\Delta_f\|\mathbf{l}_0\|_1)^{\frac{p}{3p-2}}(BT)^{\frac{2p-2}{3p-2}}} + \frac{256\Delta_f^{\frac{2p-2}{3p-2}}\|\boldsymbol{\sigma}_0\|_1^{\frac{2p}{3p-2}}\|\mathbf{l}_1\|_\infty}{\|\mathbf{l}_0\|_1^{\frac{p}{3p-2}}(BT)^{\frac{2p-2}{3p-2}}},
 \end{aligned}$$

which implies a convergence rate of $O\left((\Delta_f\|\mathbf{l}_0\|_1)^{\frac{p-1}{3p-2}}\|\boldsymbol{\sigma}_0\|_1^{\frac{p}{3p-2}}(BT)^{\frac{1-p}{3p-2}}\right)$.

C.4. Proof of Theorem 2

By Lemma C.8, $\|\mathbf{x}_{t+1} - \mathbf{x}_t\|_\infty \leq 5\eta/3$ holds for any $t \in [T]$ provided that $\|\mathbf{x}_1\|_\infty \leq 1/(3\lambda)$, which immediately implies $\|\mathbf{x}_{t+1} - \mathbf{x}_t\|_\infty \leq 1/\|\mathbf{l}_1\|_\infty$ by the choice of η in (3). Thus, under Assumption 2a, it holds that

$$\begin{aligned}
 f(\mathbf{x}_{t+1}) &\leq f(\mathbf{x}_t) + \langle \nabla f(\mathbf{x}_t), \mathbf{x}_{t+1} - \mathbf{x}_t \rangle + \frac{1}{2}\|\mathbf{x}_{t+1} - \mathbf{x}_t\|_{\mathbf{l}_0 + \mathbf{l}_1 \odot |\nabla f(\mathbf{x}_t)|}^2 \\
 &\leq f(\mathbf{x}_t) + \langle \nabla f(\mathbf{x}_t), -\eta \text{sign}(\mathbf{v}_t) \rangle + \langle \nabla f(\mathbf{x}_t), -\eta\lambda\mathbf{x}_t \rangle \\
 &\quad + \frac{1}{2}\|\mathbf{l}_0 + \mathbf{l}_1 \odot |\nabla f(\mathbf{x}_t)|\|_1\|\mathbf{x}_{t+1} - \mathbf{x}_t\|_\infty^2 \\
 &\stackrel{\text{Lemma C.8}}{\leq} f(\mathbf{x}_t) + \eta\langle \nabla f(\mathbf{x}_t), -\text{sign}(\nabla f(\mathbf{x}_t)) \rangle + \eta\langle \nabla f(\mathbf{x}_t), \text{sign}(\nabla f(\mathbf{x}_t)) - \text{sign}(\mathbf{v}_t) \rangle \\
 &\quad + \eta\lambda\|\mathbf{x}_t\|_\infty\|\nabla f(\mathbf{x}_t)\|_1 + \frac{25\eta^2}{9}(\|\mathbf{l}_0\|_1 + \langle \mathbf{l}_1, |\nabla f(\mathbf{x}_t)| \rangle)
 \end{aligned}$$

$$\begin{aligned}
 & \text{Lemmas C.3 and C.8} \\
 & \leq f(\mathbf{x}_t) - \eta \|\nabla f(\mathbf{x}_t)\|_1 + 2\eta \|\mathbf{v}_t - \nabla f(\mathbf{x}_t)\|_1 + \frac{2\eta}{3} \|\nabla f(\mathbf{x}_t)\|_1 \\
 & \quad + \frac{25\eta^2 \|\mathbf{l}_0\|_1}{9} + \frac{25\eta^2 \|\mathbf{l}_1\|_\infty \|\nabla f(\mathbf{x}_t)\|_1}{9} \\
 & \leq f(\mathbf{x}_t) - \frac{\eta}{6} \|\nabla f(\mathbf{x}_t)\|_1 + 2\eta \|\mathbf{v}_t - \nabla f(\mathbf{x}_t)\|_1 + \frac{25\eta^2 \|\mathbf{l}_0\|_1}{9},
 \end{aligned}$$

where the last step utilizes $\eta \leq 3/(50 \|\mathbf{l}_1\|_\infty)$. Similar to (13), we arrive at

$$\frac{1}{T} \sum_{t=1}^T \mathbb{E} [\|\nabla f(\mathbf{x}_t)\|_1] \leq \frac{6\Delta_f}{\eta T} + \frac{12}{T} \sum_{t=1}^T \mathbb{E} [\|\mathbf{v}_t - \nabla f(\mathbf{x}_t)\|_1] + \frac{50\eta \|\mathbf{l}_0\|_1}{3}. \quad (25)$$

Recall the notations in (11) and apply the same decomposition as in (14) to bound $\mathbb{E} [\|\mathbf{v}_t - \nabla f(\mathbf{x}_t)\|_1]$:

$$\begin{aligned}
 & \mathbb{E} [\|\mathbf{v}_t - \nabla f(\mathbf{x}_t)\|_1] = \mathbb{E} [\|\beta_1 \mathbf{m}_{t-1} + (1 - \beta_1) \mathbf{g}_t - \nabla f(\mathbf{x}_t)\|_1] \\
 & = \mathbb{E} [\|\beta_1 (\mathbf{m}_{t-1} - \nabla f(\mathbf{x}_{t-1})) + (1 - \beta_1) (\mathbf{g}_t - \nabla f(\mathbf{x}_t)) + \beta_1 (\nabla f(\mathbf{x}_{t-1}) - \nabla f(\mathbf{x}_t))\|_1] \quad (26) \\
 & \leq \beta_1 \mathbb{E} [\|\boldsymbol{\epsilon}_{t-1}\|_1] + (1 - \beta_1) \mathbb{E} [\|\mathbf{n}_t\|_1] + \beta_1 \mathbb{E} [\|\mathbf{s}_t\|_1],
 \end{aligned}$$

which holds for all $t \geq 2$. The noise term \mathbf{n}_t can be bounded by

$$\begin{aligned}
 \mathbb{E} [\|\mathbf{n}_t\|_1] &= \sum_{i=1}^d \mathbb{E} [\mathbb{E} [|\mathbf{n}_{t,i}| \mid \mathcal{F}_{t-1}]] \stackrel{\text{Lemma C.2}}{\leq} \sum_{i=1}^d \mathbb{E} \left[(\mathbb{E} [|\mathbf{n}_{t,i}|^p \mid \mathcal{F}_{t-1}])^{1/p} \right] \\
 &\stackrel{\text{Lemma C.5}}{\leq} \sum_{i=1}^d \mathbb{E} \left[\left(B^{1-p} (\boldsymbol{\sigma}_{0,i}^p + \boldsymbol{\sigma}_{1,i}^p |\nabla_i f(\mathbf{x}_t)|^p) \right)^{1/p} \right] \\
 &\stackrel{\text{Lemma C.1}}{\leq} \sum_{i=1}^d \mathbb{E} \left[B^{\frac{1-p}{p}} (\boldsymbol{\sigma}_{0,i} + \boldsymbol{\sigma}_{1,i} |\nabla_i f(\mathbf{x}_t)|) \right] \leq B^{\frac{1-p}{p}} (\|\boldsymbol{\sigma}_0\|_1 + \|\boldsymbol{\sigma}_1\|_\infty \mathbb{E} [\|\nabla f(\mathbf{x}_t)\|_1]).
 \end{aligned}$$

To bound the trajectory curvature term \mathbf{s}_t , note that the trajectory of Algorithm 2 satisfies the conditions in Lemma C.9 with $c = 2/3$ by Lemma C.8. Therefore, we deduce that

$$\mathbb{E} [\|\mathbf{s}_t\|_1] \leq \mathbb{E} \left[\frac{10\eta}{3} (\|\mathbf{l}_0\|_1 + \langle \mathbf{l}_1, |\nabla f(\mathbf{x})| \rangle) \right] \leq \frac{10\eta}{3} \|\mathbf{l}_0\|_1 + \frac{10\eta}{3} \|\mathbf{l}_1\|_\infty \mathbb{E} [\|\nabla f(\mathbf{x})\|_1].$$

Plugging the bounds for $\mathbb{E}[\|\mathbf{n}_t\|_1]$ and $\mathbb{E}[\|\mathbf{s}_t\|_1]$, then summing from 2 to T , we get

$$\begin{aligned}
 \frac{1}{T} \sum_{t=1}^T \mathbb{E}[\|\mathbf{v}_t - \nabla f(\mathbf{x}_t)\|_1] &= \frac{1}{T} \mathbb{E}[\|\mathbf{v}_1 - \nabla f(\mathbf{x}_1)\|_1] + \frac{1}{T} \sum_{t=2}^T \mathbb{E}[\|\mathbf{v}_t - \nabla f(\mathbf{x}_t)\|_1] \\
 &\leq \frac{1}{T} \mathbb{E}[\|\mathbf{n}_1\|_1] + \frac{\beta_1}{T} \sum_{t=2}^T \mathbb{E}[\|\boldsymbol{\epsilon}_{t-1}\|_1] + \frac{(1-\beta_1)}{T} \sum_{t=2}^T \mathbb{E}[\|\mathbf{n}_t\|_1] + \frac{\beta_1}{T} \sum_{t=2}^T \mathbb{E}[\|\mathbf{s}_t\|_1] \\
 &\leq \frac{\beta_1}{T} \sum_{t=1}^{T-1} \mathbb{E}[\|\boldsymbol{\epsilon}_t\|_1] + \frac{\beta_1}{T} \mathbb{E}[\|\mathbf{n}_1\|_1] + \frac{(1-\beta_1)}{T} \sum_{t=1}^T B^{\frac{1-p}{p}} (\|\boldsymbol{\sigma}_0\|_1 + \|\boldsymbol{\sigma}_1\|_\infty \mathbb{E}[\|\nabla f(\mathbf{x}_t)\|_1]) \\
 &\quad + \frac{\beta_1}{T} \sum_{t=2}^T \left(\frac{10\eta}{3} \|\mathbf{l}_0\|_1 + \frac{10\eta}{3} \|\mathbf{l}_1\|_\infty \mathbb{E}[\|\nabla f(\mathbf{x}_t)\|_1] \right) \\
 &\leq \frac{\beta_1}{T} \sum_{t=1}^{T-1} \mathbb{E}[\|\boldsymbol{\epsilon}_t\|_1] + \frac{\beta_1 (\|\boldsymbol{\sigma}_0\|_1 + \|\boldsymbol{\sigma}_1\|_\infty \|\nabla f(\mathbf{x}_1)\|_1)}{B^{\frac{p-1}{p}} T} + \frac{(1-\beta_1) \|\boldsymbol{\sigma}_0\|_1}{B^{\frac{p-1}{p}}} + \frac{10\eta\beta_1}{3} \|\mathbf{l}_0\|_1 \\
 &\quad + \frac{(1-\beta_1) \|\boldsymbol{\sigma}_1\|_\infty}{B^{\frac{p-1}{p}} T} \sum_{t=1}^T \mathbb{E}[\|\nabla f(\mathbf{x}_t)\|_1] + \frac{10\beta_1\eta \|\mathbf{l}_1\|_\infty}{3T} \sum_{t=2}^T \mathbb{E}[\|\nabla f(\mathbf{x}_t)\|_1],
 \end{aligned} \tag{27}$$

where the first inequality is due to $\mathbf{v}_1 - \nabla f(\mathbf{x}_1) = \mathbf{g}_1 - \nabla f(\mathbf{x}_1) = \mathbf{n}_1$. Next, we proceed by bounding the error term $\frac{\beta_1}{T} \sum_{t=1}^{T-1} \mathbb{E}[\|\boldsymbol{\epsilon}_t\|_1]$. Following the same recipe as in (14), we immediately obtain $\boldsymbol{\epsilon}_t = (1-\beta_2)\boldsymbol{\epsilon}_{t-1} + (1-\beta_2)\mathbf{s}_t + \beta_2\mathbf{n}_t$. Expanding this relation recursively yields

$$\boldsymbol{\epsilon}_t = \beta_2^{t-1} \mathbf{n}_1 + (1-\beta_2) \sum_{k=2}^t \beta_2^{t-k} \mathbf{n}_k + \sum_{k=2}^t \beta_2^{t-k+1} \mathbf{s}_k,$$

where we utilize $\boldsymbol{\epsilon}_1 = \mathbf{m}_1 - \nabla f(\mathbf{x}_1) = \mathbf{g}_1 - \nabla f(\mathbf{x}_1) = \mathbf{n}_1$. Next, we decompose $\boldsymbol{\epsilon}_t$ into

$$\mathbb{E}[\|\boldsymbol{\epsilon}_t\|_1] \leq \underbrace{\mathbb{E}[\|\beta_2^{t-1} \mathbf{n}_1\|_1]}_{A_t} + \underbrace{\mathbb{E}\left[\left\|\left(1-\beta_2\right) \sum_{k=2}^t \beta_2^{t-k} \mathbf{n}_k\right\|_1\right]}_{B_t} + \underbrace{\mathbb{E}\left[\left\|\sum_{k=2}^t \beta_2^{t-k+1} \mathbf{s}_k\right\|_1\right]}_{C_t},$$

which exhibits the almost identical form to that in (15), with the only difference in β . Thus, we can safely follow the derivations in Appendix C.3 to bound A_t, B_t, C_t . For A_t and B_t , we can simply replace the β in (16) and (19) by β_2 to obtain

$$\begin{aligned}
 A_t &\leq \beta_2^{t-1} B^{\frac{1-p}{p}} (\|\boldsymbol{\sigma}_0\|_1 + \|\boldsymbol{\sigma}_1\|_\infty \|\nabla f(\mathbf{x}_1)\|_1), \\
 B_t &\leq 2\sqrt{2} B^{\frac{1-p}{p}} (1-\beta_2)^{\frac{p-1}{p}} \|\boldsymbol{\sigma}_0\|_1 + 2\sqrt{2} B^{\frac{1-p}{p}} (1-\beta_2) \|\boldsymbol{\sigma}_1\|_\infty \sum_{k=2}^t \beta_2^{t-k} \mathbb{E}[\|\nabla f(\mathbf{x}_k)\|_1].
 \end{aligned}$$

For C_t , we can not directly substitute β in (20) with β_2 due to the presence of weight decay. Instead, we invoke Lemma C.9 to deduce

$$C_t \leq \mathbb{E} \left[\sum_{k=2}^t \beta_2^{t-k+1} \|\mathbf{s}_k\|_1 \right] \leq \sum_{k=2}^t \beta_2^{t-k+1} \cdot \mathbb{E} \left[\frac{10}{3} \eta (\|\mathbf{l}_0\|_1 + \langle \mathbf{l}_1, |\nabla f(\mathbf{x}_k)| \rangle) \right]$$

$$\leq \frac{10\eta\beta_2 \|\mathbf{l}_0\|_1}{3(1-\beta_2)} + \sum_{k=2}^t \frac{10}{3} \eta\beta_2^{t-k+1} \|\mathbf{l}_1\|_\infty \mathbb{E} [\|\nabla f(\mathbf{x}_k)\|_1].$$

Combining the bounds for $\mathbf{A}_t, \mathbf{B}_t, \mathbf{C}_t$ as below:

$$\begin{aligned} & \frac{1}{T} \sum_{t=1}^T \mathbb{E} [\|\boldsymbol{\epsilon}_t\|_1] \\ & \leq 2\sqrt{2}(1-\beta_2)^{\frac{p-1}{p}} B^{\frac{1-p}{p}} \|\boldsymbol{\sigma}_0\|_1 + \frac{B^{\frac{1-p}{p}} \|\boldsymbol{\sigma}_0\|_1 + B^{\frac{1-p}{p}} \|\boldsymbol{\sigma}_1\|_\infty \|\nabla f(\mathbf{x}_1)\|_1}{T(1-\beta_2)} + \frac{10\eta\beta_2 \|\mathbf{l}_0\|_1}{3(1-\beta_2)} \\ & \quad + \sum_{t=2}^T \left(2\sqrt{2}B^{\frac{1-p}{p}} \|\boldsymbol{\sigma}_1\|_\infty + \frac{10\eta \|\mathbf{l}_1\|_\infty \beta_2}{3(1-\beta_2)} \right) \frac{1}{T} \mathbb{E} [\|\nabla f(\mathbf{x}_t)\|_1]. \end{aligned}$$

Plugging the above relation into (27) and simplify:

$$\begin{aligned} & \frac{1}{T} \sum_{t=1}^T \mathbb{E} [\|\mathbf{v}_t - \nabla f(\mathbf{x}_t)\|_1] \\ & \leq 2\sqrt{2}\beta_1(1-\beta_2)^{\frac{p-1}{p}} B^{\frac{1-p}{p}} \|\boldsymbol{\sigma}_0\|_1 + \frac{\beta_1 (\|\boldsymbol{\sigma}_0\|_1 + \|\boldsymbol{\sigma}_1\|_\infty \|\nabla f(\mathbf{x}_1)\|_1)}{B^{\frac{p-1}{p}} T(1-\beta_2)} + \frac{10\eta\beta_1\beta_2 \|\mathbf{l}_0\|_1}{3(1-\beta_2)} \\ & \quad + \sum_{t=2}^T \left(2\sqrt{2}B^{\frac{1-p}{p}} \|\boldsymbol{\sigma}_1\|_\infty + \frac{10\eta \|\mathbf{l}_1\|_\infty \beta_2}{3(1-\beta_2)} \right) \frac{\beta_1}{T} \mathbb{E} [\|\nabla f(\mathbf{x}_t)\|_1] \\ & \quad + \frac{\beta_1 (\|\boldsymbol{\sigma}_0\|_1 + \|\boldsymbol{\sigma}_1\|_\infty \|\nabla f(\mathbf{x}_1)\|_1)}{B^{\frac{p-1}{p}} T} + \frac{(1-\beta_1) \|\boldsymbol{\sigma}_0\|_1}{B^{\frac{p-1}{p}}} + \frac{10\eta\beta_1}{3} \|\mathbf{l}_0\|_1 \\ & \quad + \frac{(1-\beta_1) \|\boldsymbol{\sigma}_1\|_\infty}{B^{\frac{p-1}{p}} T} \sum_{t=1}^T \mathbb{E} [\|\nabla f(\mathbf{x}_t)\|_1] + \frac{10\beta_1\eta \|\mathbf{l}_1\|_\infty}{3T} \sum_{t=2}^T \mathbb{E} [\|\nabla f(\mathbf{x}_t)\|_1] \\ & \leq \frac{2\sqrt{2}\beta_1 \|\boldsymbol{\sigma}_0\|_1}{(1-\beta_2)^{\frac{1-p}{p}} B^{\frac{p-1}{p}}} + \frac{(1-\beta_1) \|\boldsymbol{\sigma}_0\|_1}{B^{\frac{p-1}{p}}} + \frac{2\beta_1 (\|\boldsymbol{\sigma}_0\|_1 + \|\boldsymbol{\sigma}_1\|_\infty \|\nabla f(\mathbf{x}_1)\|_1)}{B^{\frac{p-1}{p}} T(1-\beta_2)} + \frac{10\eta\beta_1 \|\mathbf{l}_0\|_1}{3(1-\beta_2)} \\ & \quad + \frac{1}{T} \sum_{t=1}^T \left(2\sqrt{2}B^{\frac{1-p}{p}} \|\boldsymbol{\sigma}_1\|_\infty + \frac{10\eta\beta_1 \|\mathbf{l}_1\|_\infty}{3(1-\beta_2)} \right) \mathbb{E} [\|\nabla f(\mathbf{x}_t)\|_1] \\ & \leq \frac{2\sqrt{2} \|\boldsymbol{\sigma}_0\|_1}{(1-\beta_2)^{\frac{1-p}{p}} B^{\frac{p-1}{p}}} + \frac{(1-\beta_1) \|\boldsymbol{\sigma}_0\|_1}{B^{\frac{p-1}{p}}} + \frac{2 (\|\boldsymbol{\sigma}_0\|_1 + \|\boldsymbol{\sigma}_1\|_\infty \|\nabla f(\mathbf{x}_1)\|_1)}{B^{\frac{p-1}{p}} T(1-\beta_2)} + \frac{10\eta \|\mathbf{l}_0\|_1}{3(1-\beta_2)} \\ & \quad + \sum_{t=1}^T \frac{1}{24T} \mathbb{E} [\|\nabla f(\mathbf{x}_t)\|_1], \end{aligned}$$

where the last inequality uses the hyperparameters in (3), as depicted below:

$$2\sqrt{2}B^{\frac{1-p}{p}} \|\boldsymbol{\sigma}_1\|_\infty + \frac{10\eta\beta_1 \|\mathbf{l}_1\|_\infty}{3(1-\beta_2)} \leq \frac{1}{36} + \frac{1}{36} = \frac{1}{18}.$$

Now, it suffices to combine the above error bound for $\frac{1}{T} \sum_{t=1}^T \mathbb{E} [\|\mathbf{v}_t - \nabla f(\mathbf{x}_t)\|_1]$ with (25), which gives

$$\begin{aligned} \frac{1}{T} \sum_{t=1}^T \mathbb{E} [\|\nabla f(\mathbf{x}_t)\|_1] &\leq \frac{12\Delta_f}{\eta T} + \frac{170\eta \|\mathbf{l}_0\|_1}{1 - \beta_2} + \frac{72\sqrt{2} \|\boldsymbol{\sigma}_0\|_1}{(1 - \beta_2)^{\frac{1-p}{p}} B^{\frac{p-1}{p}}} \\ &+ \frac{36(1 - \beta_1) \|\boldsymbol{\sigma}_0\|_1}{B^{\frac{p-1}{p}}} + \frac{72 (\|\boldsymbol{\sigma}_0\|_1 + \|\boldsymbol{\sigma}_1\|_\infty \|\nabla f(\mathbf{x}_1)\|_1)}{B^{\frac{p-1}{p}} T(1 - \beta_2)}. \end{aligned}$$

Choosing $B, \beta_1, \beta_2, \eta$ according to (3) yields the desired bound.

Appendix D. Analysis for Muon and Muonlight

As established in Appendix B.4, Assumption 4b implies Assumption 4c. Accordingly, throughout this appendix, we maintain Assumption 4b as our operative assumption while utilizing the relation (10) specified in Assumption 4c.

D.1. Matrix Calculus

Lemmas D.1 and D.2 are standard textbook results (Bhatia, 1996; Horn and Johnson, 2012; Gupta et al., 2018), which we omit the proof here for simplicity.

Lemma D.1 (Properties of trace and matrix norms) *For any $\mathbf{X} \in \mathbb{R}^{m \times n}, \mathbf{Y} \in \mathbb{R}^{n \times r}, \mathbf{L}, \mathbf{L}' \in \mathbb{S}^n$*

$$1. \text{tr}(\mathbf{L}) = \|\mathbf{L}\|_*, \text{tr}(|\mathbf{X}|_m) = \text{tr}((\mathbf{X}\mathbf{X}^\top)^{1/2}) = \|\mathbf{X}\|_*.$$

$$2. \|\mathbf{XY}\|_* \leq \min \left\{ \|\mathbf{X}\|_{\text{op}} \|\mathbf{Y}\|_*, \|\mathbf{X}\|_* \|\mathbf{Y}\|_{\text{op}} \right\}.$$

Lemma D.2 (Properties of the msign(\cdot) operator) *For any $\mathbf{X} \in \mathbb{R}^{m \times n}, \mathbf{L} \in \mathbb{S}^n, a \in \mathbb{R}$*

$$1. \langle \mathbf{X}, \text{msign}(\mathbf{X}) \rangle = \|\mathbf{X}\|_*.$$

$$2. \text{msign}(a\mathbf{X}) = \text{msign}(\mathbf{X}).$$

$$3. \|\text{msign}(\mathbf{X})\|_{\mathbf{L}}^2 = \text{tr}((\text{msign}(\mathbf{X}))^\top \mathbf{L} \cdot \text{msign}(\mathbf{X})) \leq \text{tr}(\mathbf{L}).$$

Lemma D.3 (Matrix Extension of Lemma C.3) *For any $\mathbf{X}, \mathbf{Y} \in \mathbb{R}^{m \times n}$, it holds that*

$$\langle \mathbf{X}, \text{msign}(\mathbf{X}) - \text{msign}(\mathbf{Y}) \rangle \leq 2 \|\mathbf{X} - \mathbf{Y}\|_*.$$

Proof By Lemma D.2, we compute

$$\begin{aligned} \langle \mathbf{X}, \text{msign}(\mathbf{X}) - \text{msign}(\mathbf{Y}) \rangle &= \langle \mathbf{X}, \text{msign}(\mathbf{X}) \rangle - \langle \mathbf{X}, \text{msign}(\mathbf{Y}) \rangle \\ &= \|\mathbf{X}\|_* - \|\mathbf{Y}\|_* + \langle \mathbf{Y} - \mathbf{X}, \text{msign}(\mathbf{Y}) \rangle \\ &\leq \|\mathbf{X} - \mathbf{Y}\|_* + \|\mathbf{Y} - \mathbf{X}\|_* \|\text{msign}(\mathbf{Y})\|_{\text{op}} \leq 2 \|\mathbf{X} - \mathbf{Y}\|_*, \end{aligned}$$

where the first inequality uses the triangle inequality as well as the duality between nuclear norm and operator norm. \blacksquare

Lemma D.4 (Matrix Cauchy-Schwarz Inequality, Lemma 8 in An et al. (2025)) *For any $\mathbf{X} \in \mathbb{R}^{m \times n}$ and $\mathbf{L} \in \mathbb{S}^m, \mathbf{L} \succ 0$, it holds that*

$$\|\mathbf{X}\|_* \leq \sqrt{\|\mathbf{L}\|_* \text{tr}(\mathbf{X}^\top \mathbf{L}^{-1} \mathbf{X})} = \sqrt{\|\mathbf{L}\|_* \|\mathbf{X}\|_{\mathbf{L}^{-1}}^2}.$$

D.2. Technical Lemmas

Lemma D.5 (Descent Lemma) *Under Assumption 2b, if $\|\mathbf{X}' - \mathbf{X}\|_{\text{op}} \leq 1/\|\mathbf{L}_1\|_{\text{op}}$, then:*

$$f(\mathbf{X}') \leq f(\mathbf{X}) + \langle \nabla f(\mathbf{X}), \mathbf{X}' - \mathbf{X} \rangle + \frac{1}{2} \|\mathbf{X}' - \mathbf{X}\|_{\mathbf{L}(\mathbf{X})}^2$$

Proof Define $\mathbf{X}(s) = s\mathbf{X}' + (1-s)\mathbf{X}$, $\forall s \in [0, 1]$, which implies $\|\mathbf{X}(s) - \mathbf{X}\|_{\text{op}} = s\|\mathbf{X}' - \mathbf{X}\|_{\text{op}} \leq 1/\|\mathbf{L}_1\|_{\text{op}}$. By Taylor expansion, we have

$$\begin{aligned} f(\mathbf{X}') &= f(\mathbf{X}) + \langle \nabla f(\mathbf{X}), \mathbf{X}' - \mathbf{X} \rangle + \int_0^1 \langle \nabla f(\mathbf{X}(s)) - \nabla f(\mathbf{X}), \mathbf{X}' - \mathbf{X} \rangle \, ds \\ &\leq f(\mathbf{X}) + \langle \nabla f(\mathbf{X}), \mathbf{X}' - \mathbf{X} \rangle + \int_0^1 \|\nabla f(\mathbf{X}(s)) - \nabla f(\mathbf{X})\|_{(\mathbf{L}(\mathbf{X}))^{-1}} \|\mathbf{X}' - \mathbf{X}\|_{\mathbf{L}(\mathbf{X})} \, ds \\ &\stackrel{\text{Assumption 2b}}{\leq} f(\mathbf{X}) + \langle \nabla f(\mathbf{X}), \mathbf{X}' - \mathbf{X} \rangle + \int_0^1 \|\mathbf{X}(s) - \mathbf{X}\|_{\mathbf{L}(\mathbf{X})} \|\mathbf{X}' - \mathbf{X}\|_{\mathbf{L}(\mathbf{X})} \, ds \\ &= f(\mathbf{X}) + \langle \nabla f(\mathbf{X}), \mathbf{X}' - \mathbf{X} \rangle + \int_0^1 s \|\mathbf{X}' - \mathbf{X}\|_{\mathbf{L}(\mathbf{X})}^2 \, ds \\ &= f(\mathbf{X}) + \langle \nabla f(\mathbf{X}), \mathbf{X}' - \mathbf{X} \rangle + \frac{1}{2} \|\mathbf{X}' - \mathbf{X}\|_{\mathbf{L}(\mathbf{X})}^2, \end{aligned}$$

where the first inequality is due to Cauchy-Schwarz inequality, and the fact that $\|\cdot\|_{\mathbf{L}(\mathbf{X})}$ and $\|\cdot\|_{(\mathbf{L}(\mathbf{X}))^{-1}}$ are primal-dual norm pairs (Nesterov et al., 2018; An et al., 2025). \blacksquare

Lemma D.6 (Matrix Version of Lemma C.5) *Under Assumption 4b, the following holds for any $t \in [T]$:*

$$\mathbb{E} \left[\|\mathbf{N}_t\|_{|\mathbf{V}_0|_m^{-1}}^p \mid \mathcal{F}_{t-1} \right] \leq B^{1-p} \left(\|\mathbf{V}_0\|_*^{p/2} + \frac{\|\mathbf{V}_1\|_{\text{op}}^p \|\nabla_t\|_*^p}{\|\mathbf{V}_0\|_*^{p/2}} \right),$$

where \mathbf{N}_t is defined in (32).

Proof We denote $\mathbf{N}_t^b := \mathbf{G}_t^b - \nabla f(\mathbf{X}_t)$. So $\mathbf{N}_t = \frac{1}{B} \sum_{b=1}^B \mathbf{N}_t^b$. Under Assumption 4b and the convexity of $\|\cdot\|_{|\mathbf{V}_0|_m^{-1}}$, we have

$$\begin{aligned} \mathbb{E} \left[\|\mathbf{N}_t\|_{|\mathbf{V}_0|_m^{-1}}^p \mid \mathcal{F}_{t-1} \right] &= \mathbb{E} \left[\left\| \frac{1}{B} \sum_{b=1}^B \mathbf{N}_t^b \right\|_{|\mathbf{V}_0|_m^{-1}}^p \mid \mathcal{F}_{t-1} \right] \leq \mathbb{E} \left[\frac{1}{B^p} \sum_{b=1}^B \|\mathbf{N}_t^b\|_{|\mathbf{V}_0|_m^{-1}}^p \mid \mathcal{F}_{t-1} \right] \\ &\leq \frac{1}{B^p} \sum_{b=1}^B \left(\|\mathbf{V}_0\|_*^{p/2} + \frac{\|\mathbf{V}_1\|_{\text{op}}^p \|\nabla f(\mathbf{X}_t)\|_*^p}{\|\mathbf{V}_0\|_*^{p/2}} \right) = B^{1-p} \left(\|\mathbf{V}_0\|_*^{p/2} + \frac{\|\mathbf{V}_1\|_{\text{op}}^p \|\nabla f(\mathbf{X}_t)\|_*^p}{\|\mathbf{V}_0\|_*^{p/2}} \right). \end{aligned}$$

\blacksquare

Lemma D.7 (Matrix Extension of Lemmas C.6 and C.7; Lemma 4 in Section 5.2) *Given an arbitrary sequence of matrices $\{\mathbf{G}_t\}_{t=1}^T \subset \mathbb{R}^{m \times n}$, $T \in \mathbb{N}$, there exists a sequence of vectors $\{\mathbf{W}_t\}_{t=1}^T \subset$*

$\mathbb{R}^{m \times n}$ such that (i) $\|\mathbf{W}_t\|_{\text{op}} \leq 1$, (ii) every \mathbf{W}_t only depends on $\mathbf{G}_1, \dots, \mathbf{G}_{t-1}$, and (iii) they further satisfy

$$\sum_{t=1}^T \langle \mathbf{G}_t, \mathbf{W}_t \rangle \leq 2\sqrt{2} \left\| \left(\sum_{t=1}^T \mathbf{G}_t \mathbf{G}_t^\top \right)^{1/2} \right\|_* - \left\| \sum_{t=1}^T \mathbf{G}_t \right\|_*.$$

If $\{\mathbf{G}_t\}_{t=1}^T \subset \mathbb{R}^{m \times n}$, $T \in \mathbb{N}$ form a martingale difference sequence, i.e., $\mathbb{E}[\mathbf{G}_t | \mathcal{F}_{t-1}] = \mathbf{0}$ where $\mathcal{F}_t = \sigma(\mathbf{G}_1, \dots, \mathbf{G}_t)$ is the natural filtration, then there is

$$\mathbb{E} \left[\left\| \sum_{t=1}^T \mathbf{G}_t \right\|_* \right] \leq 2\sqrt{2} \mathbb{E} \left[\left\| \left(\sum_{t=1}^T \mathbf{G}_t \mathbf{G}_t^\top \right)^{1/2} \right\|_* \right].$$

Proof This lemma is motivated by the regret analysis of the ASGO optimizer (An et al., 2025; Xie et al., 2025a). Consider a closed convex set $\mathcal{W} := \left\{ \|\mathbf{W}\|_{\text{op}} \leq 1 | \mathbf{W} \in \mathbb{R}^{m \times n} \right\}$. Then, imagine there is an online algorithm given by

$$\mathbf{W}_1 = \mathbf{\Lambda}_0 = \mathbf{0}, \quad \mathbf{\Lambda}_t = \left(\mathbf{\Lambda}_{t-1}^2 + \mathbf{G}_t \mathbf{G}_t^\top \right)^{1/2}, \quad \mathbf{W}_{t+1} = \Pi_{\mathcal{W}}^{\mathbf{\Lambda}_t} (\mathbf{W}_t - \eta \mathbf{\Lambda}_t^{-1} \mathbf{G}_t), \quad \forall t \in [1, T], \quad (28)$$

where the generalized projection operator (Hazan et al., 2007; Duchi et al., 2011) is defined as

$$\Pi_{\mathcal{W}}^{\mathbf{\Lambda}}(\mathbf{W}) := \underset{\mathbf{W}' \in \mathcal{W}}{\operatorname{argmin}} \|\mathbf{W} - \mathbf{W}'\|_{\mathbf{\Lambda}}^2,$$

and $\eta \in \mathbb{R}$ is the step size to be determined later. Clearly, the construction in (28) satisfies conditions (i) and (ii). So it suffices to prove (iii). For any $\mathbf{W}_* \in \mathcal{W}$, the non-expansiveness of the generalized projection operator (Hazan et al., 2007, Lemma 8) implies

$$\begin{aligned} \|\mathbf{W}_{t+1} - \mathbf{W}_*\|_{\mathbf{\Lambda}_t}^2 &\leq \|\mathbf{W}_t - \eta \mathbf{\Lambda}_t^{-1} \mathbf{G}_t - \mathbf{W}_*\|_{\mathbf{\Lambda}_t}^2 \\ &= \|\mathbf{W}_t - \mathbf{W}_*\|_{\mathbf{\Lambda}_t}^2 + \eta^2 \|\mathbf{G}_t\|_{\mathbf{\Lambda}_t^{-1}}^2 - 2\eta \langle \mathbf{G}_t, \mathbf{W}_t - \mathbf{W}_* \rangle \end{aligned}$$

Rearranging and summing from 1 to T :

$$\begin{aligned} \sum_{t=1}^T \langle \mathbf{G}_t, \mathbf{W}_t \rangle &\leq \sum_{t=1}^T \left(\frac{\|\mathbf{W}_t - \mathbf{W}_*\|_{\mathbf{\Lambda}_t}^2 - \|\mathbf{W}_{t+1} - \mathbf{W}_*\|_{\mathbf{\Lambda}_t}^2}{2\eta} + \frac{\eta}{2} \|\mathbf{G}_t\|_{\mathbf{\Lambda}_t^{-1}}^2 + \langle \mathbf{G}_t, \mathbf{W}_* \rangle \right) \\ &= \sum_{t=1}^T \left(\frac{\|\mathbf{W}_t - \mathbf{W}_*\|_{\mathbf{\Lambda}_t}^2 - \|\mathbf{W}_t - \mathbf{W}_*\|_{\mathbf{\Lambda}_{t-1}}^2}{2\eta} + \frac{\eta}{2} \|\mathbf{G}_t\|_{\mathbf{\Lambda}_{t-1}}^2 + \langle \mathbf{G}_t, \mathbf{W}_* \rangle \right) - \frac{\|\mathbf{W}_{T+1} - \mathbf{W}_*\|_{\mathbf{\Lambda}_T}^2}{2\eta} \\ &\leq \sum_{t=1}^T \left(\frac{\|\mathbf{W}_t - \mathbf{W}_*\|_{\mathbf{\Lambda}_t - \mathbf{\Lambda}_{t-1}}^2}{2\eta} + \frac{\eta}{2} \|\mathbf{G}_t\|_{\mathbf{\Lambda}_t^{-1}}^2 + \langle \mathbf{G}_t, \mathbf{W}_* \rangle \right), \end{aligned}$$

where the first equality is due to $\Lambda_0 = \mathbf{0}$. We proceed by bounding the three terms above. For the first term:

$$\begin{aligned}
 \sum_{t=1}^T \frac{\|\mathbf{W}_t - \mathbf{W}_*\|_{\Lambda_t - \Lambda_{t-1}}^2}{2\eta} &= \frac{1}{2\eta} \sum_{t=1}^T \left\langle (\mathbf{W}_t - \mathbf{W}_*) (\mathbf{W}_t - \mathbf{W}_*)^\top, \Lambda_t - \Lambda_{t-1} \right\rangle \\
 &\leq \frac{1}{2\eta} \sum_{t=1}^T \left\| (\mathbf{W}_t - \mathbf{W}_*) (\mathbf{W}_t - \mathbf{W}_*)^\top \right\|_{\text{op}} \|\Lambda_t - \Lambda_{t-1}\|_* \\
 &\leq \frac{1}{2\eta} \sum_{t=1}^T \|\mathbf{W}_t - \mathbf{W}_*\|_{\text{op}}^2 \text{tr}(\Lambda_t - \Lambda_{t-1}) \\
 &\leq \frac{2}{\eta} \sum_{t=1}^T \text{tr}(\Lambda_t - \Lambda_{t-1}) = \frac{2 \text{tr}(\Lambda_T)}{\eta},
 \end{aligned} \tag{29}$$

where the first inequality leverages the Cauchy-Schwarz inequality; the second inequality utilizes the submultiplicativity of $\|\cdot\|_{\text{op}}$ as well as $\Lambda_t - \Lambda_{t-1} \succeq \mathbf{0}$; the third inequality is due to $\|\mathbf{W}_t - \mathbf{W}_*\|_{\text{op}} \leq \|\mathbf{W}_t\|_{\text{op}} + \|\mathbf{W}_*\|_{\text{op}} \leq 2$. For the second term,

$$\frac{\eta}{2} \sum_{t=1}^T \|\mathbf{G}_t\|_{\Lambda_t^{-1}}^2 \leq \eta \sum_{t=1}^T 2 \text{tr}(\Lambda_t - \Lambda_{t-1}) = \eta \text{tr}(\Lambda_T), \tag{30}$$

where the inequality follows from [An et al. \(2025, Eq. \(9\)\)](#). For the third term, notice that the bounds in (29) and (30) are irrelevant of \mathbf{W}_* , so we can choose \mathbf{W}_* to satisfy the following relation:

$$\sum_{t=1}^T \langle \mathbf{G}_t, \mathbf{W}_* \rangle = - \left\| \sum_{t=1}^T \mathbf{G}_t \right\|_*, \quad \text{where } \mathbf{W}_* = \underset{\mathbf{W}'_* \in \mathcal{W}}{\text{argmin}} \left\langle \sum_{t=1}^T \mathbf{G}_t, \mathbf{W}'_* \right\rangle. \tag{31}$$

Plugging in (29), (30) and (31) into the original regret bound, we obtain

$$\sum_{t=1}^T \langle \mathbf{G}_t, \mathbf{W}_t \rangle \leq \frac{2 \text{tr}(\Lambda_T)}{\eta} + \eta \text{tr}(\Lambda_T) - \left\| \sum_{t=1}^T \mathbf{G}_t \right\|_* = 2\sqrt{2} \text{tr}(\Lambda_T) - \left\| \sum_{t=1}^T \mathbf{G}_t \right\|_*,$$

where we specify $\eta = \sqrt{2}$. According to (28), we have $\Lambda_T = \left(\sum_{t=1}^T \mathbf{G}_t \mathbf{G}_t^\top \right)^{1/2}$, which completes the first part of the proof. The second part of the proof follows the same recipe as in [Lemma C.7](#). If $\{\mathbf{G}_t\}_{t=1}^T$ further form a martingale difference sequence, then after taking total expectations, it holds that

$$\begin{aligned}
 \mathbb{E} \left[\left\| \sum_{t=1}^T \mathbf{G}_t \right\|_* \right] &\leq 2\sqrt{2} \mathbb{E} \left[\left\| \left(\sum_{t=1}^T \mathbf{G}_t \mathbf{G}_t^\top \right)^{1/2} \right\|_* \right] - \mathbb{E} \left[\sum_{t=1}^T \langle \mathbf{G}_t, \mathbf{W}_t \rangle \right] \\
 &= 2\sqrt{2} \mathbb{E} \left[\left\| \left(\sum_{t=1}^T \mathbf{G}_t \mathbf{G}_t^\top \right)^{1/2} \right\|_* \right] - \sum_{t=1}^T \mathbb{E} [\langle \mathbb{E}[\mathbf{G}_t | \mathcal{F}_{t-1}], \mathbf{W}_t \rangle] \\
 &= 2\sqrt{2} \mathbb{E} \left[\left\| \left(\sum_{t=1}^T \mathbf{G}_t \mathbf{G}_t^\top \right)^{1/2} \right\|_* \right].
 \end{aligned}$$

■

Lemma D.8 (Stability with weight decay, matrix version of Lemma C.8) *Running Algorithm 4*

$$\lambda \leq \frac{1}{\eta} \left(1 - \frac{1}{2^{1/T}} \right), \text{ and } \|\mathbf{X}_1\|_{\text{op}} \leq \frac{a}{\lambda}, \quad \forall a \in (0, 1),$$

ensures that

$$\|\mathbf{X}_t\|_{\text{op}} \leq \frac{a+1}{2\lambda}, \quad \|\mathbf{X}_{t+1} - \mathbf{X}_t\|_{\text{op}} \leq \frac{a+3}{2}\eta, \quad \forall t \in [T].$$

Proof The proof of this lemma is analogous to that of Lemma C.8. Denote $1 - \eta\lambda$ by q , which implies $q \in (1/2^{1/T}, 1)$ as $\lambda \leq \frac{1}{\eta} \left(1 - \frac{1}{2^{1/T}} \right)$. By the update rule of Algorithm 4, we have

$$\begin{aligned} \|\mathbf{X}_t\|_{\text{op}} &= \left\| (1 - \eta\lambda)\mathbf{X}_{t-1} - \eta \text{msign}(\tilde{\mathbf{B}}_{t-1}) \right\|_{\text{op}} \leq q \|\mathbf{X}_{t-1}\|_{\text{op}} + \eta \\ &\leq q^2 \|\mathbf{X}_{t-2}\|_{\text{op}} + q\eta + \eta \leq \dots \leq q^{t-1} \|\mathbf{X}_1\|_{\text{op}} + \eta \sum_{i=0}^{t-2} q^i \leq \frac{aq^{t-1}}{\lambda} + \frac{\eta(1 - q^{t-1})}{1 - q} \\ &= \frac{1 - (1 - a)q^{t-1}}{\lambda} \leq \frac{1 - (1 - a) \left(\frac{1}{2} \right)^{\frac{t-1}{T}}}{\lambda} \leq \frac{a+1}{2\lambda}, \end{aligned}$$

which holds for any $t \in [T]$. Therefore, we can deduce

$$\|\mathbf{X}_{t+1} - \mathbf{X}_t\|_{\text{op}} = \left\| \eta\lambda\mathbf{X}_t + \eta \text{msign}(\tilde{\mathbf{B}}_t) \right\|_{\text{op}} \leq \eta\lambda \|\mathbf{X}_t\|_{\text{op}} + \eta \leq \frac{a+3}{2}\eta, \quad \forall t \in [T].$$

■

D.3. Proof of Theorem 3

Preliminaries Throughout this section, we define

$$\begin{aligned} \nabla_t &:= \nabla f(\mathbf{X}_t), \quad \mathbf{M}_t := (1 - \beta)\mathbf{B}_t, \\ \mathbf{E}_t &:= \mathbf{M}_t - \nabla_t, \quad \mathbf{N}_t := \mathbf{G}_t - \nabla_t, \quad \mathbf{S}_t := \nabla_{t-1} - \nabla_t. \end{aligned} \tag{32}$$

Under the above notation, the momentum term $\mathbf{B}_t = \beta\mathbf{B}_{t-1} + \mathbf{G}_t$ in Algorithm 3 can be rewritten as the one with a damping factor, i.e., $\mathbf{M}_t = \beta\mathbf{M}_{t-1} + (1 - \beta)\mathbf{G}_t$, allowing us to borrow the similar derivations for Theorems 1 and 2. Also, under the exact Newton–Schulz oracle assumption, we have $\mathbf{O}_t = \text{NewtonSchulz}(\mathbf{B}_t) = \text{msign}(\mathbf{B}_t)$. Since $\text{msign}(\cdot)$ is invariant to input scale according to Lemma D.2, so it further implies $\mathbf{O}_t = \text{msign}(\mathbf{M}_t)$. With the above preparations, we formally begin the proof.

By choosing $\eta \leq 1/\|\mathbf{L}_1\|_{\text{op}}$, we can ensure $\|\mathbf{X}_{t+1} - \mathbf{X}_t\|_{\text{op}} = \eta \|\mathbf{O}_t\|_{\text{op}} \leq 1/\|\mathbf{L}_1\|_{\text{op}}$. Recall the definitions and notations in (32), according to Lemma D.5, we have

$$\begin{aligned}
 f(\mathbf{X}_{t+1}) &\leq f(\mathbf{X}_t) - \eta \langle \nabla_t, \text{msign}(\mathbf{B}_t) \rangle + \frac{\eta^2}{2} \|\mathbf{O}_t\|_{\mathbf{L}(\mathbf{X}_t)}^2 \\
 &\stackrel{\text{Lemma D.2}}{\leq} f(\mathbf{X}_t) - \eta \langle \nabla_t, \text{msign}(\nabla_t) \rangle + \eta \langle \nabla_t, \text{msign}(\nabla_t) - \text{msign}(\mathbf{M}_t) \rangle \\
 &\quad + \frac{\eta^2}{2} \text{tr} \left(|\mathbf{L}_0|_{\text{m}} + \left| \nabla_t \mathbf{L}_1^\top \right|_{\text{m}} \right) \\
 &\stackrel{\text{Lemmas D.1 to D.3}}{\leq} f(\mathbf{X}_t) - \eta \|\nabla_t\|_* + 2\eta \|\nabla_t - \mathbf{M}_t\|_* + \frac{\eta^2 \|\mathbf{L}_0\|_*}{2} + \frac{\eta^2}{2} \|\mathbf{L}_1\|_{\text{op}} \|\nabla_t\|_* \\
 &\leq f(\mathbf{X}_t) - \frac{\eta}{2} \|\nabla_t\|_* + 2\eta \|\nabla_t - \mathbf{M}_t\|_* + \frac{\eta^2 \|\mathbf{L}_0\|_*}{2}.
 \end{aligned} \tag{33}$$

Rearranging the above relation and summing from 1 to T yields

$$\mathbb{E} \left[\frac{1}{T} \sum_{t=1}^T \|\nabla_t\|_* \right] \leq \frac{2\Delta_f}{\eta T} + \eta \|\mathbf{L}_0\|_* + 4\mathbb{E} \left[\frac{1}{T} \sum_{t=1}^T \|\mathbf{M}_t - \nabla_t\|_* \right], \tag{34}$$

where we use $\Delta_f = f(\mathbf{X}_1) - f_* \geq f(\mathbf{X}_1) - f(\mathbf{X}_{T+1})$. By (32), we have that $\mathbf{M}_t = \beta \mathbf{M}_{t-1} + (1-\beta) \mathbf{G}_t$. Hence, we follow a similar expansion as in (14) to get

$$\begin{aligned}
 \mathbf{E}_t &= \mathbf{M}_t - \nabla_t = \beta \mathbf{M}_{t-1} + (1-\beta) \mathbf{G}_t - \nabla_t \\
 &= \beta (\mathbf{M}_{t-1} - \nabla_{t-1}) + \beta (\nabla_{t-1} - \nabla_t) + (1-\beta) (\mathbf{G}_t - \nabla_t) \\
 &= \beta \mathbf{E}_{t-1} + \beta \mathbf{S}_t + (1-\beta) \mathbf{N}_t.
 \end{aligned}$$

which implies

$$\mathbf{E}_t = -\beta^t \nabla_1 + (1-\beta) \sum_{k=1}^t \beta^{t-k} \mathbf{N}_k + \sum_{k=2}^t \beta^{t-k+1} \mathbf{S}_k,$$

where we utilize $\mathbf{E}_1 = \mathbf{M}_1 - \nabla_1 = (1-\beta) \mathbf{G}_1 - \nabla_1 = (1-\beta) \mathbf{N}_1 - \beta \nabla_1$. We then decompose \mathbf{E}_t into

$$\mathbb{E} [\|\mathbf{E}_t\|_*] \leq \underbrace{\|\beta^t \nabla_1\|_*}_{A_t} + \underbrace{\mathbb{E} \left[\left\| (1-\beta) \sum_{k=1}^t \beta^{t-k} \mathbf{N}_k \right\|_* \right]}_{B_t} + \underbrace{\mathbb{E} \left[\left\| \sum_{k=2}^t \beta^{t-k+1} \mathbf{S}_k \right\|_* \right]}_{C_t},$$

and bound these terms separately.

Cumulative noise B_t Define $\tilde{\mathbf{N}}_k := \beta^{t-k} \mathbf{N}_k, k \in [1, t]$. Under Assumption 3b, we can show that

$$\begin{aligned}
 \frac{B_t}{1-\beta} &\stackrel{\text{Lemma D.7}}{\leq} 2\sqrt{2}\mathbb{E} \left[\left\| \left(\sum_{k=1}^t \tilde{\mathbf{N}}_k \tilde{\mathbf{N}}_k^\top \right)^{1/2} \right\|_* \right] \\
 &\stackrel{\text{Lemma D.4}}{\leq} 2\sqrt{2}\mathbb{E} \left[\sqrt{\left\| (\mathbf{V}_0 \mathbf{V}_0^\top)^{1/2} \right\|_* \text{tr} \left(\left(\sum_{k=1}^t \tilde{\mathbf{N}}_k \tilde{\mathbf{N}}_k^\top \right)^{1/2} |\mathbf{V}_0|_m^{-1} \left(\sum_{k=1}^t \tilde{\mathbf{N}}_k \tilde{\mathbf{N}}_k^\top \right)^{1/2} \right)} \right] \quad (35) \\
 &= 2\sqrt{2\|\mathbf{V}_0\|_*} \cdot \mathbb{E} \left[\sqrt{\text{tr} \left(\left(\sum_{k=1}^t \tilde{\mathbf{N}}_k \tilde{\mathbf{N}}_k^\top \right) |\mathbf{V}_0|_m^{-1} \right)} \right].
 \end{aligned}$$

We proceed by following the conditional expectation recursion in (18):

$$\begin{aligned}
 &\mathbb{E} \left[\sqrt{\text{tr} \left(\left(\sum_{k=1}^t \tilde{\mathbf{N}}_k \tilde{\mathbf{N}}_k^\top \right) |\mathbf{V}_0|_m^{-1} \right)} \middle| \mathcal{F}_{t-1} \right] \\
 &= \mathbb{E} \left[\left(\left(\sum_{k=1}^t \text{tr} \left(\tilde{\mathbf{N}}_k \tilde{\mathbf{N}}_k^\top |\mathbf{V}_0|_m^{-1} \right) \right)^{p/2} \right)^{1/p} \middle| \mathcal{F}_{t-1} \right] \\
 &\stackrel{\text{Lemma C.2}}{\leq} \left(\mathbb{E} \left[\left(\sum_{k=1}^t \left\| \tilde{\mathbf{N}}_k \right\|_{|\mathbf{V}_0|_m^{-1}}^2 \right)^{p/2} \middle| \mathcal{F}_{t-1} \right] \right)^{1/p} \\
 &\stackrel{\text{Lemma C.1}}{\leq} \left(\left(\sum_{k=1}^{t-1} \left\| \tilde{\mathbf{N}}_k \right\|_{|\mathbf{V}_0|_m^{-1}}^2 \right)^{p/2} + \mathbb{E} \left[\left(\text{tr} \left(\tilde{\mathbf{N}}_t \tilde{\mathbf{N}}_t^\top |\mathbf{V}_0|_m^{-1} \right) \right)^{p/2} \middle| \mathcal{F}_{t-1} \right] \right)^{1/p} \\
 &\stackrel{\text{Lemma D.6}}{\leq} \left(\left(\sum_{k=1}^{t-1} \left\| \tilde{\mathbf{N}}_k \right\|_{|\mathbf{V}_0|_m^{-1}}^2 \right)^{p/2} + B^{1-p} \beta^{p(t-t)} \left(\|\mathbf{V}_0\|_*^{p/2} + \frac{\|\mathbf{V}_1\|_{\text{op}}^p \|\nabla_t\|_*^p}{\|\mathbf{V}_0\|_*^{p/2}} \right) \right)^{1/p} \\
 &\stackrel{\text{Lemma C.1}}{\leq} \left(\left(\sum_{k=1}^{t-1} \left\| \tilde{\mathbf{N}}_k \right\|_{|\mathbf{V}_0|_m^{-1}}^2 \right)^{p/2} + B^{1-p} \beta^{p(t-t)} \|\mathbf{V}_0\|_*^{p/2} \right)^{1/p} + \frac{\beta^{(t-t)} \|\mathbf{V}_1\|_{\text{op}} \|\nabla_t\|_*}{B^{\frac{p-1}{p}} \|\mathbf{V}_0\|_*^{1/2}}.
 \end{aligned}$$

Taking total expectations on both sides and applying the above relation recursively:

$$\begin{aligned}
 \mathbb{E} \left[\sqrt{\text{tr} \left(\left(\sum_{k=1}^t \tilde{\mathbf{N}}_k \tilde{\mathbf{N}}_k^\top \right) |\mathbf{V}_0|_m^{-1} \right)} \right] &\leq \underbrace{\mathbb{E} \left[\frac{\beta^{(t-k)} \|\mathbf{V}_1\|_{\text{op}} \|\nabla_k\|_*}{B^{\frac{p-1}{p}} \|\mathbf{V}_0\|_*^{1/2}} \right] \Big|_{k=t}}_{\Phi_k|_{k=t}} \\
 &+ \mathbb{E} \left[\left(\left(\sum_{k=1}^{t-1} \left\| \tilde{\mathbf{N}}_k \right\|_{|\mathbf{V}_0|_m^{-1}}^2 \right)^{p/2} + B^{1-p} \beta^{p(t-t)} \|\mathbf{V}_0\|_*^{p/2} \right)^{1/p} \right]
 \end{aligned}$$

$$\begin{aligned}
 & \stackrel{\text{Lemma C.1}}{\leq} \left(\mathbb{E} \left[\left(\sum_{k=1}^{t-1} \left\| \tilde{\mathbf{N}}_k \right\|_{|\mathbf{V}_0|_m^{-1}}^2 \right)^{p/2} + B^{1-p} \beta^{p(t-t)} \|\mathbf{V}_0\|_*^{p/2} \right] \right)^{1/p} + \Phi_t \\
 &= \left(\mathbb{E} \left[\mathbb{E} \left[\left(\sum_{k=1}^{t-1} \left\| \tilde{\mathbf{N}}_k \right\|_{|\mathbf{V}_0|_m^{-1}}^2 \right)^{p/2} \middle| \mathcal{F}_{t-2} \right] \right] + B^{1-p} \beta^{p(t-t)} \|\mathbf{V}_0\|_*^{p/2} \right)^{1/p} + \Phi_t \\
 &\leq \left(\mathbb{E} \left[\mathbb{E} \left[\left(\sum_{k=1}^{t-2} \left\| \tilde{\mathbf{N}}_k \right\|_{|\mathbf{V}_0|_m^{-1}}^2 \right)^{p/2} \middle| \mathcal{F}_{t-3} \right] \right] + B^{1-p} \left(\beta^{p(t-(t-1))} + \beta^{p(t-t)} \right) \|\mathbf{V}_0\|_*^{p/2} \right)^{1/p} \\
 &\quad + \Phi_{t-1} + \Phi_t \leq \dots \\
 &\leq \left(B^{1-p} \|\mathbf{V}_0\|_*^{p/2} \sum_{k=1}^t \beta^{p(t-k)} \right)^{1/p} + \sum_{k=1}^t \Phi_k \\
 &\leq \frac{\|\mathbf{V}_0\|_*^{p/2}}{B^{\frac{p-1}{p}} (1 - \beta^p)^{1/p}} + \sum_{k=1}^t \mathbb{E} \left[\frac{\beta^{t-k} \|\mathbf{V}_1\|_{\text{op}} \|\nabla_k\|_*}{B^{\frac{p-1}{p}} \|\mathbf{V}_0\|_*^{1/2}} \right].
 \end{aligned}$$

Hence, we can bound B_t as

$$B_t \leq \frac{2\sqrt{2}(1 - \beta)^{\frac{p-1}{p}} \|\mathbf{V}_0\|_*}{B^{\frac{p-1}{p}}} + \frac{2\sqrt{2}(1 - \beta) \|\mathbf{V}_1\|_{\text{op}}}{B^{\frac{p-1}{p}}} \sum_{k=1}^t \mathbb{E} \left[\beta^{t-k} \|\nabla_k\|_* \right], \quad (36)$$

where we make use of $(1 - \beta^p)^{-1/p} \leq (1 - \beta)^{-1/p}$.

Trajectory curvature C_t Under Assumption 2b with $\mathbf{L}(\mathbf{X}) = |\mathbf{L}_0|_m + |\nabla f(\mathbf{X})\mathbf{L}_1^\top|_m$, together with the fact that $\|\mathbf{X}_k - \mathbf{X}_{k-1}\|_{\text{op}} = \eta \|\mathbf{O}_{k-1}\|_{\text{op}} \leq 1/\|\mathbf{L}_1\|_{\text{op}}$, we have

$$\begin{aligned}
 C_t &\leq \sum_{k=2}^t \beta^{t-k+1} \mathbb{E} [\|\mathbf{S}_k\|_*] \stackrel{\text{Lemma D.4}}{\leq} \sum_{k=2}^t \beta^{t-k+1} \mathbb{E} \left[\sqrt{\|\mathbf{L}(\mathbf{X}_k)\|_*} \|\mathbf{S}_k\|_{(\mathbf{L}(\mathbf{X}_k))^{-1}} \right] \\
 &\leq \sum_{k=2}^t \beta^{t-k+1} \mathbb{E} \left[\sqrt{\text{tr}(\mathbf{L}(\mathbf{X}_k))} \|\eta \mathbf{O}_{k-1}\|_{\mathbf{L}(\mathbf{X}_k)} \right] \\
 &\stackrel{\text{Lemma D.2}}{\leq} \eta \sum_{k=2}^t \beta^{t-k+1} \mathbb{E} [\text{tr}(\mathbf{L}(\mathbf{X}_k))] \\
 &\stackrel{\text{Lemma D.1}}{\leq} \eta \sum_{k=2}^t \beta^{t-k+1} \text{tr}(|\mathbf{L}_0|_m) + \eta \sum_{k=2}^t \beta^{t-k+1} \mathbb{E} [\|\mathbf{L}_1\|_{\text{op}} \|\nabla_k\|_*] \\
 &\leq \frac{\eta \|\mathbf{L}_0\|_*}{1 - \beta} + \eta \|\mathbf{L}_1\|_{\text{op}} \sum_{k=2}^t \beta^{t-k+1} \mathbb{E} [\|\nabla_k\|_*].
 \end{aligned}$$

Combining the bounds for A_t, B_t, C_t , and summing from 1 to T :

$$\frac{1}{T} \sum_{t=1}^T \mathbb{E} [\|\mathbf{E}_t\|_*] \leq \frac{1}{T} \sum_{t=1}^T \beta^t \|\nabla_1\|_*$$

$$\begin{aligned}
 & + \frac{2\sqrt{2}(1-\beta)^{\frac{p-1}{p}} \|\mathbf{V}_0\|_*}{B^{\frac{p-1}{p}}} + \frac{2\sqrt{2}(1-\beta) \|\mathbf{V}_1\|_{\text{op}}}{TB^{\frac{p-1}{p}}} \sum_{t=1}^T \sum_{k=1}^t \mathbb{E} \left[\beta^{(t-k)} \|\nabla_k\|_* \right] \\
 & + \frac{\eta \|\mathbf{L}_0\|_*}{1-\beta} + \frac{\eta \|\mathbf{L}_1\|_{\text{op}}}{T} \sum_{t=1}^T \sum_{k=2}^t \beta^{t-k+1} \mathbb{E} [\|\nabla_k\|_*] \\
 & \stackrel{(21)}{\leq} \frac{\|\nabla_1\|_*}{T(1-\beta)} + \frac{2\sqrt{2}(1-\beta)^{\frac{p-1}{p}} \|\mathbf{V}_0\|_*}{B^{\frac{p-1}{p}}} + \frac{\eta \|\mathbf{L}_0\|_*}{1-\beta} \\
 & + \frac{1}{T} \sum_{t=1}^T \left(\frac{2\sqrt{2} \|\mathbf{V}_1\|_{\text{op}}}{B^{\frac{p-1}{p}}} + \frac{\eta \beta \|\mathbf{L}_1\|_{\text{op}}}{1-\beta} \right) \mathbb{E} [\|\nabla_t\|_*] \\
 & \stackrel{(4)}{\leq} \frac{\|\nabla_1\|_*}{T(1-\beta)} + \frac{2\sqrt{2}(1-\beta)^{\frac{p-1}{p}} \|\mathbf{V}_0\|_*}{B^{\frac{p-1}{p}}} + \frac{\eta \|\mathbf{L}_0\|_*}{1-\beta} + \sum_{t=1}^T \frac{1}{8T} \mathbb{E} [\|\nabla_t\|_*].
 \end{aligned}$$

Plugging the above relation into (34), we obtain

$$\frac{1}{T} \sum_{t=1}^T \mathbb{E} [\|\nabla_t\|_*] \leq \frac{4\Delta_f}{\eta T} + \frac{8 \|\nabla_1\|_*}{T(1-\beta)} + \frac{16\sqrt{2}(1-\beta)^{\frac{p-1}{p}} \|\mathbf{V}_0\|_*}{B^{\frac{p-1}{p}}} + \frac{10\eta \|\mathbf{L}_0\|_*}{1-\beta}.$$

Finally, choosing B, β, η according to (4) and following the similar steps as in Appendix C.3, we can obtain the convergence rate $O \left((\Delta_f \|\mathbf{L}_0\|_*)^{\frac{p-1}{3p-2}} \|\mathbf{V}_0\|_*^{\frac{p}{3p-2}} (BT)^{\frac{1-p}{3p-2}} \right)$.

D.4. Proof of Theorem 4

Preliminaries For Algorithm 4, we define

$$\begin{aligned}
 \nabla_t &:= \nabla f(\mathbf{X}_t), \quad \mathbf{M}_t := (1-\beta_2)\mathbf{B}_t, \quad \widetilde{\mathbf{M}}_t := (1-\beta_2)\widetilde{\mathbf{B}}_t, \\
 \mathbf{E}_t &:= \mathbf{M}_t - \nabla_t, \quad \mathbf{N}_t := \mathbf{G}_t - \nabla_t, \quad \mathbf{S}_t := \nabla_{t-1} - \nabla_t.
 \end{aligned} \tag{37}$$

Based on the above notation, we have $\mathbf{M}_t = \beta_2 \mathbf{M}_{t-1} + (1-\beta_2) \mathbf{G}_t$ and $\widetilde{\mathbf{M}}_t = \beta_1 \mathbf{M}_t + (1-\beta_2) \mathbf{G}_t$. We also have $\mathbf{O}_t = \text{NewtonSchulz}(\widetilde{\mathbf{B}}_t) = \text{msign}(\widetilde{\mathbf{M}}_t)$. Now, we begin the proof as follows.

By Lemma D.8 and $\|\mathbf{X}_1\|_{\text{op}} \leq 1/(3\lambda)$, $\|\mathbf{X}_{t+1} - \mathbf{X}_t\|_{\text{op}} \leq 5\eta/3$ holds for any $t \in [T]$, which immediately implies $\|\mathbf{X}_{t+1} - \mathbf{X}_t\|_{\text{op}} \leq 1/\|\mathbf{L}_1\|_{\text{op}}$ by the choice of η in (5). Thus, we invoke Lemma D.5 to deduce that

$$\begin{aligned}
 f(\mathbf{X}_{t+1}) &\leq f(\mathbf{X}_t) - \eta \left\langle \nabla_t, \text{msign}(\widetilde{\mathbf{B}}_t) + \lambda \mathbf{X}_t \right\rangle \\
 &\quad + \frac{1}{2} \text{tr} \left((\mathbf{X}_{t+1} - \mathbf{X}_t)^\top \mathbf{L}(\mathbf{X}_t) (\mathbf{X}_{t+1} - \mathbf{X}_t) \right) \\
 &\stackrel{\text{Lemma D.2}}{\leq} f(\mathbf{X}_t) - \eta \langle \nabla_t, \text{msign}(\nabla_t) \rangle + \eta \left\langle \nabla_t, \text{msign}(\nabla_t) - \text{msign}(\widetilde{\mathbf{M}}_t) \right\rangle \\
 &\quad + \eta \lambda \|\mathbf{X}_t\|_{\text{op}} \|\nabla_t\|_* + \frac{1}{2} \|\mathbf{X}_{t+1} - \mathbf{X}_t\|_{\text{op}}^2 \|\mathbf{L}(\mathbf{X}_t)\|_* \\
 &\stackrel{\text{Lemmas D.1 to D.3 and D.8}}{\leq} f(\mathbf{X}_t) - \eta \|\nabla_t\|_* + 2\eta \left\| \nabla_t - \widetilde{\mathbf{M}}_t \right\|_* + \frac{2\eta}{3} \|\nabla_t\|_* + \frac{25\eta^2}{9} \text{tr} \left(|\mathbf{L}_0|_{\text{m}} + \left| \nabla_t \mathbf{L}_1^\top \right|_{\text{m}} \right)
 \end{aligned}$$

$$\begin{aligned}
 &\stackrel{\text{Lemma D.1}}{\leq} f(\mathbf{X}_t) - \frac{\eta}{3} \|\nabla_t\|_* + 2\eta \left\| \nabla_t - \widetilde{\mathbf{M}}_t \right\|_* + \frac{25\eta^2 \|\mathbf{L}_0\|_*}{9} + \frac{25\eta^2 \|\mathbf{L}_1\|_{\text{op}} \|\nabla_t\|_*}{9} \\
 &\stackrel{(5)}{\leq} f(\mathbf{X}_t) - \frac{8\eta}{25} \|\nabla_t\|_* + 2\eta \left\| \nabla_t - \widetilde{\mathbf{M}}_t \right\|_* + \frac{25\eta^2 \|\mathbf{L}_0\|_*}{9},
 \end{aligned}$$

where the second inequality uses Cauchy-Schwarz inequality and the fact that $\|\cdot\|_{\text{op}}$ is submultiplicative; the last step is due to $\eta \leq 3/(625 \|\mathbf{L}_1\|_{\text{op}})$. Rearranging the above relation and summing from 1 to T yields

$$\frac{1}{T} \sum_{t=1}^T \mathbb{E} [\|\nabla_t\|_*] \leq \frac{25\Delta_f}{8\eta T} + \frac{625\eta}{72} \|\mathbf{L}_0\|_* + \frac{25}{4T} \sum_{t=1}^T \mathbb{E} \left[\left\| \widetilde{\mathbf{M}}_t - \nabla_t \right\|_* \right], \quad (38)$$

Recall the notations in (37) and decompose $\mathbb{E} \left[\left\| \widetilde{\mathbf{M}}_t - \nabla_t \right\|_* \right]$ as follows:

$$\begin{aligned}
 \mathbb{E} \left[\left\| \widetilde{\mathbf{M}}_t - \nabla_t \right\|_* \right] &= \mathbb{E} [\|\beta_1 \mathbf{M}_t + (1 - \beta_2) \mathbf{G}_t - \nabla_t\|_*] \\
 &= \mathbb{E} [\|\beta_1 (\mathbf{M}_t - \nabla_t) + (1 - \beta_2) (\mathbf{G}_t - \nabla_t) + (\beta_1 - \beta_2) (\nabla_t)\|_*] \\
 &\leq \beta_1 \mathbb{E} [\|\mathbf{E}_t\|_*] + (1 - \beta_2) \mathbb{E} [\|\mathbf{N}_t\|_*] + |\beta_1 - \beta_2|_{\text{m}} \mathbb{E} [\|\nabla_t\|_*],
 \end{aligned} \quad (39)$$

which holds for all $t \in [T]$. The noise term \mathbf{N}_t can be bounded by

$$\begin{aligned}
 \mathbb{E} [\|\mathbf{N}_t\|_*] &\stackrel{\text{Lemma D.4}}{\leq} \mathbb{E} \left[\sqrt{\|\mathbf{V}_0\|_{\text{m}} \text{tr} \left(\mathbf{N}_t^\top |\mathbf{V}_0|_{\text{m}}^{-1} \mathbf{N}_t \right)} \right] \\
 &= \sqrt{\|\mathbf{V}_0\|_*} \mathbb{E} \left[\mathbb{E} \left[\|\mathbf{N}_t\|_{|\mathbf{V}_0|_{\text{m}}^{-1}} \mid \mathcal{F}_{t-1} \right] \right] \\
 &\stackrel{\text{Lemma C.2}}{\leq} \sqrt{\|\mathbf{V}_0\|_*} \mathbb{E} \left[\left(\mathbb{E} \left[\|\mathbf{N}_t\|_{|\mathbf{V}_0|_{\text{m}}^{-1}}^p \mid \mathcal{F}_{t-1} \right] \right)^{1/p} \right] \\
 &\stackrel{\text{Lemma D.6}}{\leq} \sqrt{\|\mathbf{V}_0\|_*} \mathbb{E} \left[\left(B^{1-p} \left(\|\mathbf{V}_0\|_*^{p/2} + \frac{\|\mathbf{V}_1\|_{\text{op}}^p \|\nabla_t\|_*^p}{\|\mathbf{V}_0\|_*^{p/2}} \right) \right)^{1/p} \right] \quad (40) \\
 &\stackrel{\text{Lemma C.1}}{\leq} B^{\frac{1-p}{p}} \sqrt{\|\mathbf{V}_0\|_*} \mathbb{E} \left[\|\mathbf{V}_0\|_*^{1/2} + \frac{\|\mathbf{V}_1\|_{\text{op}} \|\nabla_t\|_*}{\|\mathbf{V}_0\|_*^{1/2}} \right] \\
 &= B^{\frac{1-p}{p}} \|\mathbf{V}_0\|_* + B^{\frac{1-p}{p}} \|\mathbf{V}_1\|_{\text{op}} \mathbb{E} [\|\nabla_t\|_*].
 \end{aligned}$$

As for the error term \mathbf{E}_t , we mainly adopt the same procedures as in Appendix D.3. Following (14), \mathbf{E}_t could be expressed as $\mathbf{E}_t = \beta_2 \mathbf{E}_{t-1} + \beta_2 \mathbf{S}_t + (1 - \beta_2) \mathbf{N}_t$, implying

$$\mathbf{E}_t = -\beta_2^t \nabla_1 + (1 - \beta_2) \sum_{k=1}^t \beta_2^{t-k} \mathbf{N}_k + \sum_{k=2}^t \beta_2^{t-k+1} \mathbf{S}_k,$$

where we utilize $\mathbf{E}_1 = \mathbf{M}_1 - \nabla_1 = (1 - \beta) \mathbf{G}_1 - \nabla_1 = (1 - \beta) \mathbf{N}_1 - \beta \nabla_1$. Then, it holds that

$$\mathbb{E} [\|\mathbf{E}_t\|_*] \leq \underbrace{\|\beta_2^t \nabla_1\|_*}_{A_t} + \underbrace{\mathbb{E} \left[\left\| (1 - \beta_2) \sum_{k=1}^t \beta_2^{t-k} \mathbf{N}_k \right\|_* \right]}_{B_t} + \underbrace{\mathbb{E} \left[\left\| \sum_{k=2}^t \beta_2^{t-k+1} \mathbf{S}_k \right\|_* \right]}_{C_t}.$$

For B_t , we can safely replace the β in (36) by β_2 to derive

$$B_t \leq \frac{2\sqrt{2}(1-\beta_2)^{\frac{p-1}{p}} \|\mathbf{V}_0\|_*}{B^{\frac{p-1}{p}}} + \frac{2\sqrt{2}(1-\beta_2) \|\mathbf{V}_1\|_{\text{op}}}{B^{\frac{p-1}{p}}} \sum_{k=1}^t \mathbb{E} \left[\beta_2^{t-k} \|\nabla_k\|_* \right],$$

For C_t , we need to cope with weight decay carefully. By Lemma D.8, we have $\|\mathbf{X}_t - \mathbf{X}_{t-1}\|_{\text{op}} \leq 5\eta/3 \leq 1/\|\mathbf{L}\|_{\text{op}}$. So we can utilize Assumption 2b in the following way:

$$\begin{aligned} C_t &\leq \sum_{k=2}^t \beta_2^{t-k+1} \mathbb{E} [\|\mathbf{S}_k\|_*] \stackrel{\text{Lemma D.4}}{\leq} \sum_{k=2}^t \beta_2^{t-k+1} \mathbb{E} \left[\sqrt{\|\mathbf{L}(\mathbf{X}_k)\|_*} \|\mathbf{S}_k\|_{(\mathbf{L}(\mathbf{X}_k))^{-1}} \right] \\ &\leq \sum_{k=2}^t \beta_2^{t-k+1} \mathbb{E} \left[\sqrt{\|\mathbf{L}(\mathbf{X}_k)\|_*} \|\mathbf{X}_k - \mathbf{X}_{k-1}\|_{\mathbf{L}(\mathbf{X}_k)} \right] \\ &\leq \sum_{k=2}^t \beta_2^{t-k+1} \mathbb{E} \left[\sqrt{\|\mathbf{L}(\mathbf{X}_k)\|_* \cdot \|\mathbf{X}_k - \mathbf{X}_{k-1}\|_{\text{op}}^2 \cdot \|\mathbf{L}(\mathbf{X}_k)\|_*} \right] \\ &\stackrel{\text{Lemma D.8}}{\leq} \sum_{k=2}^t \beta_2^{t-k+1} \mathbb{E} \left[\text{tr}(\mathbf{L}(\mathbf{X}_k)) \cdot \frac{5\eta}{3} \right] \\ &\stackrel{\text{Lemma D.1}}{\leq} \frac{5\eta}{3} \sum_{k=2}^t \beta_2^{t-k+1} \text{tr}(|\mathbf{L}_0|_{\text{m}}) + \eta \sum_{k=2}^t \beta_2^{t-k+1} \mathbb{E} [\|\mathbf{L}_1\|_{\text{op}} \|\nabla_k\|_*] \\ &\leq \frac{5\eta \|\mathbf{L}_0\|_*}{3(1-\beta_2)} + \frac{5\eta}{3} \|\mathbf{L}_1\|_{\text{op}} \sum_{k=2}^t \beta_2^{t-k+1} \mathbb{E} [\|\nabla_k\|_*], \end{aligned}$$

where the fourth inequality leverages Cauchy-Schwarz inequality and $\|AB\|_{\text{op}} \leq \|A\|_{\text{op}} \|B\|_{\text{op}}, \forall A \in \mathbb{R}^{m \times n}, B \in \mathbb{R}^{n \times r}$. Combining the bounds for A_t, B_t, C_t , and summing from 1 to T :

$$\begin{aligned} \frac{1}{T} \sum_{t=1}^T \mathbb{E} [\|\mathbf{E}_t\|_*] &\leq \frac{1}{T} \sum_{t=1}^T \beta_2^t \|\nabla_1\|_* + \frac{5\eta \|\mathbf{L}_0\|_*}{3(1-\beta_2)} + \frac{5\eta \|\mathbf{L}_1\|_{\text{op}}}{3T} \sum_{t=1}^T \sum_{k=2}^t \beta_2^{t-k+1} \mathbb{E} [\|\nabla_k\|_*] \\ &\quad + \frac{2\sqrt{2}(1-\beta_2)^{\frac{p-1}{p}} \|\mathbf{V}_0\|_*}{B^{\frac{p-1}{p}}} + \frac{2\sqrt{2}(1-\beta_2) \|\mathbf{V}_1\|_{\text{op}}}{TB^{\frac{p-1}{p}}} \sum_{t=1}^T \sum_{k=1}^t \mathbb{E} \left[\beta_2^{(t-k)} \|\nabla_k\|_* \right] \\ &\stackrel{(2)}{\leq} \frac{\|\nabla_1\|_*}{T(1-\beta_2)} + \frac{2\sqrt{2}(1-\beta_2)^{\frac{p-1}{p}} \|\mathbf{V}_0\|_*}{B^{\frac{p-1}{p}}} + \frac{5\eta \|\mathbf{L}_0\|_*}{3(1-\beta_2)} \\ &\quad + \frac{1}{T} \sum_{t=1}^T \left(\frac{2\sqrt{2} \|\mathbf{V}_1\|_{\text{op}}}{B^{\frac{p-1}{p}}} + \frac{5\eta \beta_2 \|\mathbf{L}_1\|_{\text{op}}}{3(1-\beta_2)} \right) \mathbb{E} [\|\nabla_t\|_*]. \end{aligned}$$

Plugging the above bound for $\mathbb{E} [\|\mathbf{E}_t\|_*]$, the bound for $\mathbb{E} [\|\mathbf{N}_t\|_*]$ in (40) into (39):

$$\begin{aligned} \frac{1}{T} \sum_{t=1}^T \mathbb{E} [\|\widetilde{\mathbf{M}}_t - \nabla_t\|_*] &\leq \frac{\beta_1}{T} \sum_{t=1}^T \mathbb{E} [\|\mathbf{E}_t\|_*] + \frac{1-\beta_2}{T} \sum_{t=1}^T \mathbb{E} [\|\mathbf{N}_t\|_*] + \frac{|\beta_1 - \beta_2|_{\text{m}}}{T} \sum_{t=1}^T \mathbb{E} [\|\nabla_t\|_*] \\ &\leq \frac{\beta_1 \|\nabla_1\|_*}{T(1-\beta_2)} + \frac{2\sqrt{2}\beta_1(1-\beta_2)^{\frac{p-1}{p}} \|\mathbf{V}_0\|_*}{B^{\frac{p-1}{p}}} + \frac{5\beta_1 \eta \|\mathbf{L}_0\|_*}{3(1-\beta_2)} + \frac{(1-\beta_2) \|\mathbf{V}_0\|_*}{B^{\frac{p-1}{p}}} \end{aligned}$$

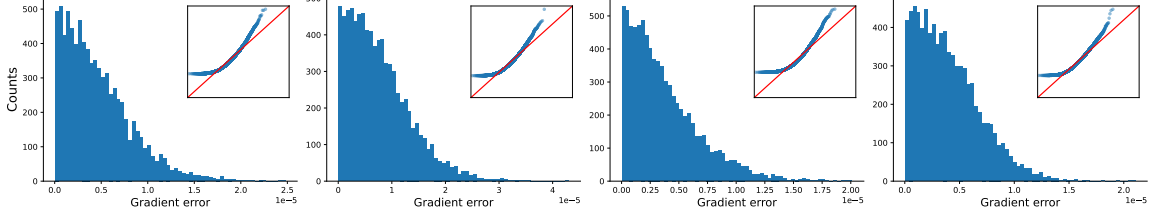


Figure 4: Noise histograms of nanoGPT on C4 at initialization sampled from different coordinates. Q-Q plots are shown at the top-right of each histogram, visualizing the distribution compared with a Gaussian (the red diagonal reference line).

$$\begin{aligned}
 & + \frac{1}{T} \sum_{t=1}^T \left(\frac{(2\sqrt{2}\beta_1 + 1 - \beta_2) \|\mathbf{V}_1\|_{\text{op}}}{B^{\frac{p-1}{p}}} + \frac{5\eta\beta_1\beta_2 \|\mathbf{L}_1\|_{\text{op}}}{3(1-\beta_2)} \right) \mathbb{E}[\|\nabla_t\|_*] + \frac{3}{20T} \sum_{t=1}^T \mathbb{E}[\|\nabla_t\|_*] \\
 & \stackrel{(5)}{\leq} \frac{\beta_1 \|\nabla_1\|_*}{T(1-\beta_2)} + \frac{(2\sqrt{2} + 1)\beta_1 \|\mathbf{V}_0\|_*}{(1-\beta_2)^{\frac{1-p}{p}} B^{\frac{p-1}{p}}} + \frac{5\beta_1\eta \|\mathbf{L}_0\|_*}{3(1-\beta_2)} + \frac{159}{1000T} \sum_{t=1}^T \mathbb{E}[\|\nabla_t\|_*],
 \end{aligned}$$

where the first inequality is due to $|\beta_1 - \beta_2|_m \leq 3/20$ as indicated by (5); the last step is due to

$$\frac{(2\sqrt{2}\beta_1 + 1 - \beta_2) \|\mathbf{V}_1\|_{\text{op}}}{B^{\frac{p-1}{p}}} + \frac{5\eta\beta_1\beta_2 \|\mathbf{L}_1\|_{\text{op}}}{3(1-\beta_2)} \leq \frac{1}{1000} + \frac{5 \times 3}{3 \times 625} = \frac{9}{1000}.$$

Therefore, we plug in this relation into the initial bound in (38) to obtain

$$\begin{aligned}
 & \frac{1}{T} \sum_{t=1}^T \mathbb{E}[\|\nabla_t\|_*] \leq \frac{25\Delta_f}{8\eta T} + \frac{625\eta}{72} \|\mathbf{L}_0\|_* \\
 & + \frac{25\beta_1 \|\nabla_1\|_*}{4T(1-\beta_2)} + \frac{25(2\sqrt{2} + 1)\beta_1 \|\mathbf{V}_0\|_*}{4(1-\beta_2)^{\frac{1-p}{p}} B^{\frac{p-1}{p}}} + \frac{125\beta_1\eta \|\mathbf{L}_0\|_*}{12(1-\beta_2)} + \frac{159}{160T} \sum_{t=1}^T \mathbb{E}[\|\nabla_t\|_*], \\
 & \implies \frac{1}{T} \sum_{t=1}^T \mathbb{E}[\|\nabla_t\|_*] \leq \frac{500\Delta_f}{\eta T} + \frac{1000 \|\nabla_1\|_*}{T(1-\beta_2)} + \frac{3829 \|\mathbf{V}_0\|_*}{(1-\beta_2)^{\frac{1-p}{p}} B^{\frac{p-1}{p}}} + \frac{1875\eta \|\mathbf{L}_0\|_*}{1-\beta_2}.
 \end{aligned}$$

Setting $B, \beta_1, \beta_2, \eta$ according to (5) completes the proof.

Appendix E. Experimental Details

We present the omitted details in Section 6.

E.1. Experimental Setup and Methodology

We conduct all experiments for the NanoGPT model using PyTorch and Distributed Data Parallel (DDP) across eight NVIDIA 4090 GPUs (24GB VRAM each). Our implementation extends the codebase provided by [Semenov et al. \(2025\)](#), incorporating additional modules for noise visualization. All models are trained for 16k steps with a global batch size of 256 sequences. This is

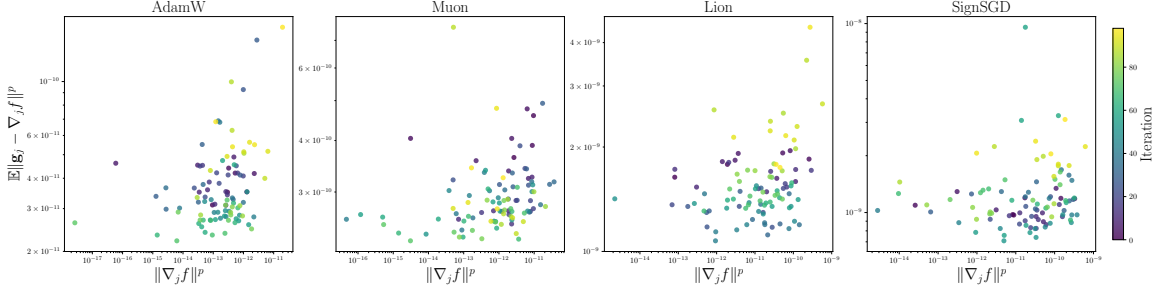


Figure 5: Verification of Assumption 4a. x-axis: $|\nabla_j f|^p$, y-axis: $\mathbb{E}[\|\mathbf{g}_j - \nabla_j f\|^p]$.

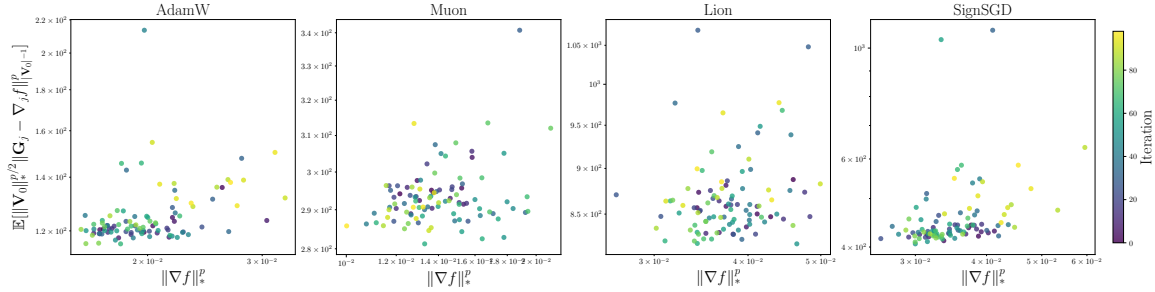


Figure 6: Verification of Assumption 4b. x-axis: $\|\nabla f\|_*^p$, y-axis: $\mathbb{E}[\|\mathbf{V}_0\|_*^{p/2} \|\mathbf{G}_j - \nabla f\|_{|\mathbf{V}_0|_*^{-1}}^p]$.

achieved via a per-GPU batch size of 8 and 64 gradient accumulation steps per round. We use a sequence length of 512, totaling approximately $1 \times$ the Chinchilla-optimal token count as proposed by Hoffmann et al. (2022). For the AdamW, Muon, and Muonlight optimizers, we adopt the standard hyperparameters for 124M-parameter models suggested by Semenov et al. (2025), specifically a learning rate $\eta = 10^{-3}$ and weight decay $\lambda = 0.1$. For vector sign-based optimizers (Lion and SignSGD), we scale the learning rate down by a factor of 10 to $\eta = 10^{-4}$ and increase the weight decay to $\lambda = 1$. This order-of-magnitude adjustment ensures that the effective weight decay remains consistent across all optimizers. Finally, we employ a linear warm-up period of 2000 iterations at the start of pretraining. Results are presented in Figure 3.

E.2. Estimating the Heavy-Tail Index p

Following the methodology of Zhang et al. (2020c), we estimate the heavy-tail index p using the estimator introduced by Simsekli et al. (2019). To visualize this, we randomly sample coordinates from the model and plot the resulting noise histograms. These results, including quantile-quantile (Q-Q) plots, are presented in Figure 4. In these Q-Q plots, a Gaussian distribution would align perfectly with the red diagonal reference line; the fact that our observed curves deviate above the diagonal indicates that the model experiences heavy-tailed noise at these coordinates.

E.3. Validating the Noise Model

To empirically characterize the evolution of noise throughout the pretraining phase, we save model checkpoints at fixed intervals. At each checkpoint, we compute the heavy-tail coefficient p by applying the tail index estimator to gradients calculated over several mini-batches. Simultaneously, we estimate the gradient noise by aggregating stochastic gradients over subsequent iterations. We

then plot the distribution of the empirical gradient norms against their expected values. Figures 1 and 2 show the noise distribution in nanoGPT’s attention layer on the C4 dataset with checkpoint at iteration $t = 0$, while Figures 5 and 6 show the case when iteration $t = 4000$.⁷ These trends are consistent across all layers of the network.

7. Note that Assumptions 4b and 4c are equivalent in some sense, experimental on one implies the other.